



DET NORSKE VERITAS™

Final Report

Subtask 2.3: Characterization of the Toughness of Pipe Containing ERW Seam Defects

Pipeline Hazardous Materials Safety Administration
U.S. Department of Transportation
Washington, DC 20590

Report No./DNV Reg No.: TAOUS813GTQU (PP017533)
May 8, 2013



Subtask 2.3: Characterization of the Toughness of Pipe Containing ERW Seam Defects For: Pipeline and Hazardous Materials Safety Administration U.S. Department of Transportation Washington, DC 20590 Account Ref.:	DET NORSKE VERITAS (U.S.A.), INC. Materials & Corrosion Technology Center 5777 Frantz Road Dublin, OH 43017-1886, United States Tel: (614) 761-1214 Fax: (614) 761-1633 http://www.dnv.com http://www.dnvusa.com
--	--

Date of First Issue:	February 27, 2013	Project No.	PP017533
Report No.:		Organization Unit:	Materials & Corrosion Technology Ctr.
Revision No.:		Subject Group:	

Summary:
 Please see Executive Summary.

Prepared by:	Greg T. Quickel, M.S. Senior Engineer	Signature 
Verified by:	John A. Beavers, Ph.D., FNACE Director – Forensic Investigation	Signature 
Approved by:	Oliver C. Moghissi, Ph.D. Director, Materials & Corrosion Technology Center	Signature 

<input checked="" type="checkbox"/>	No distribution without permission from the client or responsible organizational unit (however, free distribution for internal use within DNV after 3 years)	Key Words	
<input type="checkbox"/>	No distribution without permission from the client or responsible organizational unit		
<input type="checkbox"/>	Strictly confidential		
<input type="checkbox"/>	Unrestricted distribution		

Rev. No. / Date:	Reason for Issue:	Prepared by:	Approved by:	Verified by

© 2013 Det Norske Veritas (U.S.A.), Inc.
 All rights reserved. This publication or parts thereof may not be reproduced or transmitted in any form or by any means, including photocopying or recording, without the prior written consent of Det Norske Veritas (U.S.A.), Inc.

Executive Summary

The purpose of Subtask 2.3 was to identify the best method(s) to characterize the toughness properties of electric resistance welded (ERW) seams. There were three proposed activities in Subtask 2.3; (1) A search of the literature to identify current and new practices for characterizing seam weld properties, (2) Charpy V-notch (CVN) impact testing, and (3) J fracture toughness testing. CVN testing was recommended (based on a literature search) for assessing the toughness of ERW seams. Accordingly, J fracture toughness testing, which was a small effort, was not performed. This subtask's outcome has implications for standards development, although that was beyond the present scope.

The purpose of the literature search task was to identify current and possible novel methods to characterize seam properties. The open literature and DNV documents were reviewed. The open literature search was performed using the search engines Engineering Village and Science Direct. The keywords in the search included pipelines, electric resistance weld, electric resistance welding, low frequency ERW (LFERW), ERW, toughness, seam toughness. The internal DNV documents included those that would not be found in the open literature (e.g., EPRG and Line Pipe Symposium Papers) and literature in our files that may have been older than that searched by the search engines.

The findings from the literature search support the use of the Charpy test for the assessment of the toughness of line pipe steels in general, and the ERW weld seams in particular. The vast majority of the studies found a good correlation between the Charpy test results and the results of the more expensive and complicated fracture mechanics type tests. Furthermore, the integrity predictions using Charpy tests were consistent with the results of full scale burst tests. Test cost is a significant advantage of the Charpy test over the fracture mechanics test. The low cost of the Charpy test allows replicate tests to be performed to better characterize the scatter in the toughness data and provide better prediction of the material toughness.

Previous research points to a number of ways to optimize the Charpy test for characterizing the toughness of line pipe steels. These include:

1. The Charpy specimens should not be flattened.
2. Full thickness Charpy specimens should be used. No machining of the surfaces of the pipe should be performed in the vicinity of the seam weld.
3. The notch in the Charpy specimen should be accurately located by metallography.
4. Full-temperature curves should be obtained.

5. A sufficient number of replicate tests should be performed to establish the range of scatter in the Charpy test data.

Recommendations 1 and 2 can be achieved by machining only the ID surface of the pipe sample to produce one flat surface and one curved surface for the test specimen. With respect to Recommendation 3, the location of the notch should be based on the location of the defects in the pipe. The notch should be placed at the bond line of the weld for lack of fusion defects, while the notch should be placed off the bond line for hook cracks.

The purpose of the CVN testing was to 1) establish the Charpy toughness of the base metal and seam weld in areas that are known to be defect free; 2) evaluate the effect of circumferential location of the notch with respect to the seam on toughness; and 3) evaluate the variation in toughness along the bond line in close proximity to and away from seam weld defects. This information can be used to assist in the development of procedures for establishing the seam toughness of pipe joints containing seam defects.

CVN testing was performed on specimens from two pipe sections where the notch varied in circumferential location from the bond line. The terminus of a hook crack with a “low degree of hook” is typically 1 mm from the bond line whereas the terminus of a hook crack with a “high degree of hook” is a typically 2 mm from the bond line. Two millimeters is typically well outside the boundaries of the coarse-grained heat affected zone (HAZ), in fine-grained HAZ material. Metallography indicated that one of the pipe sections contained a non-post weld heat treated (PWHT) low frequency (LF) ERW seam and the other contained a PWHT high frequency (HF) ERW seam. The results indicated a significant decrease in the Charpy energy for the non-PWHT pipe with decreasing distance from the bond line. The percent shear and lateral expansion data were generally consistent with the Charpy energy data, exhibiting significant changes with distance from the bond line.

The results of CVN testing of specimens removed from the PWHT pipe did not show a dramatic change in properties with circumferential distance from the bond line. Metallography revealed that the seam weld was heated to a temperature that enabled grain refinement, resulting in a more uniform microstructure (compared to the non-PWHT pipe) at and away from the bond line. A PWHT seam weld typically has better toughness than a seam weld that is not PWHT. The uniformity of the microstructure resulted in a higher toughness at the bond line and less variation in toughness with distance from the bond line than the non-PWHT pipe.

CVN testing was also performed on bond line specimens removed from the seam weld, at and away from non-destructive examination (NDE) features. Metallography of eleven of the NDE features revealed two surface breaking lack-of-fusion (LOF) defects and three non-surface

breaking LOF defects. The LOF defects were identified in one of the four pipe sections examined.

Surprisingly, the Charpy energies (upper shelf) were higher adjacent to the confirmed LOF defects compared to away from the defects. At lower temperatures (lower shelf), the Charpy energies were all similar. For the remainder of the NDE features evaluated, there was no obvious trend in Charpy behavior as a function of distance from the features. A larger sampling of bond line defects would help provide some confidence in determining how Charpy energies vary with axial distance from LOF or other types of seam weld defects.

It is our experience that failure pressure calculations using CorLAS™ on various LF ERW failures, where the pipe dimensions, tensile properties, and flaw geometry were known, have revealed very low (<1 ft lb back-calculated) Charpy energies are needed to cause failure. While the data are very limited in this study, they do not support the notion that CVN tests of the bond line can be used in integrity assessments of bond line defects. Additional testing can help determine whether CVN tests are useful in this regard. In the meantime, hydrostatic tests of segments of a pipeline or of cut-outs containing bond line defects in the seam weld can be performed to establish the range of bond line Charpy energies by the following steps:

1. Perform a series of hydrostatic pressure tests.
2. Measure the pipe geometry and initiating flaw (length and depth).
3. Measure the tensile properties of the pipe steel.
4. Use CorLAS™ or some other fracture mechanics model to back-calculate the Charpy energy to cause failure.

DNV also recommends performing CVN tests of base metal and seam weld specimen in order to create/add to archived data for pipelines. These data can be helpful when pipeline failures occur, when mechanical properties of pipelines are needed for calculations, etc.

Table of Contents

1.0 BACKGROUND 1

 1.1 Literature Search..... 1

 1.1.1 Approach..... 1

 1.1.1.1 Results 1

 1.1.2 Discussion 6

 1.1.3 Recommendations 8

 1.2 Charpy V-notch Impact Testing..... 9

2.0 APPROACH 9

3.0 DEFECT FREE PIPE, PHASE 1 11

4.0 PHASE 2, VARIATION IN CVN ENERGY BASED ON SPECIMEN LOCATION 12

 4.1 Variation in CVN Energy as a Function of Circumferential Notch Location 13

 4.1.1 Pipe Section 1..... 13

 4.1.2 Pipe Section 4..... 14

 4.2 Variation in CVN Energy as a Function of Specimen Axial Location with Respect to Seam Defects..... 15

 4.2.1 Pipe Section 1..... 16

 4.2.2 Pipe Section 2..... 17

 4.2.3 Pipe Section 4..... 17

 4.2.4 Pipe Section 5..... 18

5.0 CONCLUSIONS..... 19

 5.1 Literature Search..... 19

 5.2 Charpy V-notch Impact Testing..... 20

6.0 REFERENCES 22

List of Tables

Table 1.	Length and nominal dimensions of Pipe Sections 1 through 5.	23
Table 2.	Results of Charpy V-notch impact tests for transverse, unflattened base metal samples removed from Pipe Section 1.	23
Table 3.	Results of Charpy V-notch impact tests for transverse, unflattened seam weld samples removed from Pipe Section 1.....	24
Table 4.	Results of Charpy V-notch impact tests for transverse, unflattened base metal samples removed from Pipe Section 2.	24
Table 5.	Results of Charpy V-notch impact tests for transverse, unflattened seam weld samples removed from Pipe Section 2.....	25
Table 6.	Results of Charpy V-notch impact tests for transverse, unflattened base metal samples removed from Pipe Section 3.	25
Table 7.	Results of Charpy V-notch impact tests for transverse, unflattened seam weld samples removed from Pipe Section 3.....	26
Table 8.	Results of Charpy V-notch impact tests for transverse, unflattened base metal samples removed from Pipe Section 4.	26
Table 9.	Results of Charpy V-notch impact tests for transverse, unflattened seam weld samples removed from Pipe Section 4.....	27
Table 10.	Results of Charpy V-notch impact tests for transverse, unflattened base metal samples removed from Pipe Section 5.	27
Table 11.	Results of Charpy V-notch impact tests for transverse, unflattened seam weld samples removed from Pipe Section 5.....	28
Table 12.	Summary of upper shelf impact energies (full size) for base metal and seam weld samples removed from the pipe sections.....	28
Table 13.	Summary of 85% fracture appearance transition temperatures (FATT's) for base metal and seam weld samples removed from the pipe sections.	29
Table 14.	Summary of full size ¹ 85% fracture appearance transition temperatures (FATT's) for base metal and seam weld samples removed from the pipe sections.	29
Table 15.	Summary of the full-scale pipe ¹ 85% fracture appearance transition temperatures (FATT's) for base metal and seam weld samples removed from the pipe sections.....	30

List of Tables (continued)

Table 16.	Results of Charpy V-notch impact tests for transverse, unflattened seam weld samples removed from Pipe Section 1, at and away from the bond line	31
Table 17.	Results of Charpy V-notch impact tests for transverse, unflattened seam weld samples removed from Pipe Section 4, at and away from the bond line	31
Table 18.	Results of Charpy V-notch impact tests for transverse, unflattened seam weld samples removed from Pipe Section 1, adjacent to NDE features.	32
Table 19.	Results of Charpy V-notch impact tests for transverse, unflattened seam weld samples removed from Pipe Section 1, away from NDE features.	33
Table 20.	Results of analyses of Charpy V-notch impact tests for transverse, unflattened seam weld samples tested at 320 and 120 °F. Samples were removed from Pipe Section 1.	34
Table 21.	Results of Charpy V-notch impact tests for transverse, unflattened seam weld samples removed from Pipe Section 2 adjacent to an NDE feature.	34
Table 22.	Results of Charpy V-notch impact tests for transverse, unflattened seam weld samples removed from Pipe Section 2, away from NDE feature.	35
Table 23.	Results of analyses of Charpy V-notch impact tests for transverse, unflattened seam weld samples tested at 120 and 80 °F. Samples were removed from Pipe Section 2.	36
Table 24.	Results of Charpy V-notch impact tests for transverse, unflattened seam weld samples removed from Pipe Section 4 adjacent to an NDE feature.	36
Table 25.	Results of Charpy V-notch impact tests for transverse, unflattened seam weld samples removed from Pipe Section 4, away an NDE feature.	37
Table 26.	Results of analyses of Charpy V-notch impact tests for transverse, unflattened seam weld samples tested at 200 and 40 °F. Samples were removed from Pipe Section 4.	37
Table 27.	Results of Charpy V-notch impact tests for transverse, unflattened seam weld samples removed from Pipe Section 5 adjacent to NDE features.	38
Table 28.	Results of Charpy V-notch impact tests for transverse, unflattened seam weld samples removed from Pipe Section 5, away from NDE features.	38

List of Tables (continued)

Table 29. Results of analyses of Charpy V-notch impact tests for transverse, unflattened seam weld samples tested at 320 and 140 °F. Samples were removed from Pipe Section 5. 39



List of Figures

Figure 1. Percent shear from Charpy V-notch tests as a function of temperature for transverse, unflattened base metal samples removed from Pipe Section 1. 40

Figure 2. Charpy V-notch impact energy (full-size-equivalent) as a function of temperature for transverse, unflattened base metal samples removed from Pipe Section 1. 40

Figure 3. Percent shear from Charpy V-notch tests as a function of temperature for transverse, unflattened seam weld samples removed from Pipe Section 1. 41

Figure 4. Charpy V-notch impact energy (full-size-equivalent) as a function of temperature for transverse, unflattened seam weld samples removed from Pipe Section 1. 41

Figure 5. Percent shear from Charpy V-notch tests as a function of temperature for transverse, unflattened base metal samples removed from Pipe Section 2. 42

Figure 6. Charpy V-notch impact energy (full-size-equivalent) as a function of temperature for transverse, unflattened base metal samples removed from Pipe Section 2. 42

Figure 7. Percent shear from Charpy V-notch tests as a function of temperature for transverse, unflattened seam weld samples removed from Pipe Section 2. 43

Figure 8. Charpy V-notch impact energy (full-size-equivalent) as a function of temperature for transverse, unflattened seam weld samples removed from Pipe Section 2. 43

Figure 9. Percent shear from Charpy V-notch tests as a function of temperature for transverse, unflattened base metal samples removed from Pipe Section 3. 44

Figure 10. Charpy V-notch impact energy (full-size-equivalent) as a function of temperature for transverse, unflattened base metal samples removed from Pipe Section 3. 44

Figure 11. Percent shear from Charpy V-notch tests as a function of temperature for transverse, unflattened seam weld samples removed from Pipe Section 3. 45

List of Figures (continued)

Figure 12. Charpy V-notch impact energy (full-size-equivalent) as a function of temperature for transverse, unflattened seam weld samples removed from Pipe Section 3. 45

Figure 13. Percent shear from Charpy V-notch tests as a function of temperature for transverse, unflattened base metal samples removed from Pipe Section 4. 46

Figure 14. Charpy V-notch impact energy (full-size-equivalent) as a function of temperature for transverse, unflattened base metal samples removed from Pipe Section 4. 46

Figure 15. Percent shear from Charpy V-notch tests as a function of temperature for transverse, unflattened seam weld samples removed from Pipe Section 4. 47

Figure 16. Charpy V-notch impact energy (full-size-equivalent) as a function of temperature for transverse, unflattened seam weld samples removed from Pipe Section 4. 47

Figure 17. Percent shear from Charpy V-notch tests as a function of temperature for transverse, unflattened base metal samples removed from Pipe Section 5. 48

Figure 18. Charpy V-notch impact energy (full-size-equivalent) as a function of temperature for transverse, unflattened base metal samples removed from Pipe Section 5. 48

Figure 19. Percent shear from Charpy V-notch tests as a function of temperature for transverse, unflattened seam weld samples removed from Pipe Section 5. 49

Figure 20. Charpy V-notch impact energy (full-size-equivalent) as a function of temperature for transverse, unflattened seam weld samples removed from Pipe Section 5. 49

Figure 21. Plot of Charpy energy (full-size-equivalent) vs. distance of the notch from the bond line for Pipe Section 1. 50

Figure 22. Stereo light photomicrograph of transverse Mount M1-7, which was removed from an NDE feature adjacent to CVN specimens C1-7A and C1-7B (4% Nital Etchant). 51

Figure 23. Light photomicrograph showing the microstructure adjacent to the bond line of transverse Mount M4-1 (4% Nital Etchant). 52

List of Figures (continued)

Figure 24. Light photomicrograph showing the typical base metal of transverse Mount M4-1 (4% Nital Etchant). 52

Figure 25. Plot of percent shear vs. distance of the notch from the bond line for Pipe Section 1. 53

Figure 26. Plot of lateral expansion vs. distance of the notch from the bond line for Pipe Section 1. 54

Figure 27. Plot of Charpy energy (full-size-equivalent) vs. distance of the notch from the bond line for Pipe Section 4. 55

Figure 28. Stereo light photomicrograph of transverse Mount M4-1, which was removed from an NDE feature adjacent to CVN Specimens C4-1A and C4-1B (4% Nital Etchant). 56

Figure 29. Light photomicrograph showing the microstructure adjacent to the bond line of transverse Mount M4-1 (4% Nital Etchant). 57

Figure 30. Light photomicrograph showing the typical base metal of transverse Mount M4-1 (4% Nital Etchant). 57

Figure 31. Plot of percent shear vs. distance of the notch from the bond line for Pipe Section 4. 58

Figure 32. Plot of lateral expansion vs. distance of the notch from the bond line for Pipe Section 4. 59

Figure 33. Photograph of a portion of Pipe Section prior to removal of Mount M4-1 and CVN specimens C4-40a/b and C4-1a/b. 60

Figure 34. Light photomicrograph of transverse Mount M1-8, which was removed from an NDE feature adjacent to CVN specimens C1-8A and C1-8B (4% Nital Etchant). 61

Figure 35. Light photomicrograph of transverse Mount M1-5, which was removed from an NDE feature adjacent to CVN specimens C1-5A and C1-5B (4% Nital Etchant). 61

Figure 36. Plot of Charpy energy (full-size-equivalent) vs. distance from NDE features and confirmed bond line defects for Pipe Section 1. 62

Figure 37. Plot of percent shear vs. distance from NDE features and confirmed bond line defects for Pipe Section 1. 63

List of Figures (continued)

Figure 38. Plot of lateral expansion vs. distance from NDE features and confirmed bond line defects for Pipe Section 1. 64

Figure 39. Plot of Charpy energy (full-size-equivalent) vs. distance from an NDE feature for Pipe Section 2. 65

Figure 40. Plot of percent shear vs. distance from an NDE feature for Pipe Section 2. 66

Figure 41. Plot of lateral expansion vs. distance from an NDE feature for Pipe Section 2. 67

Figure 42. Plot of Charpy energy (full-size-equivalent) vs. distance from an NDE feature for Pipe Section 4. 68

Figure 43. Plot of percent shear vs. distance from an NDE feature Pipe Section 4. 69

Figure 44. Plot of lateral expansion vs. distance from an NDE feature for Pipe Section 4. 70

Figure 45. Plot of Charpy energy (full-size-equivalent) vs. distance from NDE features for Pipe Section 5. 71

Figure 46. Plot of percent shear vs. distance from NDE features for Pipe Section 5. 72

Figure 47. Plot of lateral expansion vs. distance from NDE features for Pipe Section 5. 73

1.0 BACKGROUND

The purpose of Subtask 2.3 was to identify the best method(s) to characterize the toughness properties of ERW seams. There were three activities in Subtask 2.3; (1) A search of the literature to identify current and new practices for characterizing seam weld properties, (2) Charpy V-notch (CVN) impact testing, and (3) J fracture toughness testing. CVN testing was recommended (based on a literature search) for assessing the toughness of ERW seams. Accordingly, J fracture toughness testing, which was a small effort, was not performed. This subtask's outcome has implications for standards development, although that was beyond the present scope.

1.1 Literature Search

1.1.1 Approach

The purpose of the literature search task was to identify current and possible novel methods to characterize seam properties. The open literature and DNV documents were reviewed. The open literature search was performed using the search engines Engineering Village and Science Direct. The keywords in the search included pipelines, electric resistance weld, electric resistance welding, LFERW, ERW, toughness, seam toughness. The internal DNV documents included those that would not be found in the open literature (e.g., EPRG and Line Pipe Symposium Papers) and literature in our files that may have been older than that searched by the search engines.

1.1.1.1 Results

In this section of the report, summaries of relevant documents from the literature are presented in chronological order.

Mayfield and Maxey [Mayfield 1982] investigated the fatigue characteristic of the ERW weld zone of several line pipe steels. The scope of the research involved characterizing the initial defects in the weld zone of the pipe samples, characterizing the mechanical properties of the samples, and evaluating the fatigue behavior of the base metal and weld zones in air and a sodium chloride solution using small laboratory samples and full-scale tests of pipe sections. Charpy tests were used to characterize the fracture toughness and no other toughness techniques were evaluated. It was concluded that the behavior of the full-scale pipe sections could be accurately predicted using the laboratory scale specimens with respect to both the fatigue behavior and the cycles to failure. This observation supports the notion that the Charpy tests can be used to adequately characterize the fracture toughness of the seam welds. It also was found that the largest steel-to-steel variation in mechanical properties was associated with the Charpy test results as opposed to the standard tensile tests. For two pipe steels, the plateau energy of the

base metal and weld zone were similar while for two others, the energy of the weld zone was $\frac{1}{4}$ of that of the base metal. Other conclusions from the research included; the weld zone and the base metal exhibited similar fatigue crack-growth rates, even for the low toughness weld zones and there was not a large effect of corrosion on the fatigue behavior.

Williams and Eiber [Williams 1984, Williams 1985] developed a notched tensile test procedure for measuring the ductility of the seam weld of ERW pipe. The tensile strength of a side notched flattened strap specimen, with the notch located at the ERW weld, is compared with the tensile strength of an un-notched axial specimen. The ratio of the tensile strengths is used to judge the weld ductility, with a value of 1.0 or greater indicating an acceptable level of weld ductility. While the technique may be valuable as a quality assurance tool for pipe mills, it is not obvious how the results could be used in burst pressure models that require a toughness input value.

Hashimoto and Sudo [Hashimoto 1987] evaluated the effects of metallurgical factors on the toughness of flash welded joints of sheet steels. Factors considered included the inclusion content of the base metal and the microstructure and hardness across the welded interface. The toughness was assessed based on Charpy impact properties. It was found that the impact properties deteriorated primarily as a result of the presence of elongated inclusions in the weld. The toughness of the weld decreased with an increase in the inclusion content of the base metal and upset distance of the weld. This deterioration also was associated with a change in the microstructure of the weld from bainitic ferrite to fine polygonal ferrite and an increase in hardness.

Fields et al. [Fields 1989], in a study by the National Institute of Standards and Technology (NIST), conducted an independent assessment of whether special standards should apply to the inspection and operation of older ERW pipelines as a result of the 1988 failure of a petroleum product pipeline operated by Shell Pipeline Corporation. The scope of work involved an independent assessment of a metallurgical analysis of the failure, performed by Battelle, a review of historical failures of ERW pipelines, and a review of integrity management methods for these pipelines. NIST agreed with the findings of the Battelle failure analysis, concluding that the failure initiated at a pre-existing hook crack near the ERW seam. There was no evidence of in-service growth of the defect, but a pressure surge on the pipeline was a contributing factor in the failure. The NIST study also found that failures in pre-1970 ERW pipelines greatly outnumber those of ERW pipelines produced after 1970 but the former incidents contribute a relatively small fraction (<5%) of the total number of pipeline failures. Therefore, NIST concluded that special standards are not warranted for the entire length of these older pipelines, except in high consequence areas. For these areas, it was concluded that periodic hydrostatic testing be performed to eliminate large flaws that potentially could grow in service. At the time the report was prepared (1989), inline inspection was rejected as an alternative integrity management

technique because the available nondestructive inspection techniques were not capable of detecting injurious defects. NIST recommended additional measures to reduce the risks associated with pipeline failures in high consequence areas such as remote control valves. The NIST report did not address the issue of toughness measurements of ERW seam welds.

The Office of Pipeline Safety (OPS 1989) analyzed previous ERW pipe failures on hazardous liquid and gas transmission pipelines in response to two ERW seam failures in Minnesota on hazardous liquid pipelines operated by Williams Pipeline Company. The OPS incident information database, along with other available information regarding ERW pipe, was reviewed with the goal of addressing the safety and reliability of ERW pipelines. It was found that over 95 % of the ERW seam failures occurred on pipelines constructed prior to 1970. The two principle causes of the failures in hazardous liquid service, where a metallurgical analysis was performed, were manufacturing defects, or environmental attack of those defects. It was concluded that the decrease in the number of failures for post-1970 ERW pipelines was so significant that it probably cannot be attributed to any factors other than the change from low frequency to high frequency welding and quality control improvements. The data collected were so compelling that they warranted immediate action, in the form of two Alert Notices. In this study, the issues of seam toughness and test techniques for assessing seam toughness were not addressed.

Groeneveld and Barnes [Groeneveld 1991] undertook a study to determine whether the seam weld quality of modern autogenously welded pipe has improved, justifying more widespread use of this type of pipe in critical applications. Six heavy wall pipes fabricated prior to 1991 were evaluated; five prepared using the using the high frequency ERW process and one prepared using the high frequency induction (HFI) process. Seam weld toughness of the line pipe steels was evaluated using CVN impact testing and the AGA weld ductility test [Williams 1984]. Five of the six pipes exhibited good Charpy properties, with low 85% shear transition temperatures and high upper shelf energies. The sixth joint exhibited a significant variation on the impact properties from one end to the other. This behavior was attributed to poor control of the weld normalization treatment. The AGA weld ductility test failed to identify the heat treatment issue with the one pipe steel. The parameter used in the test to assess weld quality (notched bar tensile strength to longitudinal ultimate tensile strength) exceeded 1.0 for all six pipe steels in spite of the fact that the fracture surfaces were brittle in the case of the pipe with the improper heat treatment.

Pargeter [Pargeter 1992] described the results of a project in which the susceptibility of ERW line pipe to pressure reversals was assessed. Ten modern ERW line pipe steels and one early vintage ERW line pipe steel, which had a history of pressure reversals, were evaluated. The welds in the line pipe were characterized by means of metallography, tensile testing, the AGA weld line ductility test developed by Williams [Williams, 1984], hardness surveys, API pipe

flattening tests, residual stress measurements, and toughness testing. Two types of toughness tests were used; standard Charpy testing and CTOD testing; testing was performed with the notch located on the weld line and 1 mm from the weld line. Susceptibility to pressure reversals was evaluated by repeated loading of notched bend specimens and full-scale pressure tests.

Five of the 11 line pipe steels evaluated exhibited poor toughness properties based on the Charpy testing. The toughness properties were generally worse at the bond line¹ than 1 mm from the bond line. The same five steels exhibited low CTOD values at 0 C. Thus, there was generally good agreement between the two techniques. An exception was where there was a poor microstructure near the outer wall of the steel as a result of overheating. The CTOD sample identified the problem but this was not the case with the Charpy specimens because the region was machined from the specimen. Accordingly, it was recommended that a suitable regime for evaluating ERW seams should include Charpy testing. The more expensive CTOD testing may be required, based on results of metallographic examination. With respect to pressure reversals, the repeated load three point bend test reproduced the susceptibility of the older ERW pipe steel to pressure reversals. Two of the newer steels also exhibited evidence of pressure reversals. Susceptibility to pressure reversals correlated with lower tearing resistance in the CTOD tests.

Orth et al. [Orth 1996] performed a project for PRCI on “Toughness Specifications of ERW Bond Lines for Line Pipe Applications.” The objective of the project was to develop techniques that can be used to characterize the toughness of ERW bond lines in a repeatable manner and develop minimum toughness requirements for ERW line pipe on a fitness for service (FFS) basis. The focus of the study was new ERW line pipe and all of the testing was performed on post-1970 vintage ERW pipe samples. Accordingly, the test results are not directly applicable to LFERW line pipe. However, the assessment of the toughness testing techniques is directly applicable to the current project.

Six ERW pipe samples were characterized using Charpy test, and CTOD test techniques. These data were combined with data for 20 pipe samples taken from the literature to provide a database of ERW pipe properties. This database was used to develop criteria that can distinguish good quality ERW from that which can be expected to cause problems in service from ERW defects. The minimum CTOD and Charpy requirements to prevent fracture initiation in a through wall flaw in an ERW pipe were developed using the failure assessment diagram (FAD) approach found in PD-6493. The predictions from these analyses were compared with performance type test results. These performance tests included service history, the API - 5L pipe flattening test, the notched tensile test described by Williams and Eiber [Williams, 1985] and fatigue tests described by Pargerter [1992].

¹ A bond line or fusion line is where the two abutting edges of skelp are fused together. In cross-section, the bond line typically has a white appearance, is perpendicular to the OD surface, and is very thin (50 to 100 µm thick).

It was found that the CTOD and Charpy performance criteria correctly predicted all of the pipes that failed the performance type tests. The CTOD and Charpy performance criteria correctly predicted 75% of the pipes that passed the experimental performance type tests. The remaining 25% were predicted to fail the performance tests, but passed. It was concluded that the CTOD and Charpy requirements were reasonably accurate, yet somewhat conservative. The FAD approach is known to be conservative so it is difficult to ascertain whether the toughness test technique, the assessment method, or both contributed to the conservatism. In any case, the results of the study are promising with respect to the use of the relatively simple Charpy test technique for assessing the toughness of LFERW seams.

Other findings of the study that are relevant to the ongoing research include:

- A slight deviation of the notch in a Charpy test from the bond line can produce significantly better impact resistance properties than are actually characteristic of the ERW bond line,
- There was extensive scatter in the Charpy data for the bond line, independent of scatter associated with Item 1, when samples were tested in the transition temperature range, and,
- Removal of the OD of the pipe to machine sub-size samples greatly affected the Charpy results.

The implications of these findings are that:

- The notch in the Charpy specimen should be accurately located by metallography.
- A sufficient number of replicate tests should be performed to establish the range of scatter in the Charpy test data, and
- Full thickness Charpy samples should be used.

In this study, no attempt was made to assess the effect of flattening the samples on toughness behavior. However, no flattening was performed on the Charpy test samples while a flattening procedure for the CTOD samples was used that avoided straining of the seam weld. In the case of the Charpy samples, the OD pipe surface was left intact while the ID surface was machined away from the seam weld. This produced one flat surface, perpendicular to the notch, in the sample.

Gianetto et al. [Gianetto, 2002] quantified the properties of the welds and base metals of a number of vintage double submerged arc weld (DSAW) and ERW line pipe steels. Toughness was measured using Charpy and J-Integral/CTOD testing techniques. Full Charpy curves were

obtained using sub-sized specimens. The J-Integral/CTOD testing was performed at room temperature using full thickness edge notched specimens loaded in bending. Crack length was measured using a compliance technique. A linear correlation was observed between the J-integral at 0.2 mm crack growth and the upper shelf Charpy transition temperature for the base metal and welds. However, the Charpy transition temperature of the older pipes was considerably higher than the more modern pipe. For the J-Integral/CTOD test specimens, the initiation toughness was found to be a function of the remaining uncracked ligament. Accordingly, it was recommended that the constraint in the test specimens should be similar to the constraint in the crack geometry being assessed.

Limon and Katz [Limon 2008] presented the results of a case study of an ERW seam weld failure in a natural gas pipeline. It was concluded from the analysis that a pre-existing lack of fusion defect grew by fatigue, ultimately failing in service by brittle fracture. In the analysis, Charpy and J-integral tests were used to characterize the toughness of the seam weld of the failed pipe joint. For the latter, the specimen geometry and type of loading was not provided in the paper. The Charpy tests provided less scatter and consistently lower toughness values than the J-integral tests. The scatter in the J-integral tests results was attributed to difficulty in locating the pre-crack in the specimen at the seam weld. There was good agreement between the observed and predicted failure pressure when the lower bound toughness from the J-integral tests was used in a fracture mechanics assessment based on API 579 Level II.

1.1.2 Discussion

Three basic types of techniques for measuring toughness were identified from the literature survey; the AGA weld ductility test, Fracture mechanics tests (J-integral and CTOD), and Charpy V-notch impact tests.

With the AGA weld ductility test, the tensile strength of a side notched flattened strap specimen, with the notch located at the ERW weld, is compared with the tensile strength of an un-notched axial specimen. The ratio of the tensile strengths is used to judge the weld ductility, with a value of 1.0 or greater indicating an acceptable level of weld ductility. While the technique may be valuable as a quality assurance tool for pipe mills, it is not obvious how the results could be used in burst pressure models that require a toughness input value.

The fracture mechanics techniques involve loading a fatigue pre-cracked sample and measuring the response of the sample to the applied load. Several different specimen geometries can be used for these fracture mechanics tests, including compact tension specimens, and edge notch specimens loaded in tension or bending. The latter geometry and loading was most typically used in the references identified in the literature.

The J-integral is an elastic-plastic crack driving force parameter that incorporates the crack length and applied load. According, crack length is measured along with the applied load, in a rising load controlled test, to calculate the applied J as a function of crack length. Crack length of the specimen can be measured using compliance or electric potential drop techniques. The J-integral at 0.2 mm of crack extension is a commonly reported value for toughness. Further details on the technique can be found in ASTM E 813 (Standard Test Method for J_{IC} , a Measure of Fracture Toughness).

The critical crack tip opening displacement (CTOD) at one or more of several crack extension events is another parameter that is used as a measure of fracture toughness of pipeline steels. The value of CTOD may correspond to δ_c , the onset of unstable brittle crack extension with no significant prior slow stable crack extension, δ_u , the onset of unstable brittle crack extension following prior slow stable crack extension, or δ_m , the first attainment of a maximum force plateau for fully plastic behavior. In a CTOD test, the crosshead or clip gage displacement rate is controlled and the load versus clip gage crack opening displacement is recorded. The CTOD is calculated from the measured clip gage crack opening displacement. Further details on the technique can be found in ASTM E 1290 (Standard Test Method for CTOD Crack-Tip Opening Displacement (CTOD) Fracture Toughness).

The CVN impact test involves subjecting a Charpy specimen to a single application of an impact of a moving mass that has sufficient energy to break the specimen placed in its path, and a device for measuring the energy absorbed by the broken specimen. A typical Charpy specimen used for steels has dimensions of 10 mm × 10 mm × 55 mm with a 2 mm deep notch in the square cross section that is centered in the long direction of the specimen, producing a cross sectional area of 80 mm². The tests can be performed at a single specified temperature, or over a range of temperature in order to establish the upper and lower shelf energies and the transition temperature. Parameters measured in a single Charpy test include the impact energy, the percent shear area on the fracture surface, and the lateral expansion. The percent shear on a fracture surface is typically calculated as the difference between the total fractured area and the area of flat fracture. The lateral expansion is defined as the increase in the width of the specimen perpendicular to the direction of applied force in the Charpy test. In general, the Charpy energy increases with an increase in the % shear area on the fracture surface or an increase in the lateral expansion of the specimen.

The Charpy V-notch (CVN) impact test has been used extensively in mechanical testing of steel products, in research, and in procurement specifications for over three decades. Where correlations with fracture mechanics parameters are available, it is possible to specify CVN toughness values that would ensure elastic-plastic or plastic behavior for fracture of fatigue-cracked specimens subjected to minimum operating temperatures and maximum in service rates

of loading. Further details on the technique can be found in ASTM E 23 (Standard Test Methods for Notch Bar Impact Testing of Metallic Materials).

There was generally good agreement between the two techniques (fracture mechanics and Charpy impact) used to characterize the toughness of the seam welds. For example, Gianetto et al. [Gianetto, 2002] found a linear correlation between the J-integral at 0.2 mm crack growth and the upper shelf Charpy transition temperature for the base metal and welds of a number of line pipe steels. Similarly, Pargeter [Pargeter 1992] found good agreement between standard Charpy testing and CTOD testing of ERW line pipe steels. It also was found that both techniques were capable of accurately predicting behavior based on other performance tests such as service history. Orth et al. [Orth 1996] concluded that the CTOD and Charpy requirements were reasonably accurate, yet somewhat conservative. This conservatism may relate as much with how the data were used as opposed to the inherent conservatism of the results from the testing. For example, the FAD approach used by Orth et al. [Orth 1996] is known to be conservative so it is difficult to ascertain whether the toughness test technique, the assessment method, or both contributed to the conservatism.

Limitations and difficulties were encountered with both techniques. For example, Pargeter [Pargeter 1992] found that the practice of machining the OD surface from Charpy specimens, to produce a flat specimen, produced non-conservative results where there was hardened microstructures in the samples near the free surface.

1.1.3 Recommendations

The findings from the literature search support the use of the Charpy test for the assessment of the toughness of line pipe steels in general, and the ERW weld seams in particular. The vast majority of the studies found a good correlation between the Charpy test results and the results of the more expensive and complicated fracture mechanics type tests. Furthermore, the integrity predictions using Charpy tests were consistent with the results of full-scale burst tests. Test cost is a significant advantage of the Charpy test over the fracture mechanics test. The low cost of the Charpy test allows replicate tests to be performed to better characterize the scatter in the toughness data and provide better prediction of the material toughness.

Previous research points to a number of ways to optimize the Charpy test for characterizing the toughness of line pipe steels. These include:

1. The Charpy specimens should not be flattened.
2. Full thickness Charpy specimens should be used. No machining of the surfaces of the pipe should be performed in the vicinity of the seam weld.
3. The notch in the Charpy specimen should be accurately located by metallography.

4. Full-temperature curves should be obtained.
5. A sufficient number of replicate tests should be performed to establish the range of scatter in the Charpy test data.

Recommendations 1 and 2 can be achieved by machining only the ID surface of the pipe sample to produce one flat surface and one curved surface for the test specimen. With respect to Recommendation 3, the location of the notch should be based on the location of the defects in the pipe. The notch should be placed at the bond line of the weld for lack of fusion defects, while the notch should be placed off the bond line for hook cracks.

1.2 Charpy V-notch Impact Testing

Charpy V-notch testing is one of the easiest and most common techniques used to characterize the fracture toughness of line pipe steels. Charpy type impact specimens are machined and notched and loaded with two fixed points. The fixed points are on the notched side of the specimens. An impact hammer connected to a pendulum of the Charpy test machine is raised to a pre-determined height. The hammer is released and impacts the specimen on the un-notched side, resulting in three-point loading. The height of the hammer after impacting the specimen correlates to the energy absorbed. The test temperatures, sub-size impact energy, full size impact energies, % shear, and lateral expansion are reported for each tested sample.

In the Charpy testing activity, the technique was used to characterize the toughness of five pipe joints that reportedly contained seam weld defects. The test temperatures, sub-size impact energy, full size impact energies, % shear, and lateral expansion were reported for each tested sample. The specimens were ground, polished, and etched to determine the bond line location for all Charpy specimens where the notch was intended to be close to or at the bond line of the seam weld.

In this subtask, the following were evaluated: 1) the effect of circumferential location of the notch with respect to the seam on toughness and 2) the variation in toughness along the bond line in close proximity and away from seam weld defects. This information can be used to assist in the development of procedures for establishing the seam toughness of pipe joints containing seam defects.

2.0 APPROACH

The procedures used in the research and testing were in accordance with industry-accepted standards. Three of the general standards governing terminology, specific metallographic procedures, and mechanical testing used are as follows:

- ASTM E7, “Standard Terminology Relating to Metallography.”

- ASTM E3, “Standard Methods of Preparation of Metallographic Specimens.”
- ASTM E23, “Standard Test Methods for Notched Bar Impact Testing of Metallic Materials.”

The testing consisted of two phases. The goal of Phase 1 was to establish the Charpy toughness of the base metal and seam weld in areas that are known to be defect free. Five pipe sections were received and photographed. The pipe section lengths and nominal wall thicknesses/diameters were recorded. Full pipe ring samples were removed from the sections and CVN specimens were machined from each full ring. The CVN specimens were machined without traditional flattening in order to avoid failure of low toughness samples. The outside diameter (OD) surface and inside diameter (ID) surfaces at the seam weld/notch were not ground; only the ID surface away from the seam weld/notch was ground. The transverse face of the seam weld CVN specimens were polished to a 1 micron finish and etched with Nital Etchant in order to clearly identify the bond line. The base metal and seam weld samples were then notched and tested at various temperatures to produce full curves.

The goals of Phase 2 were to:

- Assess the effect of circumferential notch location, with respect to the seam weld on measured toughness, and
- Assess the effect of axial specimen location with respect to seam defect locations on measured toughness.

The full Charpy curves from Phase 1 (Charpy impact energy vs temperature) for each pipe section were analyzed to determine 1) a temperature (Temperature A) that was in the upper shelf region for both the base metal and seam weld and 2) a temperature (Temperature B) that was in the upper shelf region for the base metal and lower shelf region for the seam weld. The Phase 2 testing was performed at these two temperatures.

For the evaluation of the effect of circumferential notch location on toughness, the notch of the CVN specimens was located at the bond line, 1 and 2 mm clockwise (CW) of the bond line, and 1 and 2 mm counterclockwise (CCW) of the bond line. For the assessment of the effect of axial specimen location on toughness, the CVN specimens were removed at and away from reported non-destructive examination (NDE) features. Where specimens were removed adjacent to NDE features, Specimen A (tested at Temperature A) was closer to the feature than Specimen B (tested at Temperature B). Additionally, the un-notched faces of the specimens were adjacent to each other so the material properties for Specimen A and B were similar.

The CVN specimens were machined and polished as they were in Phase 1. The specimens were tested at various locations; at each location, one specimen was tested at a Temperature A and the other adjacent specimen was tested at a Temperature B. These temperatures varied for the different pipe joints. Additionally, mounted metallographic cross-sections were removed from some of the NDE features to determine if a bond line defect was present.

3.0 DEFECT FREE PIPE, PHASE 1

Table 1 shows the lengths and dimensions (nominal diameters and wall thicknesses) of Pipe Sections 1 through 5. An additional portion of Pipe Section 2 was delivered following Phase 1 testing of Pipe Section 2 and therefore there is a Pipe Section 2a and a Pipe Section 2b. The table shows that the diameters of the pipe sections are either 12 inch or 16-inch nominal and the wall thicknesses are either 0.250 inch or 0.344 inch.

Table 2 through Table 11 show the raw data for CVN testing of the base metal and seam weld samples while Figure 1 through Figure 20 show the Charpy percent shear and impact energy curves. The data were analyzed to determine the upper shelf Charpy energies and 85% fracture appearance transition temperature (FATT) values.

Table 12 is a summary of the upper shelf energies for the base metal and seam weld samples removed from the pipe sections. The table shows that the upper shelf energies for the base metal samples ranged from 16.2 to 47.2 ft·lbs, with an average value of 30.6 ft·lbs. The upper shelf energies for the seam weld samples ranged from 7.4 to 25.6 ft·lbs, with an average value of 18.7 ft·lbs. There was a relatively large difference in the upper shelf values in comparing the base metal to the seam weld values, except for Pipe Section 2, with the base metal values higher than the seam weld values. The values are typical for low frequency (LF) electrical resistance welded (ERW) line pipe steel.

Table 13 is a summary of the 85% FATT values for the base metal and seam weld samples removed from the pipe sections. The table shows that the 85% FATT values for the base metal samples ranged from 38.0 to 136 °F, with an average value of 84.7 °F. The 85% FATT values for the seam weld samples ranged from 85.2 to 230 °F, with an average value of 140 °F. The 85% FATT's for the Pipe Sections 2, 3 and 4 are better than typical for LF ERW pipe and the 85% FATT's for the other pipe sections are typical for LF ERW pipe.

The CVN test results can be adjusted to account for material constraint effects by applying temperature shifts to the data. Various methods can be used to adjust the 85% FATT's; two methods are used below. The first method (*full size*²) adjusts the 85% FATT for sub-size

² "API Recommended Practice 579 – Fitness for Service, 1st Edition, January 2000, American Petroleum Institute, Section F.4.3.3.d. Page F9. API 5L Method.

specimens to a value that would be expected if full size CVN specimens were tested. The full-size 85% FATT's (brittle to ductile transition temperatures) for the samples are shown in Table 14. The table shows that the average 85% FATT (full size) for the base metal samples ranged from 77.5 to 144 °F, with an average value of 105 °F. The average 85% FATT for the seam weld samples ranged from 108 to 232 °F, with an average value of 158 °F. Comparison of Table 13 and Table 14 shows that all FATT values shifted to higher temperatures with increasing specimen thickness, as expected, but the Charpy specimens from the thickest pipe section (5) resulted in the smallest shift.

The second method (*full-scale*)³ adjusts the 85% FATT obtained from the Charpy tests to a predicted FATT from the Battelle Drop-Weight Tear Test (BDWTT). The predicted 85% FATT from the BDWTT test most closely represents the expected FATT for full-scale pipe. The full-scale 85% FATT's (brittle to ductile transition temperatures), based on the nominal wall thicknesses of the pipe sections, are shown in Table 15. The table shows that the average 85% FATT (full scale) for the base metal samples ranged from 22.3 to 114 °F, with an average value of 65.7 °F. The average 85% FATT (full-scale) for the seam weld samples ranged from 67.4 to 203 °F, with an average value of 119 °F. Comparison of Table 13 and Table 15 shows that all FATT values shifted to lower temperatures, which is often the case for thin walled pipe when using the full-scale adjustment. In some instances, this particular equation will cause the FATT values to shift to higher temperatures using the full-scale adjustment.

4.0 PHASE 2, VARIATION IN CVN ENERGY BASED ON SPECIMEN LOCATION

Test temperatures for Phase 2 were determined by analyzing the impact energy vs. temperature curves to find a temperature (Temperature A) that was in the upper shelf region for both the base metal and seam weld and 2) a temperature (Temperature B) that was in the upper shelf region for the base metal and lower shelf region for the seam weld. The concept is that tests at Temperature B would be more sensitive to specimen location than tests at Temperature A. Determination of the A Temperatures was relatively easy and the values for Pipe Sections 1, 2, 4, and 5 were chosen to be 320 °F, 120 °F, 200 °F, and 320 °F, respectively.⁴ Determination of B Temperatures was more challenging. For most of the curves, a value at the extreme upper shelf of the base metal was in the transition region for the seam weld. Therefore, the B Temperatures were chosen to be near or above the impact energy value that correlated to the corresponding 85% FATT of the base metal. The B Temperatures for Pipe Sections 1, 2, 4, and 5 were chosen to be 120 °F, 80 °F, 40 °F, and 140 °F, respectively.

3 Rosenfeld, M.J., "A Simple Procedure for Synthesizing Charpy Impact Energy Transition Curves From Limited Test Data," International Pipeline Conference, Volume 1, ASME, 1996.

4 These temperatures were chosen to be on the upper shelf for the base metal and seam weld and are not necessarily representative of pipeline operating temperatures.

4.1 Variation in CVN Energy as a Function of Circumferential Notch Location

For this part of the project, the notch on the CVN specimens from Pipe Sections 1 and 4 were machined counter-clockwise (minus) and clockwise (plus) of the bond line as described above. The terminus of a hook crack with a “low degree of hook” is typically 1 mm from the bond line; whereas, the terminus of a hook crack with a “high degree of hook” is a typically 2 mm from the bond line. Two millimeters is typically well outside the boundaries of the coarse-grained heat affected zone (HAZ), in fine-grained HAZ material.

4.1.1 Pipe Section 1

Table 16 shows the results of the testing for specimens removed from Pipe Section 1. Figure 21 is a plot of Charpy energy versus distance of the notch from the bond line for Pipe Section 1. The figure shows that 1) the Charpy energies decreased when the distance from the bond line decreased and 2) that a majority of the specimens tested at 320 °F had higher Charpy energies than those tested at 120 °F. The Charpy energies at 320 °F were approximately 2 to 4 times higher when the notches were 1 mm from the bond line, and 4 to 6 times higher when the notches were 2 mm from the bond line, relative to when the notch was at the bond line. The Charpy energies at 320 °F were higher when the notches were on the minus side of the bond line compared to when the notches were on the plus side of the bond line. The variations in the Charpy energies were less dramatic for CVN specimens tested at 120 °F. The Charpy energy at 120 °F was approximately 2 to 3 times lower when the notch was at the bond line, relative to when the notches were away from the bond line.

Metallography of the seam welds (performed when evaluating the defects below) was used to help understand why the Charpy energies measured for Pipe Section 1 in this study are lower near the bond line than away from it. Figure 22 is a stereo light photomicrograph of Mount M1-7 from Pipe Section 1. The bond line of the weld is white and is almost not discernible at this magnification. The HAZ of the bond line is about 3 mm wide and has a rectangular shape. Contact marks are present on the OD surface. These features are all typical of seam welds in LF ERW pipe. The photomicrograph does not show any evidence that the seam weld was PWHT. PWHT seam welds typically have a HAZ as wide as the contact marks near the OD surface (~15 mm in Figure 22) and somewhat narrower near the ID surface. Note that similar morphologies were present for the seam welds for Pipe Sections 2, 3, and 5.

The absence of a PWHT is not uncommon for early vintage ERW pipe because API 5L/5LX did not require post weld heat-treating of seam welds until 1967. The requirement was to heat the seam to at least 1000°F, or remove all untempered martensite.⁵

5 American Petroleum Institute, “API Specification for Line Pipe,” API Standard 5L. 22nd Edition. March 1967.

Figure 23 and Figure 24 are light photomicrographs of Mount M1-7 from Pipe Section 1, showing the microstructures at the bond line and in the base metal, respectively. Figure 23 shows large, coarse grains (CG) at/adjacent to the bond line, which are typical of ERW pipe not subjected to a PWHT. Post weld heat-treating that results in grain recrystallization, such as a normalization treatment, can refine the grains. A normalizing heat treatment⁶ for steel containing 0.2 wt% carbon would require a temperature of approximately 1600°F.⁷ Figure 24 is a light photomicrograph of Mount M1-7 showing the base metal microstructure. The microstructure consists of pearlite, ferrite, and inclusions and is typical for early vintage ERW pipe. Comparison of Figure 23 and Figure 24 confirms that the seam weld was not PWHT to a sufficient temperature for grain refinement. The variation in microstructure with distance from the bond line is consistent with the measured variation in Charpy energy.

Figure 25 is a plot of percent shear versus distance of the notch from the bond line for Pipe Section 1. The figure shows that 1) the percent shear values were similar when the notch was at the bond line compared to away from the bond line, 2) the percent shear values were at or close to 100% for samples tested at 320 °F, and 3) the percent shear values for samples tested at 120 °F ranged between approximately 30 and 60 % shear.

Figure 26 is a plot of lateral expansion versus distance of the notch from the bond line for Pipe Section 1. The figure shows that 1) the values were lower when the notch at the bond line compared to away from the bond line, 2) that the values for the specimens tested at 320 °F were greater than the values for the samples at 120 °F, and 3) that the variation in the values when the notch was at, compared to away from the bond line, was greater for specimens tested at 320 °F compared to specimens tested at 120 °F.

4.1.2 Pipe Section 4

Table 17 shows the results of the testing for specimens removed from Pipe Section 4. Figure 27 is a plot of Charpy energy versus distance of the notch from the bond line for Pipe Section 4. The figure shows that 1) the Charpy energies decreased when the distance from the bond line decreased and 2) that the specimens tested at 200 °F had higher Charpy energies than those tested at 40 °F. The Charpy energy at 40 °F was approximately 2 times lower when the notch was at the bond line compared to when the notches were away from the bond line. The variation in the impact values were less dramatic for CVN specimens tested at 200 °F; the Charpy energy when the notch was at the bond line, compared to the Charpy energies when the notches were away from the bond line, was slightly (no less than 15%) lower.

6 Heating the material to a temperature above the transformation region followed by an air cool to a temperature well below the transformation range. ASM International. "ASM Materials Engineering Dictionary." 1992.

7 ASTM International. "ASM Handbook. Volume 4. Heat Treating. 1991.

Metallography of the seam weld (performed when evaluating the defects below) of Pipe Section 4 revealed a wide HAZ that was wider near the OD surface; see Figure 28. This morphology suggests that the seam weld was PWHT, which typically results in increased toughness of the seam weld when heated to a sufficient temperature. The hourglass shape of the bond line HAZ and lack of contact marks at this magnification indicates that the seam weld is high frequency (HF) ERW.

Figure 29 and Figure 30 are light photomicrographs of Mount M4-1 from Pipe Section 4, showing the microstructures at/adjacent to the bond line and in the base metal, respectively. The figures show a small variation (fairly uniform microstructure) in the grain size at both locations. The grains appear to be slightly larger in the base metal compared to at/adjacent to the bond line. These microstructures confirm that the seam weld was normalized as a result of a post weld heat treatment. The post weld heat treatment is likely why the variation in the toughness was much smaller in Pipe Section 4 compared to Pipe Section 1.

Figure 31 is a plot of percent shear versus distance of the notch from the bond line for Pipe Section 4. All of the specimens tested at 200 °F resulted in 100% shear and a majority of the specimens tested at 40 °F resulted in 100% shear. The percent shear value was much less for the specimen tested at 40 °F when the notch was at the bond line compared to the specimens tested when the notch away from the bond line.

Figure 32 is a plot of lateral expansion versus distance of the notch from the bond line for Pipe Section 4. The figure shows that 1) the values were less when the notch was at the bond line compared to away from the bond line, 2) that the values for the specimens tested at 200 °F were greater than the values for the specimens at 40 °F, and 3) that the variation in the values when the notch was at, compared to away from the bond line, was slightly greater for specimens tested at 40 °F compared to values tested at 200 °F.

4.2 Variation in CVN Energy as a Function of Specimen Axial Location with Respect to Seam Defects

CVN specimens were removed from Pipe Section 1, 2, 4, and 5 at various axial locations, at and away from NDE features. The features were marked on the pipe sections prior to arrival at DNV. Figure 33 is a photograph of Pipe Section 4 illustrating CVN specimen locations and a mount location. The vertical blue lines bound the NDE feature. The figure shows that Specimens C4-1B/A were taken adjacent to the NDE feature, that Specimen A was closer to the NDE feature than Specimen B, and that the un-notched faces of the specimens were adjacent to one another. The figure also shows specimens away from the NDE feature, which have a -40 specimen designation at this location, compared to the specimens adjacent to the NDE feature, which have a -1 designation at this location.

4.2.1 Pipe Section 1

Table 18 shows the raw data for CVN specimens removed from Pipe Section 1 adjacent to NDE features, tested at A (320 °F) and B (120 °F) temperatures. Metallographic cross-sections removed from eight of the NDE features identified two OD surface breaking bond line defects (lack-of-fusion defects) out of eight NDE features. Figure 34 is a light photomicrograph of Mount M1-8, which was removed from an NDE feature adjacent to CVN specimen C1-8A. The figure shows a lack-of-fusion (LOF) defect. Three of the eight mounts contained non surface breaking LOF defects. Very small amounts of discontinuous oxide were present at the bond line for these three mounts. Figure 35 is a light photomicrograph of Mount M1-5, which was removed from the NDE feature adjacent to CVN specimen C1-5A. The figure shows the oxide at the bond line. Table 19 shows the raw data for CVN specimens removed from Pipe Section 1 away from NDE features, tested at A and B temperatures. The table shows that the specimens were between 0.3 and 0.9 feet from the nearest defects.

Table 20 is a summary of the Charpy energies for specimens tested at A and B temperatures, for seam weld samples removed at and away from NDE features in Pipe Section 1. Figure 36 is a plot of Charpy energy versus distance from the nearest NDE feature or confirmed defect. Surprisingly, the Charpy energies for specimens tested at 320 °F, adjacent to 1) confirmed LOF defects and 2) NDE features, were higher (on average) than away from the NDE features. The figure shows that a majority of the Charpy energies were between approximately 1 and 20 ft lbs, with values for two specimens tested at 320 °F being higher. The variation in toughness (for toughness values of mainly 10 ft lbs and below) was lower for the specimens tested at 120 °F than for specimens tested at 320 °F. The values for specimens tested at 320 °F were typically higher than those tested at 120 °F.

Figure 37 is a plot of percent shear versus distance from the nearest NDE features or confirmed defects. There does not appear to be a large variation in percent shear for specimen tested adjacent to NDE features/defects compared to specimens tested away from them. The figure shows that the percent shear values for specimens tested at 320 °F are at or near 100% shear and they are all greater than specimens tested at 120 °F. The figure shows that the percent shear values for specimens tested at 120 °F were between approximately 20 to 70% shear.

Figure 38 is a plot of lateral expansion versus distance from the nearest NDE features or confirmed defects. The values for specimens tested at 320 °F, adjacent to 1) confirmed surface breaking LOF defects and 2) NDE features, were (on average) higher than away from NDE features. The figure shows that a majority of the values are between approximately 0 and 20 mils. A majority of the values for specimens tested at 320 °F are greater than the values for specimens tested at 120 °F.

4.2.2 Pipe Section 2

Table 21 shows the raw data for CVN specimens removed from Pipe Section 2 adjacent to an NDE feature, tested at A (120 °F) and B (80 °F) temperatures. A metallographic cross-section removed from the NDE feature did not identify a bond line defect. Table 22 shows the raw data for CVN specimens removed from Pipe Section 2 away from the NDE feature, tested at 120 °F and 80 °F. The table shows that the specimens were between 1.5 and 6.0 feet from the NDE feature.

Table 23 is a summary of the Charpy energies for specimens tested at A and B temperatures, for seam weld samples removed from Pipe Section 2. Figure 39 is a plot of Charpy energy versus distance from the NDE feature. The figure shows that there is a significant amount of scatter in the data, more so than in for Pipe 1. The variation in toughness (toughness of mainly 10 ft lbs and below) was lower for the specimens tested at 80 °F than for those tested at 120 °F. The Charpy energy for the specimen tested at 120 °F, adjacent to an NDE feature, was higher than values away from the NDE feature. On the other hand, the opposite was the case for the tests conducted at 80 °F. The figure also shows that a majority of the Charpy energies were between approximately 1 and 20 ft lbs, with a value for one specimen tested at 120 °F being higher. The values for specimens tested at 120 °F were typically higher than those tested at 80 °F.

Figure 40 is a plot of percent shear versus distance from the NDE feature. The figure shows that the value for the specimen tested adjacent to the NDE feature was higher than the values for the specimens tested away from the feature. There was a large variation in the percent shear at both test temperatures. The Phase 1 upper shelf Charpy energy results for base metal and seam weld samples removed from Pipe Section 2 were similar, resulting in a small difference between test Temperature A and B. This small difference for the two temperatures may explain the large specimen-to-specimen variation in the percent shear. The test temperatures were likely in the transition region (not completely upper or low shelf) for some locations on the seam weld.

Figure 41 is a plot of lateral expansion versus distance from the NDE feature. Overall, the figure shows that the values are between approximately 0 and 20 mils and there is a large amount of scatter in the data. A majority of the values for specimens tested at 120 °F are greater than the values for those tested at 80 °F. The value for the specimen tested adjacent to the NDE feature at 120 °F was higher than the values for the specimens tested away from the feature, while the opposite was the case for the samples tested at 80 °F.

4.2.3 Pipe Section 4

Table 24 shows the raw data for CVN specimens removed from Pipe Section 4 adjacent to an NDE feature, tested at A (200 °F) and B (40 °F) temperatures. A metallographic cross-section removed from the NDE feature did not identify a bond line defect. Table 25 shows the raw data

for CVN specimens removed from Pipe Section 4 away from the NDE feature, tested at 200 °F and 40 °F. The table shows that the specimens were between 0.8 and 4.0 feet from the NDE feature.

Table 26 is a summary of the Charpy energies for specimens tested at A and B temperatures, for seam weld samples removed from Pipe Section 4. Figure 42 is a plot of Charpy energy versus axial distance from the NDE feature. The Charpy energy for the specimen tested at 200 °F, adjacent to the NDE feature, was lower than away from the NDE feature. The Charpy energy for the specimen tested at 40 °F, adjacent to the NDE feature, was similar to those away from the NDE feature. The figure shows that a majority of the Charpy energies were between approximately 15 and 35 ft lbs. The Charpy energy for specimens tested at 40 °F was relatively good. The values for specimens tested at 200 °F were higher than those tested at 40 °F.

Figure 43 is a plot of percent shear versus axial distance from the NDE feature for Pipe Section 4. The figure shows that 1) the percent shear values were 100% for samples tested at 200 °F and 2) that the percent shear values for samples tested at 40 °F ranged between approximately 20 and 70 % shear. The percent shear values for the specimen tested adjacent to the feature at 40°F was higher than the values for the specimens tested away from the feature.

Figure 44 is a plot of lateral expansion versus distance from the NDE feature. The value for the specimen tested adjacent to the NDE feature at 200 °F was lower than the values for the specimens tested away from the feature. The value for the specimen tested adjacent to the NDE feature at 40 °F was similar to the values for the specimens tested away from the feature. The figure shows that the values are between approximately 5 and 25 mils and that the values for specimens tested at 200 °F are greater than the values for those tested at 40 °F.

4.2.4 Pipe Section 5

Table 27 shows the raw data for CVN specimens removed from Pipe Section 5 adjacent NDE features, tested at A (320 °F) and B (140 °F) temperatures. A metallographic cross-section removed from one of the NDE features did not identify a bond line defect. Table 28 shows the raw data for CVN specimens removed from Pipe Section 5 away from the NDE features, tested at 320 °F and 140 °F. The table shows that the specimens were 0.3 feet from the NDE features.

Table 29 is a summary of the Charpy energies for specimens tested at A and B temperatures, for seam weld samples removed from Pipe Section 5. Figure 45 is a plot of Charpy energy versus distance from the NDE features. The values for the specimens tested adjacent to the features at 320 °F were similar to the values for the specimens tested away. The values for the specimens tested adjacent to the features at 140 °F were slightly greater than those tested away. The figure shows that the Charpy energies were between approximately 4 and 14 ft lbs and that the values for the specimens tested at 320 °F were higher than those tested at 140 °F. The values for

specimens tested at 320 °F were around 14 ft lbs and the values for specimens tested at 140 °F ranged from approximately 4 to 8 ft lbs.

Figure 46 is a plot of percent shear versus distance from the NDE feature for Pipe Section 5. There was not a large variation in the percent shear for specimens tested adjacent to the features compared to away. The figure shows that 1) all of the percent shear values were 100% for samples tested at 320 °F and 2) that the percent shear values for samples tested at 140 °F ranged between approximately 30 and 50 % shear.

Figure 47 is a plot of lateral expansion versus distance of the notch from the NDE feature for Pipe Section 5. The figure shows that 1) the values were similar for specimens tested at features for their respective temperature compared to away and 2) that the values for the specimens tested at 320 °F were greater than the values for the samples at 120 °F.

5.0 CONCLUSIONS

5.1 Literature Search

The findings from the literature search support the use of the Charpy test for the assessment of the toughness of line pipe steels in general, and the ERW weld seams in particular. The vast majority of the studies found a good correlation between the Charpy test results and the results of the more expensive and complicated fracture mechanics type tests. Furthermore, the integrity predictions using Charpy tests were consistent with the result of full-scale burst tests. Test cost is a significant advantage of the Charpy test over the fracture mechanics test. The low cost of the Charpy test allows replicate tests to be performed to better characterize the scatter in the toughness data and provide better prediction of the material toughness.

Previous research points to a number of ways to optimize the Charpy test for characterizing the toughness of line pipe steels. These include:

1. The Charpy specimens should not be flattened.
2. Full thickness Charpy specimens should be used. No machining of the surfaces of the pipe should be performed in the vicinity of the seam weld.
3. The notch in the Charpy specimen should be accurately located by metallography.
4. Full-temperature curves should be obtained.
5. A sufficient number of replicate tests should be performed to establish the range of scatter in the Charpy test data.

Recommendations 1 and 2 can be achieved by machining the ID surface of the pipe sample to produce one flat surface and one curved surface for the test specimen. With respect to

Recommendation 3, the location of the notch should be based on the location of the defects in the pipe. The notch should be placed at the bond line for lack of fusion defects, while the notch should be placed off the bond line for hook cracks.

5.2 Charpy V-notch Impact Testing

CVN testing was performed on specimens from two pipe sections where the notch varied in circumferential location from the bond line. The terminus of a hook crack with a “low degree of hook” is typically 1 mm from the bond line whereas the terminus of a hook crack with a “high degree of hook” is typically 2 mm from the bond line. Two millimeters is typically well outside the boundaries of the coarse-grained HAZ, in fine-grained HAZ material. Metallography indicated that one of the pipes contained a non-post weld heat-treated (PWHT) LF ERW seam and the other contained a PWHT high frequency (HF) ERW seam. The results indicated a significant decrease in the Charpy energy for the non-PWHT pipe with decreasing distance from the bond line. This pipe consisted of coarse grains (typically brittle) at the bond line and a typical base metal microstructure away from the bond line. This variation in the microstructure, with circumferential distance from the bond line, results in larger differences when comparing the Charpy energy at and away from the bond line. These statements are based on:

1. A two-to-four fold decrease in Charpy energy for a specimen tested at 320 °F, at the bond line, compared to those tested 1 mm away from the bond line.
2. A four-to-six fold decrease in Charpy energy for a specimen tested at 320 °F, at the bond line, compared to those tested 2 mm away from the bond line.
3. A two-to-three fold decrease in Charpy energy for a specimen tested at 120 °F, at the bond line, compared to those tested 1 to 2 mm away from the bond line.

The percent shear and lateral expansion data were generally consistent with the Charpy energy data, exhibiting significant changes with distance from the bond line.

The results of CVN testing of specimens removed from the PWHT pipe did not show a dramatic change in properties with circumferential distance from the bond line. Metallography revealed that the seam weld was heated to a temperature that enables grain refinement, resulting in a more uniform microstructure (compared to the non-PWHT pipe) at and away from the bond line. A PWHT seam weld typically has better toughness than a seam weld that is not PWHT. The uniformity of the microstructure resulted in a higher toughness at the bond line and less variation in toughness with distance from the bond line than the non-PWHT pipe. These statements are based on:

1. A minor decrease in Charpy energy for a specimen tested at 200 °F, at the bond line, compared to those tested 1 to 2 mm away from the bond line.

2. A two-fold decrease in Charpy energy for a specimen tested at 40 °F, at the bond line, compared to those tested 1 to 2 mm away from the bond line.

CVN testing was also performed on bond line specimens removed from the seam weld, at and away from NDE features. Metallography of eleven of the NDE features revealed two surface breaking lack-of-fusion (LOF) defects and three non-surface breaking LOF defects. The LOF defects were identified in one of the four pipe sections examined.

Surprisingly, the Charpy energies (tested at 320 °F, upper shelf) were higher adjacent to the confirmed LOF defects compared to away from the defects. At lower temperatures (120 °F, lower shelf), the Charpy energies were all similar. For the remainder of the NDE features evaluated, there was no obvious trend in Charpy behavior as a function of distance from the features. A larger sampling of bond line defects would help provide some confidence in determining how Charpy energies vary with axial distance from LOF or other types of seam weld defects.

It is our experience that failure pressure calculations using CorLAS™ on various LF ERW failures, where the pipe dimensions, tensile properties, and flaw geometry were known, have revealed very low (<1 ft lb back-calculated) Charpy energies are needed to cause failure.⁸ While the data are very limited in this study, they do not support the notion that CVN tests of the bond line can be used in integrity assessments of bond line defects. Additional testing can help determine whether CVN tests are useful in this regard. In the meantime, hydrostatic tests of segments of a pipeline or of cutouts containing bond line defects in the seam weld can be performed to establish the range of bond line Charpy energies by the following steps:

1. Perform a series of hydrostatic pressure tests.
2. Measure the pipe geometry and initiating flaw (length and depth).
3. Measure the tensile properties of the pipe steel.
4. Use CorLAS™ or some other fracture mechanics model to back calculate the Charpy energy to cause failure.

DNV also recommends performing CVN tests of base metal and seam weld specimen in order to create/add to archived data for pipelines. These data can be helpful when pipeline failures occur, when mechanical properties of pipelines are needed for calculations, etc.

⁸ If the flaw dimensions, pipe dimensions, tensile properties, and failure pressure are known, then the Charpy toughness of the pipe steel at the flaw can be estimated by adjusting the input toughness in the failure pressure model until the predicted and actual failure pressures are the same.

6.0 REFERENCES

Fields, 1989: R. J. Fields, E. N. Pugh, D. T. Read, and J.H. Smith, “An Assessment of the Performance and Reliability of Older ERW Pipelines,” NISTIR 89-4136, National Institute of Standards and Technology, July 1989.

Gianetto, 2002: J. A. Gianetto, D. K. Mak, R. Bouchard, S. Xu, and W.R. Tyson, “Characterization of the Microstructure and Toughness of DSAW and ERW Seam Welds of Older Linepipe Steels,” Proceedings of IPC 2002, Paper 27157, 2002.

Groeneveld, 1991: T. P. Groeneveld and C. R. Barnes, “Seam-weld Quality of Modern ERW/HFI Line Pipe,” NG-18 Report 198, American Gas Association, September 1991.

Hashimoto, 1987: S. Hashimoto and M. Sudo, “Effects of Metallurgical Factors on Toughness of Flash Welded Joint of Sheet Steel,” Journal of the Iron and Steel Institute of Japan, Vol. 73, No. 8, p 1018, June 1987.

Limon, 2008: S. Limon and D. Katz, “A Case Study: ERW Seam Weld Failure,” Corrosion 2008, Paper 08150, NACE International, 2008.

Mayfield, 1982: M. E. Mayfield and W. A. Maxey, “ERW Weld Zone Characteristics,” NG-18 Report No. 130, American Gas Association, June 18, 1982.

OPS, 1989: Anonymous, “Electric Resistance Weld Pipe Failures of Hazardous Liquid and Gas Transmission Pipelines,” Technical Report OPS 89-1, Office of Pipeline Safety, August 1989.

Orth, 1996: F.J. Orth, et al., “Toughness Specifications of ERW Bond Lines for Line Pipe Applications,” EWI Project No. 07450CAP, Contract PR-185-9127, PRCI International, Arlington VA, December 23, 1996.

Pargeter, 1992: R. J. Pargeter, “Assessment of ERW Welds in Modern High Strength Line Pipe,” International Conference on Pipeline Reliability, CanMet, Calgary, June 1992.

Williams, 1984: D. N. Williams, “A Method for Evaluating the Ductility of the Seam Weld in ERW Pipe, NG-18 Report No. 141, American Gas Association, May 18, 1984.

Williams, 1985: D. N. Williams and R. J. Eiber, “Test Measures ERW Line Pipe Weld Ductility,” Oil and Gas Journal, pp. 96-106, April 8, 1985.

Table 1. Length and nominal dimensions of Pipe Sections 1 through 5.

Pipe Section	Length (feet)	Nominal Diameter (inches)	Nominal Wall Thickness (inches)
1	15.4	12	0.250
2a	11.8	16	0.250
2b	6.00	16	0.250
3	2.15	16	0.250
4	6.9	12	0.250
5	2.37	16	0.344

Table 2. Results of Charpy V-notch impact tests for transverse, unflattened base metal samples removed from Pipe Section 1.

Sample ID	Temperature, °F	Sub-size ¹ Impact Energy, ft-lbs	Full Size Impact Energy, ft-lbs	Shear, %	Lateral Expansion, mils
1	-10	2.5	3.9	0	3
2	15	4	6.3	0	6
3	40	8.5	13.2	15	12
4	65	12.5	19.6	30	21
5	90	17.5	27.4	60	32
6	115	26.5	41.3	85	39
7	140	29	45	98	46
8	165	28.5	44.2	98	48
9	190	30	46.9	100	50
10	215	30	46.7	100	47

¹ Specimen cross-section = 0.394 inches by 0.253 inches.

Table 3. Results of Charpy V-notch impact tests for transverse, unflattened seam weld samples removed from Pipe Section 1.

Sample ID	Temperature, °F	Sub-size ¹ Impact Energy, ft-lbs	Full Size Impact Energy, ft-lbs	Shear, %	Lateral Expansion, mils
1	15	2	3.2	0	2
2	40	5.5	8.7	10	8
3	65	7.5	11.8	20	11
4	90	5.5	8.7	45	10
5	115	6	9.6	55	10
6	140	7.5	12	65	9
7	185	10	15.9	85	18
8	225	13.5	21.4	90	23
9	250	13.5	21.4	95	23
10	300	13.5	21.4	100	21

¹ Specimen cross-section = 0.394 inches by 0.248 inches.

Table 4. Results of Charpy V-notch impact tests for transverse, unflattened base metal samples removed from Pipe Section 2.

Sample ID	Temperature, °F	Sub-size ¹ Impact Energy, ft-lbs	Full Size Impact Energy, ft-lbs	Shear, %	Lateral Expansion, mils
1	-55	1.5	2.4	0	1
2	-20	4	6.3	0	4
3	5	6	9.5	5	6
4	30	6	9.5	20	9
5	55	8.5	13.4	55	10
6	80	14	22.1	85	22
7	105	15	23.6	100	24
8	115	14.5	22.9	100	25
9	130	16	25.2	100	25
10	155	15	23.6	100	26

¹ Specimen cross-section = 0.395 inches by 0.250 inches.

Table 5. Results of Charpy V-notch impact tests for transverse, unflattened seam weld samples removed from Pipe Section 2.

Sample ID	Temperature, °F	Sub-size ¹ Impact Energy, ft-lbs	Full Size Impact Energy, ft-lbs	Shear, %	Lateral Expansion, mils
1	-20	2.5	3.9	0	3
2	5	1	1.6	5	3
3	30	4	6.2	10	3
4	55	2	3.1	50	8
5	80	12	18.7	55	39
6	105	17	26.5	90	40
7	130	16	24.9	75	34
8	155	16	24.9	100	41
9	180	15	23.4	100	37
10	205	18	28	100	31

¹ Specimen cross-section = 0.395 inches by 0.253 inches.

Table 6. Results of Charpy V-notch impact tests for transverse, unflattened base metal samples removed from Pipe Section 3.

Sample ID	Temperature, °F	Sub-size ¹ Impact Energy, ft-lbs	Full Size Impact Energy, ft-lbs	Shear, %	Lateral Expansion, mils
1	-55	2	3.1	0	1
2	-20	0.5	0.8	0	7
3	5	3	4.7	10	7
4	30	5	7.8	35	6
5	55	9	14	85	14
6	80	11	17.1	98	20
7	105	11	17.1	100	21
8	115	10	15.5	100	18
9	130	10	15.5	100	21
10	155	10	15.5	100	21

¹ Specimen cross-section = 0.395 inches by 0.254 inches.

Table 7. Results of Charpy V-notch impact tests for transverse, unflattened seam weld samples removed from Pipe Section 3.

Sample ID	Temperature, °F	Sub-size ¹ Impact Energy, ft-lbs	Full Size Impact Energy, ft-lbs	Shear, %	Lateral Expansion, mils
1	-20	0.5	0.8	0	0
2	30	0.5	0.8	0	13
3	55	2.5	4	30	14
4	60	0.5	0.8	45	14
5	70	0.5	0.8	55	12
6	80	4	6.4	80	21
7	105	4.5	7.2	98	23
8	130	4	6.4	100	32
9	155	5	8	100	32
10	180	5	8	100	30

¹ Specimen cross-section = 0.395 inches by 0.246 inches.

Table 8. Results of Charpy V-notch impact tests for transverse, unflattened base metal samples removed from Pipe Section 4.

Sample ID	Temperature, °F	Sub-size ¹ Impact Energy, ft-lbs	Full Size Impact Energy, ft-lbs	Shear, %	Lateral Expansion, mils
1	-100	1	1.7	0	0
2	-65	2	3.3	15	1
3	-40	4	6.6	30	4
4	-15	6	10	45	8
5	10	13	21.6	75	21
6	35	15	24.9	80	26
7	60	17	28.3	90	30
8	110	22	36.6	95	30
9	135	17	28.3	100	29
10	160	20.5	34.1	100	34

¹ Specimen cross-section = 0.394 inches by 0.237 inches.

Table 9. Results of Charpy V-notch impact tests for transverse, unflattened seam weld samples removed from Pipe Section 4.

Sample ID	Temperature, °F	Sub-size ¹ Impact Energy, ft-lbs	Full Size Impact Energy, ft-lbs	Shear, %	Lateral Expansion, mils
1	-40	0.5	0.8	0	0
2	-15	4	6.2	5	3
3	10	5.5	8.5	15	21
4	35	7	10.8	30	9
5	60	10	15.5	55	10
6	85	10	15.5	75	9
7	110	12.5	19.3	100	27
8	135	16	24.7	100	22
9	160	16	24.7	100	14
10	185	12.5	19.3	100	16

1 Specimen cross-section = 0.394 inches by 0.255 inches.

Table 10. Results of Charpy V-notch impact tests for transverse, unflattened base metal samples removed from Pipe Section 5.

Sample ID	Temperature, °F	Sub-size ¹ Impact Energy, ft-lbs	Full Size Impact Energy, ft-lbs	Shear, %	Lateral Expansion, mils
1	10	1	1.2	0	2
2	35	2	2.3	0	4
3	60	5	5.8	15	8
4	85	6	7	25	11
5	110	15	17.5	60	22
6	135	20	23.3	85	33
7	160	21	24.5	95	32
8	185	22	25.6	98	32
9	210	24	28	100	33
10	235	29	33.8	100	32

1 Specimen cross-section = 0.394 inches by 0.338 inches.

Table 11. Results of Charpy V-notch impact tests for transverse, unflattened seam weld samples removed from Pipe Section 5.

Sample ID	Temperature, °F	Sub-size ¹ Impact Energy, ft-lbs	Full Size Impact Energy, ft-lbs	Shear, %	Lateral Expansion, mils
1	35	0	0	0	0
2	60	1	1.1	10	0
3	85	0	0	10	0
4	110	1	1.1	20	4
5	135	2	2.1	30	4
6	160	2	2.1	50	4
7	250	11	11.7	85	3
8	275	16	16.9	100	7
9	300	11	11.7	98	5
10	320	13	13.8	100	7

¹ Specimen cross-section = 0.393 inches by 0.372 inches.

Table 12. Summary of upper shelf impact energies (full size) for base metal and seam weld samples removed from the pipe sections.

	Upper Shelf Impact Energy (Full Size), Ft-lbs		
	Base Metal	Seam Weld	Difference
Pipe Section 1	47.2	23.4	23.8
Pipe Section 2	25.3	25.6	0.3
Pipe Section 3	16.2	7.4	8.8
Pipe Section 4	32.8	23.2	9.6
Pipe Section 5	31.3	14.0	17.3
Average	30.6	18.7	11.9
Range	16.2 – 47.2	7.4 – 25.6	–

Table 13. Summary of 85% fracture appearance transition temperatures (FATT's) for base metal and seam weld samples removed from the pipe sections.

	85% FATT, °F		
	Base Metal	Seam Weld	Difference
Pipe Section 1	115	178	67
Pipe Section 2	78.4	113	34.6
Pipe Section 3	56.3	85.2	28.9
Pipe Section 4	38.0	93.5	55.5
Pipe Section 5	136	230	94
Average	84.7	140	55.3
Range	38.0 – 136	85.2 – 230	–

Table 14. Summary of full size¹ 85% fracture appearance transition temperatures (FATT's) for base metal and seam weld samples removed from the pipe sections.

	85% FATT, °F (Full Size)		
	Base Metal	Seam Weld	Difference
Pipe Section 1	137	201	64
Pipe Section 2	101	134	33
Pipe Section 3	77.5	108	30.5
Pipe Section 4	63.2	115	51.8
Pipe Section 5	144	232	88
Average	105	158	53
Range	77.5 – 144	108 – 232	–

1 “API Recommended Practice 579 – Fitness for Service, 1st Edition, January 2000, American Petroleum Institute, Section F.4.3.3.d . Page F9. API 5L Method.

Table 15. Summary of the full-scale pipe¹ 85% fracture appearance transition temperatures (FATT's) for base metal and seam weld samples removed from the pipe sections.

	85% FATT, °F (Full-Scale Pipe)		
	Base Metal	Seam Weld	Difference
Pipe Section 1	95.9	160	64.1
Pipe Section 2	59.6	93.1	33.5
Pipe Section 3	36.6	67.4	30.8
Pipe Section 4	22.3	73.7	51.4
Pipe Section 5	114	203	89.0
Average	65.7	119	53.3
Range	22.3 - 114	67.4 - 203	–

- 1 Rosenfeld, M.J., “A Simple Procedure for Synthesizing Charpy Impact Energy Transition Curves From Limited Test Data,” International Pipeline Conference, Volume 1, ASME, 1996.

Table 16. Results of Charpy V-notch impact tests for transverse, unflattened seam weld samples removed from Pipe Section 1, at and away from the bond line

Sample ID	Distance to Nearest NDE Feature (ft)	Distance from Bond Line (mm)	Temp. °F	Sub-size Impact Energy, ft-lbs	Full Size Impact Energy, ft-lbs	Shear, %	Lateral Expansion, mils
C1-26A	2 and 2.4	0	320	7	11.4	100	18
C1-26B			120	6.5	10.6	60	9
C1-260A		+1	320	12	19.9	98	19
C1-260B			120	14	23.2	45	16
C1-261A		+2	320	30	49.3	100	33
C1-261B			120	15	24.6	60	13
C1-262A		-1	320	29	47.6	100	46
C1-262B			120	14	23	35	17
C1-263A		-2	320	40	65.4	100	40
C1-263B			120	19	31.1	55	17

Table 17. Results of Charpy V-notch impact tests for transverse, unflattened seam weld samples removed from Pipe Section 4, at and away from the bond line

Sample ID	Distance to Nearest NDE Feature (ft)	Distance from Bond Line (mm)	Temp. °F	Sub-size Impact Energy, ft-lbs	Full Size Impact Energy, ft-lbs	Shear, %	Lateral Expansion, mils
C4-41A	2.0	0	200	22	34.4	100	23
C4-41B			40	10	15.6	20	7
C4-410A		+1	200	25	39.1	100	23
C4-410B			40	22	34.4	100	17
C4-411A		+2	200	25	39.1	100	26
C4-411B			40	22	34.4	100	17
C4-412A		-1	200	23	35.8	100	32
C4-412B			40	20	31.1	55	8
C4-413A		-2	200	25	38.9	100	33
C4-413B			40	21.5	33.5	100	23

Table 18. Results of Charpy V-notch impact tests for transverse, unflattened seam weld samples removed from Pipe Section 1, adjacent to NDE features.

Sample ID	Description of Feature Near CVN Sample Following Metallography	Temperature, °F	Sub-size Impact Energy, ft-lbs	Full Size Impact Energy, ft-lbs	Shear, %	Lateral Expansion, mils
C1-1A	OD LOF Defect	320	10	16	100	15
C1-1B		120	5.0	7.9	55	5
C1-2A	No BL defect identified	320	11	17.5	100	16
C1-2B		120	4.0	6.3	45	2
C1-3A	No BL defect identified	320	8	12.7	100	11
C1-3B		120	4	6.3	50	2
C1-4A	No BL defect identified	320	31	50.5	100	41
C1-4B		120	5	8.1	65	8
C1-5A	BL contained discontinuous regions of oxide	320	12	19.7	100	15
C1-5B		120	3	4.9	50	4
C1-6A	BL contained discontinuous regions of oxide	320	9.0	14.6	100	14
C1-6B		120	3.5	5.7	40	7
C1-7A	BL contained discontinuous regions of oxide	320	6.5	10.5	95	8
C1-7B		120	5	8.1	60	2
C1-8A	OD LOF Defect	320	20	31.9	100	20
C1-8B		120	3	4.8	20	3

OD = Outside diameter; LOF = Lack of fusion; BL = Bond line

Table 19. Results of Charpy V-notch impact tests for transverse, unflattened seam weld samples removed from Pipe Section 1, away from NDE features.

Sample ID	Distance to Nearest NDE Feature(s) (ft)	Temperature, °F	Sub-size Impact Energy, ft-lbs	Full Size Impact Energy, ft-lbs	Shear, %	Lateral Expansion, mils
C1-20A	0.8	320	10	15.8	100	15
C1-20B		120	3	4.7	35	6
C1-21A	0.7 and 0.6	320	6	9.5	100	10
C1-21B		120	6	9.5	40	6
C1-22A	0.9 and 0.9	320	7	11	95	6
C1-22B		120	2	3.2	30	0
C1-23A	0.6 and 0.5	320	6	9.8	100	14
C1-23B		120	4	6.5	40	7
C1-24A	0.6 and 0.3	320	4.5	7.2	100	6
C1-24B		120	4.5	7.3	65	6
C1-25A	0.7 and 0.8	320	10	16.1	100	7
C1-25B		120	5	8.2	60	8
C1-26A	2 and 2.4	320	7	11.4	100	18
C1-26B		120	6.5	10.6	60	9
C1-27A	0.9	320	3	4.8	100	8
C1-27B		120	1	1.6	25	5

Table 20. Results of analyses of Charpy V-notch impact tests for transverse, unflattened seam weld samples tested at 320 and 120 °F. Samples were removed from Pipe Section 1.

	Temperature (°F)	Full Size Impact Energy (ft-lbs)		Shear %		Lateral Expansion (mils)	
		Average	Range	Average	Range	Average	Range
C1 adjacent to confirmed LOF defects	320	18.5	10.5 – 31.9	99	95 – 100	14	8 – 20
C1 adjacent to NDE features	320	26.9	12.7 – 50.5	100	100	23	11 – 41
C1 away from NDE features	320	10.7	4.8 – 16.1	99	95 – 100	10.5	6 – 18
C1 adjacent to confirmed LOF defects	120	6.3	4.8 – 8.1	45	20 – 60	4.2	2 – 7
C1 adjacent to NDE features	120	6.9	6.3 – 8.1	53	45 – 65	4.0	2 – 8
C1 away from NDE features	120	6.5	1.6 – 10.6	44	25 – 65	5.9	0 – 9

Table 21. Results of Charpy V-notch impact tests for transverse, unflattened seam weld samples removed from Pipe Section 2 adjacent to an NDE feature.

Sample ID	Description of Feature Near CVN Sample Following Metallography	Temp. °F	Sub-size Impact Energy, ft-lbs	Full Size Impact Energy, ft-lbs	Shear, %	Lateral Expansion, mils
C2-1A	No BL defect identified	120	15	22.7	100	20
C2-1B		80	2	3	100	2

BL = Bond line



Table 22. Results of Charpy V-notch impact tests for transverse, unflattened seam weld samples removed from Pipe Section 2, away from NDE feature.

Sample ID	Distance to NDE Feature (ft)	Temperature, °F	Sub-size Impact Energy, ft-lbs	Full Size Impact Energy, ft-lbs	Shear, %	Lateral Expansion, mils
C2-20A	3.7	120	7	10.6	50	10
C2-20B		80	3	4.5	10	4
C2-21A	1.7	120	9.5	14.4	50	13
C2-21B		80	5	7.6	20	10
C2-22A	2.0	120	13	19.5	100	18
C2-22B		80	7	10.5	100	14
C2-23A	4.0	120	5	7.4	20	8
C2-23B		80	3	4.5	100	5
C2-24A	6.0	120	6	8.9	100	7
C2-24B		80	5	7.3	25	3
C2-30A	6.0	120	5	7.4	75	5
C2-30B		80	3	4.4	35	4
C2-31A	4.0	120	10	14.9	90	5
C2-31B		80	5	7.5	89	6
C2-32A	2.0	120	3	4.4	75	5
C2-32B		80	1	1.5	45	0
C2-33A	1.5	120	3.5	5.3	98	13
C2-33B		80	4	6.1	80	5

Table 23. Results of analyses of Charpy V-notch impact tests for transverse, unflattened seam weld samples tested at 120 and 80 °F. Samples were removed from Pipe Section 2.

	Temperature (°F)	Full Size Impact Energy (ft-lbs)		Shear %		Lateral Expansion (mils)	
		Average	Range	Average	Range	Average	Range
C2 adjacent to NDE feature	120	22.7	1	100	1	20	1
C2 away from NDE feature	120	10.3	4.4 – 19.5	82	50 – 100	9.3	5 – 18
C2 adjacent to NDE feature	80	3.0	1	100	1	2	1
C2 away from NDE feature	80	6.0	1.5 – 10.5	47.1	10 – 100	5.7	0 – 14

1 – There was only one reported NDE feature on the pipe and therefore only on set of CVN specimens at the feature.

Table 24. Results of Charpy V-notch impact tests for transverse, unflattened seam weld samples removed from Pipe Section 4 adjacent to an NDE feature.

Sample ID	Description of Feature Near CVN Sample Following Metallography	Temp. °F	Sub-size Impact Energy, ft-lbs	Full Size Impact Energy, ft-lbs	Shear, %	Lateral Expansion, mils
C4-1A	No BL defect identified	200	12	18.3	100	13
C4-1B		40	11	16.8	65	11

BL = Bond line

Table 25. Results of Charpy V-notch impact tests for transverse, unflattened seam weld samples removed from Pipe Section 4, away an NDE feature.

Sample ID	Distance to NDE Feature (ft)	Temp. °F	Sub-size Impact Energy, ft-lbs	Full Size Impact Energy, ft-lbs	Shear, %	Lateral Expansion, mils
C4-40A	0.8	200	19	29	100	22
C4-40B		40	13.5	20.6	60	15
C4-41A	2.0	200	22	34.4	100	23
C4-41B		40	10	15.6	20	7
C4-42A	4.0	200	16	25.4	100	20
C4-42B		140	9	14.3	45	8

Table 26. Results of analyses of Charpy V-notch impact tests for transverse, unflattened seam weld samples tested at 200 and 40 °F. Samples were removed from Pipe Section 4.

	Temp. (°F)	Full Size Impact Energy (ft-lbs)		Shear %		Lateral Expansion (mils)	
		Average	Range	Average	Range	Average	Range
C4 adjacent to NDE feature	200	18.3	1	100	1	13	1
C4 away from NDE feature	200	29.6	25.4 – 34.4	100	100	21.7	20 – 23
C4 adjacent to NDE feature	40	16.8	1	65	1	11	1
C4 away from NDE feature	40	16.8	14.3 – 20.6	41.7	20 – 60	10	7 – 15

1 – There was only one reported NDE feature on the pipe and therefore only one set of CVN specimens at the feature.

Table 27. Results of Charpy V-notch impact tests for transverse, unflattened seam weld samples removed from Pipe Section 5 adjacent to NDE features.

Sample ID	Description of Feature Near CVN Sample Following Metallography	Temp. °F	Sub-size Impact Energy, ft-lbs	Full Size Impact Energy, ft-lbs	Shear, %	Lateral Expansion, mils
C5-1A	No BL defect identified	320	13	13.7	100	8
C5-1B		140	5	5.3	40	2
C5-2A	Not examined	320	13.5	14.3	100	12
C5-2B		140	7	7.4	30	1

BL = Bond line

Table 28. Results of Charpy V-notch impact tests for transverse, unflattened seam weld samples removed from Pipe Section 5, away from NDE features.

Sample ID	Distance to Nearest NDE Feature(s) (ft)	Temp. °F	Sub-size Impact Energy, ft-lbs	Full Size Impact Energy, ft-lbs	Shear, %	Lateral Expansion, mils
C5-50A	0.3 and 0.3	320	13	13.8	100	10
C5-50B		140	3.5	3.7	35	0
C5-51A	0.3	320	13.5	14.5	100	12
C5-51B		140	4	4.3	45	1

Table 29. Results of analyses of Charpy V-notch impact tests for transverse, unflattened seam weld samples tested at 320 and 140 °F. Samples were removed from Pipe Section 5.

	Temp. (°F)	Full Size Impact Energy (ft-lbs)		Shear %		Lateral Expansion (mils)	
		Average	Range	Average	Range	Average	Range
C5 adjacent to NDE features	320	14	13.7 – 14.3	100	100	10	8 – 12
C5 away from NDE features	320	14.2	13.8 – 14.5	100	100	11	10 – 12
C5 adjacent to NDE features	140	6.4	5.3 – 7.4	35	30 – 40	1.5	1 – 2
C5 away from NDE features	140	3.9	3.7 – 4	40	35 – 45	0.5	0 – 1

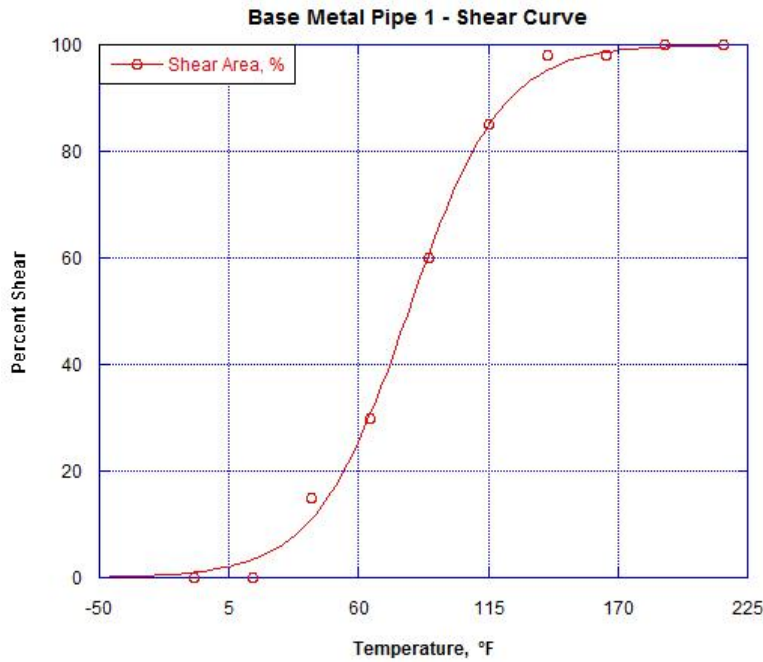


Figure 1. Percent shear from Charpy V-notch tests as a function of temperature for transverse, unflattened base metal samples removed from Pipe Section 1.

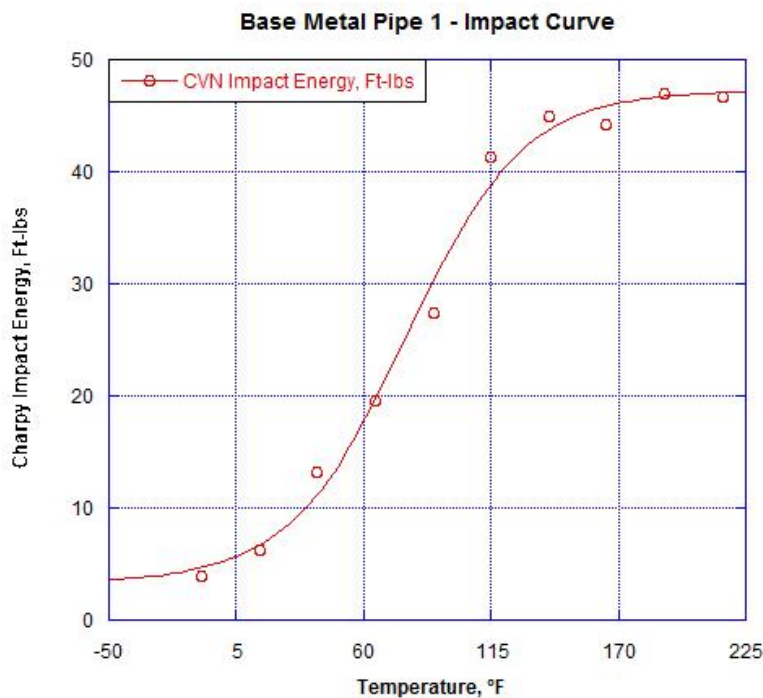


Figure 2. Charpy V-notch impact energy (full-size-equivalent) as a function of temperature for transverse, unflattened base metal samples removed from Pipe Section 1.

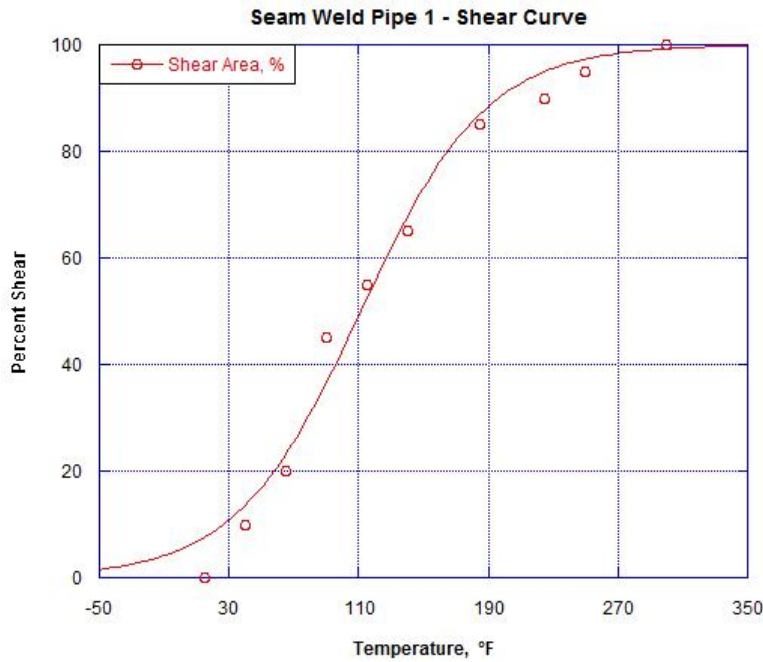


Figure 3. Percent shear from Charpy V-notch tests as a function of temperature for transverse, unflattened seam weld samples removed from Pipe Section 1.

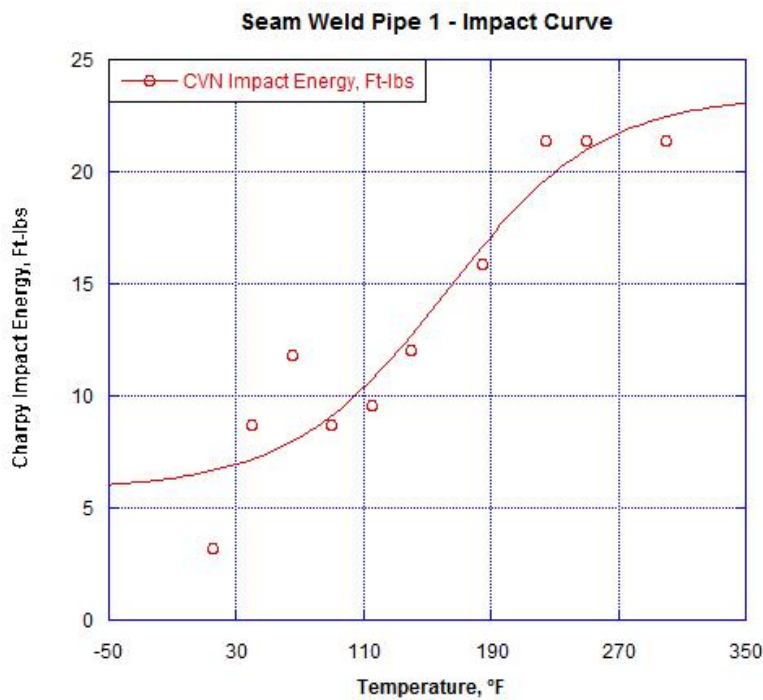


Figure 4. Charpy V-notch impact energy (full-size-equivalent) as a function of temperature for transverse, unflattened seam weld samples removed from Pipe Section 1.

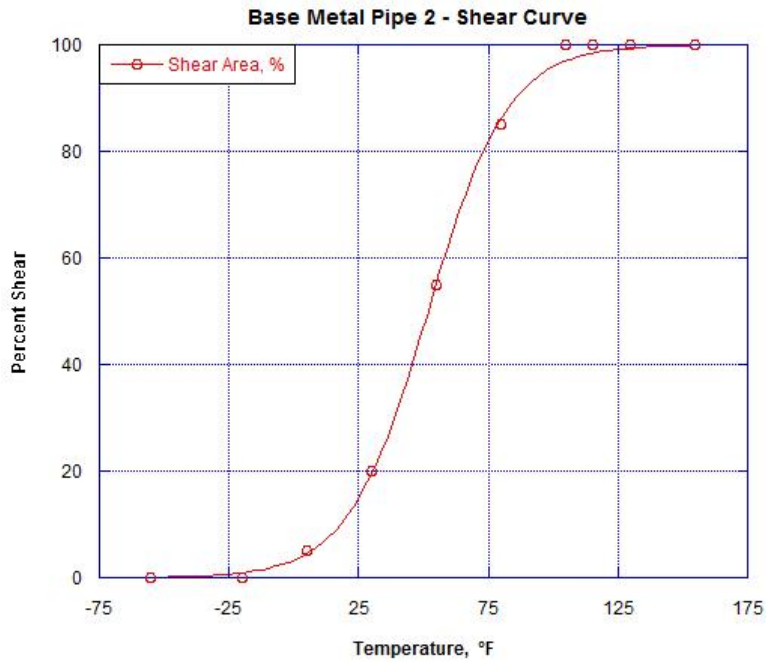


Figure 5. Percent shear from Charpy V-notch tests as a function of temperature for transverse, unflattened base metal samples removed from Pipe Section 2.

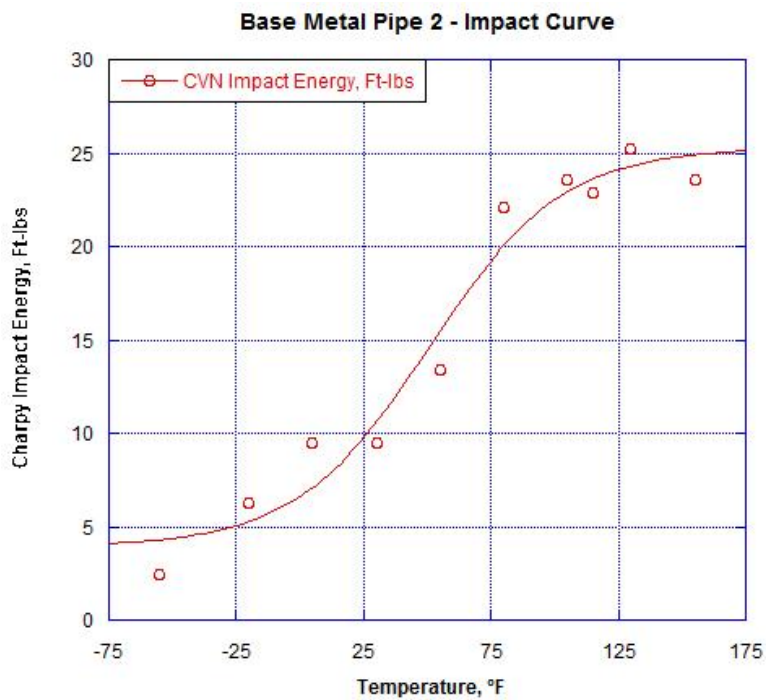


Figure 6. Charpy V-notch impact energy (full-size-equivalent) as a function of temperature for transverse, unflattened base metal samples removed from Pipe Section 2.

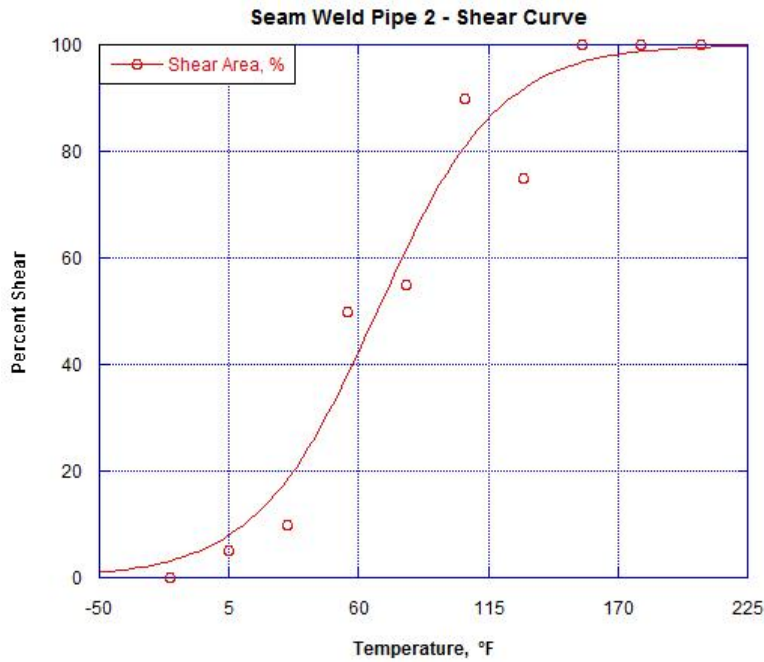


Figure 7. Percent shear from Charpy V-notch tests as a function of temperature for transverse, unflattened seam weld samples removed from Pipe Section 2.

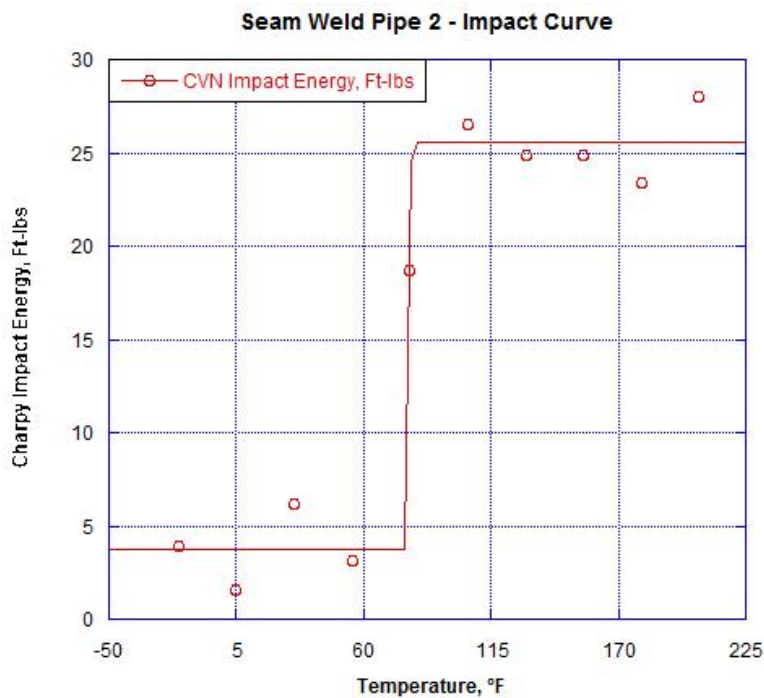


Figure 8. Charpy V-notch impact energy (full-size-equivalent) as a function of temperature for transverse, unflattened seam weld samples removed from Pipe Section 2.

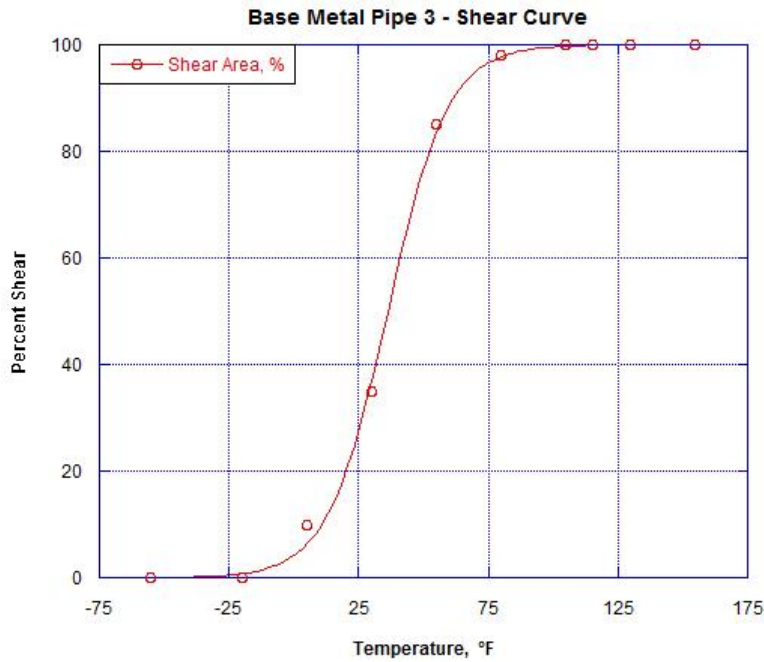


Figure 9. Percent shear from Charpy V-notch tests as a function of temperature for transverse, unflattened base metal samples removed from Pipe Section 3.

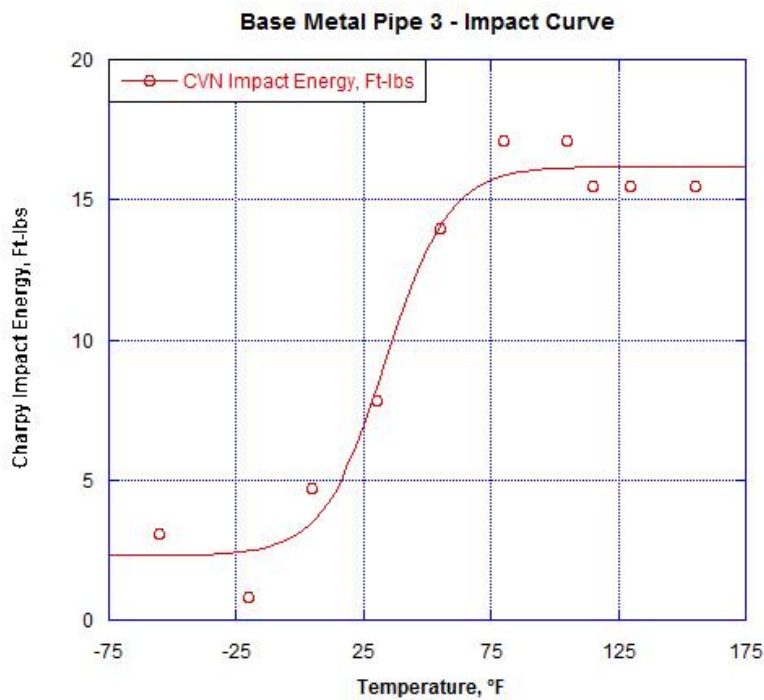


Figure 10. Charpy V-notch impact energy (full-size-equivalent) as a function of temperature for transverse, unflattened base metal samples removed from Pipe Section 3.

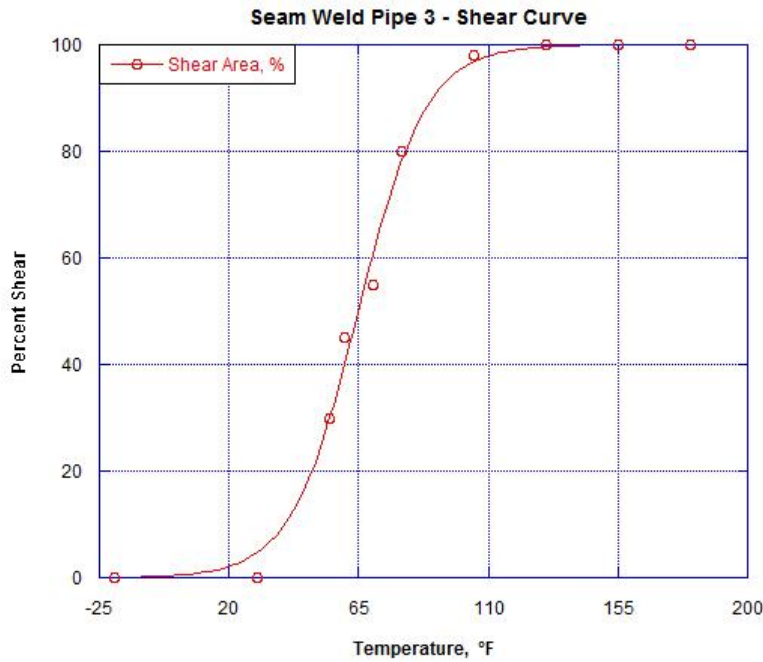


Figure 11. Percent shear from Charpy V-notch tests as a function of temperature for transverse, unflattened seam weld samples removed from Pipe Section 3.

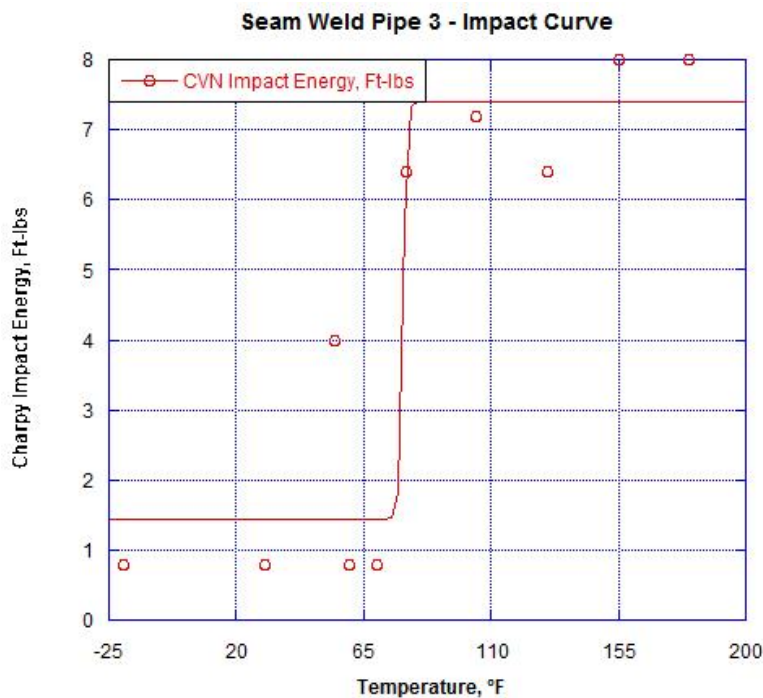


Figure 12. Charpy V-notch impact energy (full-size-equivalent) as a function of temperature for transverse, unflattened seam weld samples removed from Pipe Section 3.

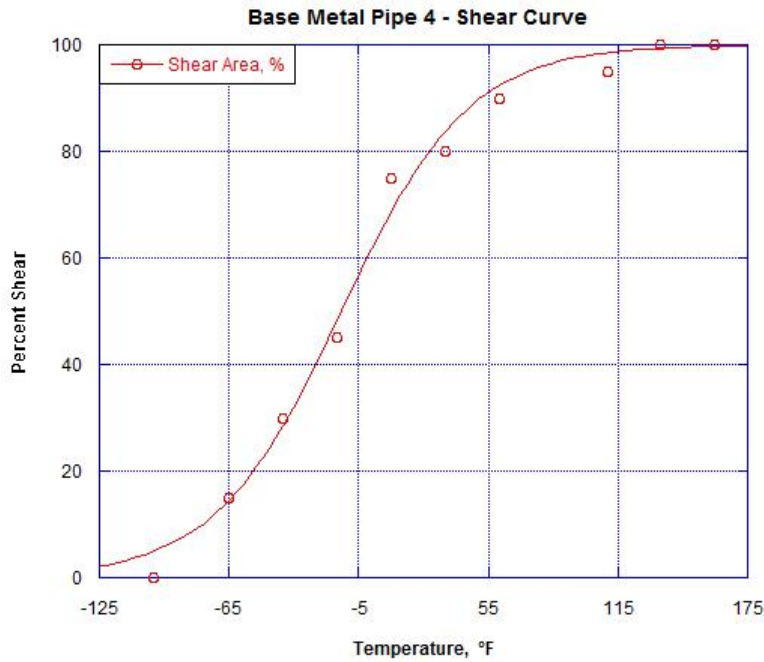


Figure 13. Percent shear from Charpy V-notch tests as a function of temperature for transverse, unflattened base metal samples removed from Pipe Section 4.

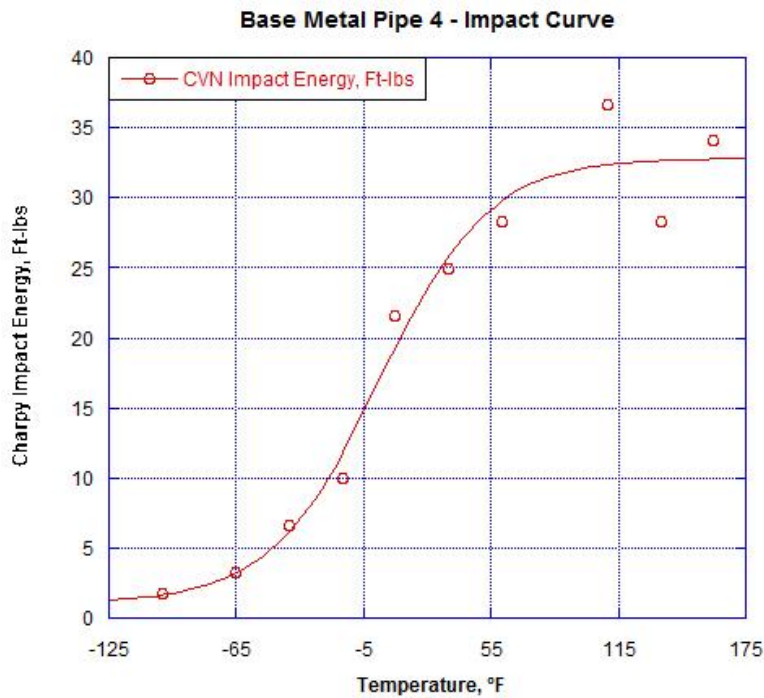


Figure 14. Charpy V-notch impact energy (full-size-equivalent) as a function of temperature for transverse, unflattened base metal samples removed from Pipe Section 4.

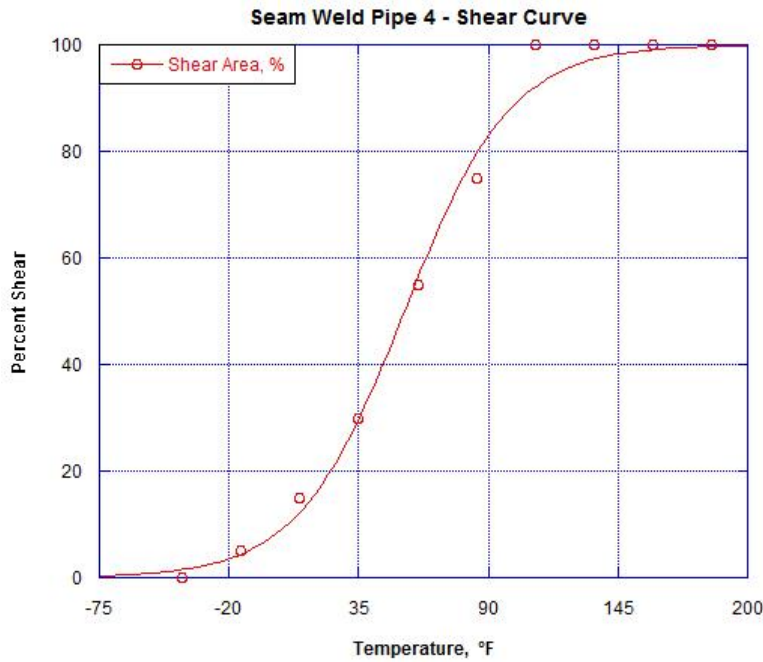


Figure 15. Percent shear from Charpy V-notch tests as a function of temperature for transverse, unflattened seam weld samples removed from Pipe Section 4.

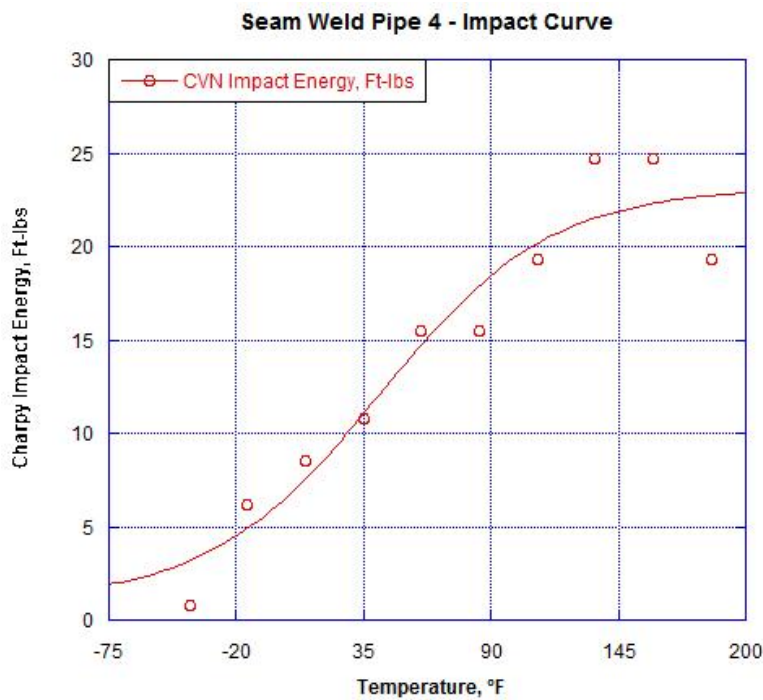


Figure 16. Charpy V-notch impact energy (full-size-equivalent) as a function of temperature for transverse, unflattened seam weld samples removed from Pipe Section 4.

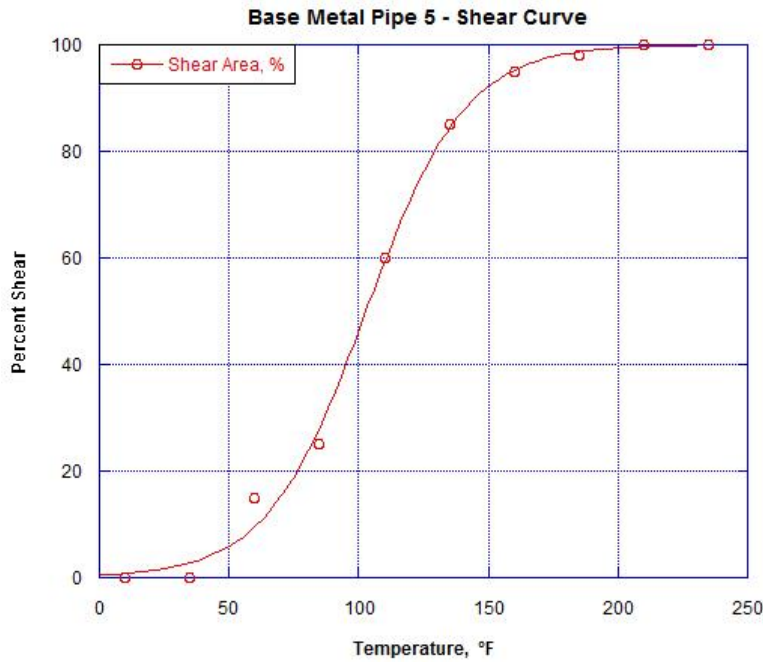


Figure 17. Percent shear from Charpy V-notch tests as a function of temperature for transverse, unflattened base metal samples removed from Pipe Section 5.

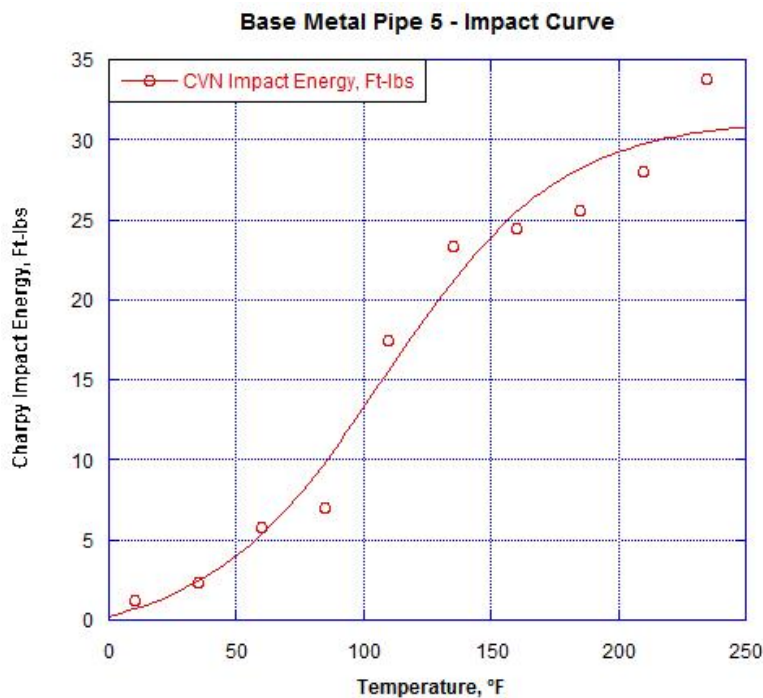


Figure 18. Charpy V-notch impact energy (full-size-equivalent) as a function of temperature for transverse, unflattened base metal samples removed from Pipe Section 5.

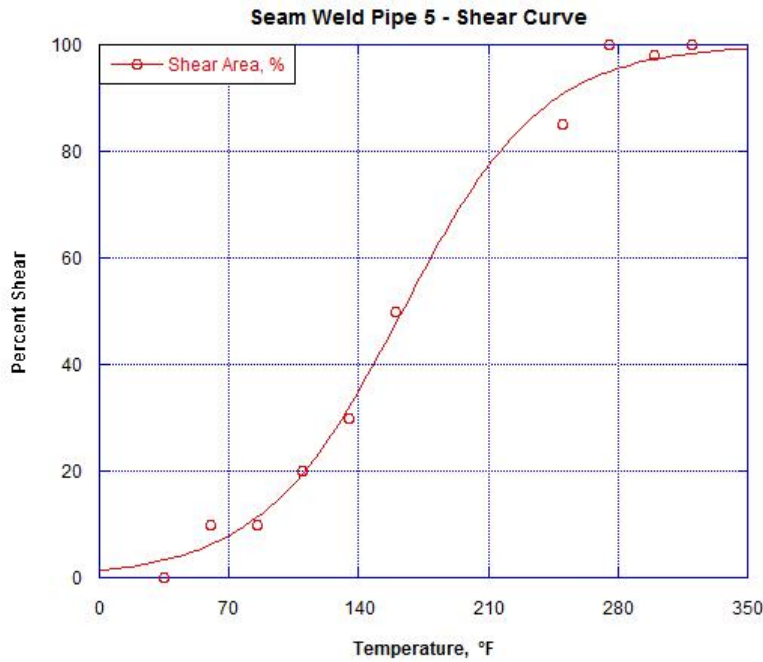


Figure 19. Percent shear from Charpy V-notch tests as a function of temperature for transverse, unflattened seam weld samples removed from Pipe Section 5.

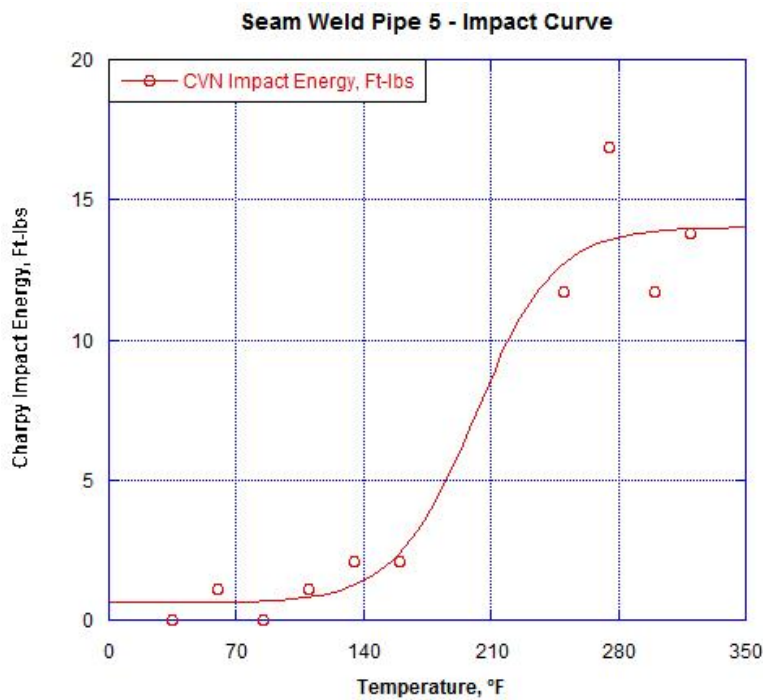


Figure 20. Charpy V-notch impact energy (full-size-equivalent) as a function of temperature for transverse, unflattened seam weld samples removed from Pipe Section 5.

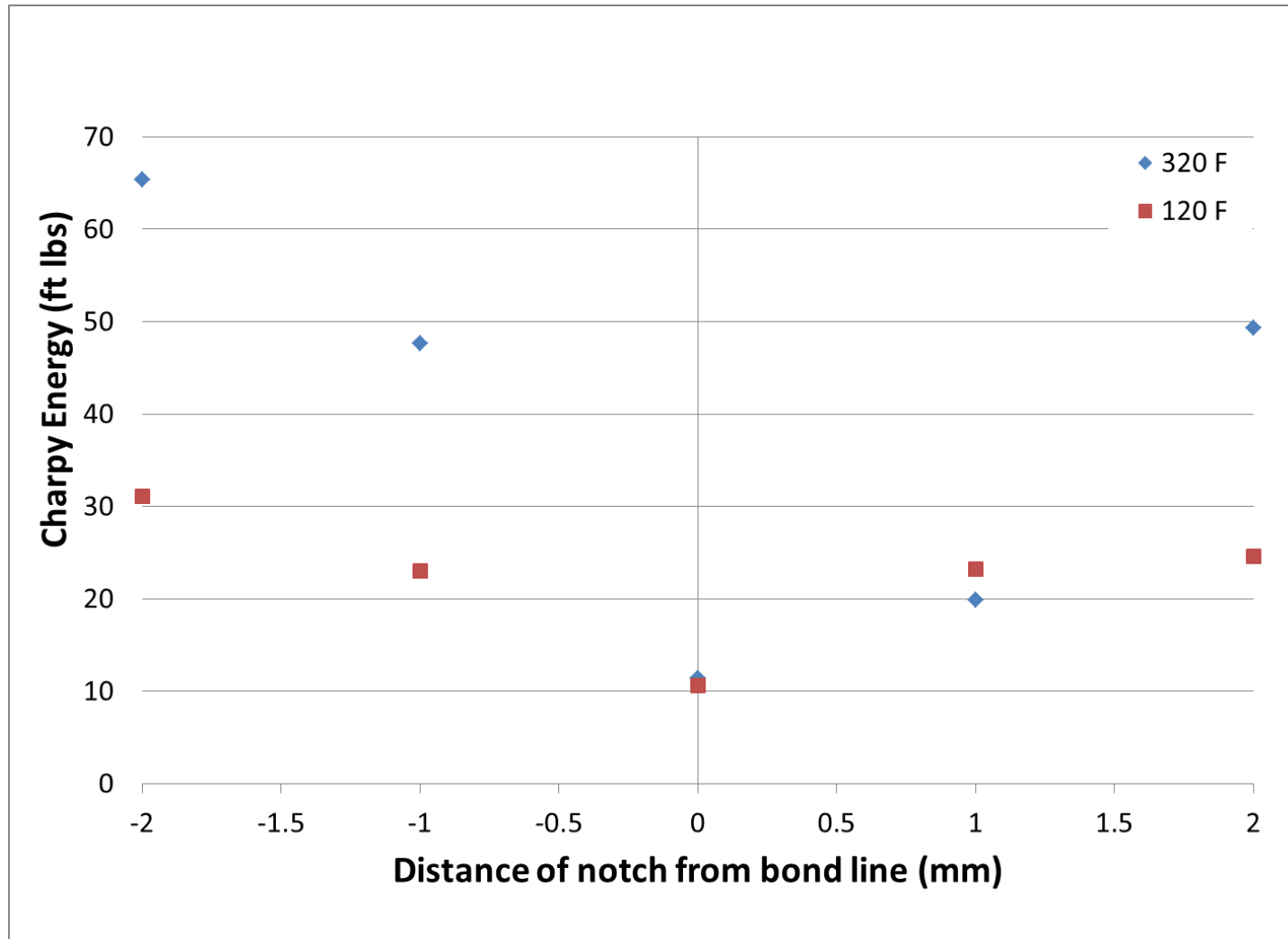


Figure 21. Plot of Charpy energy (full-size-equivalent) vs. distance of the notch from the bond line for Pipe Section 1.

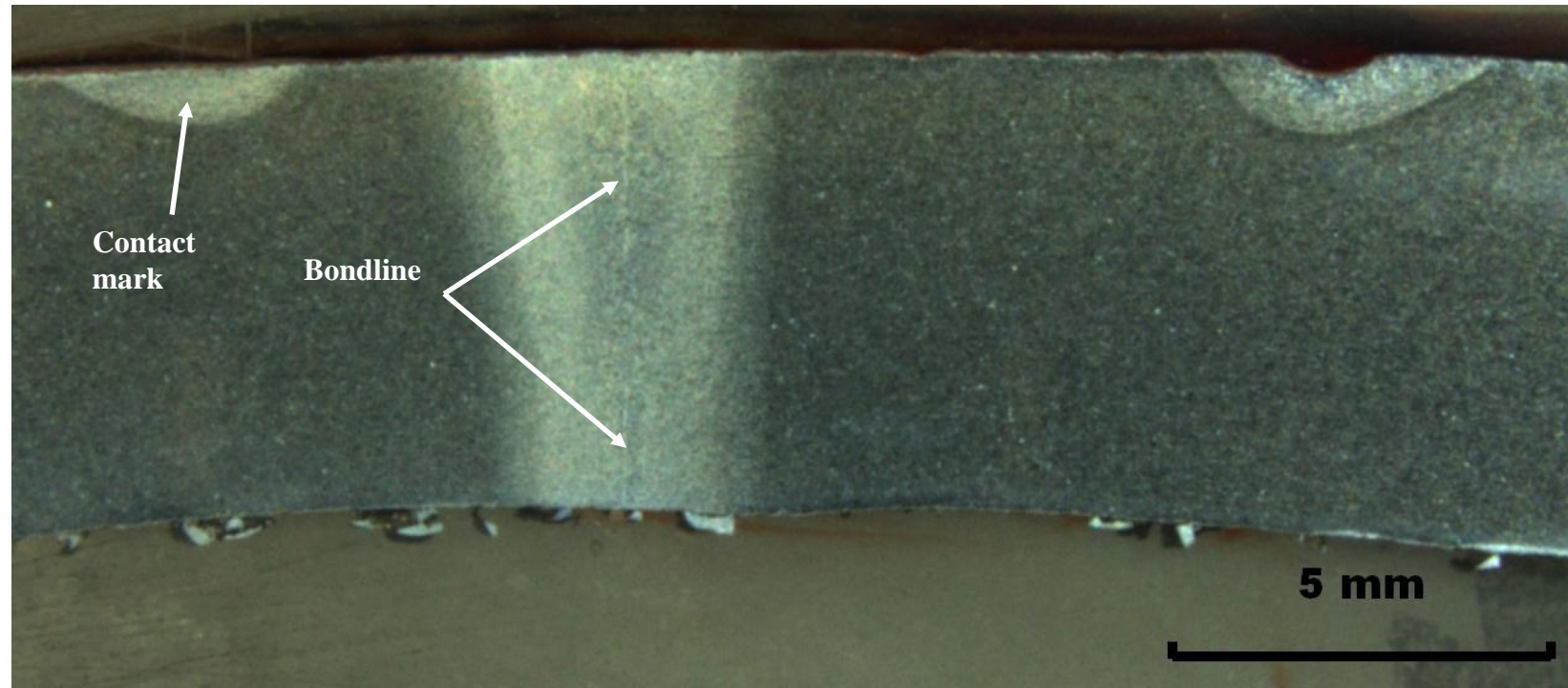


Figure 22. Stereo light photomicrograph of transverse Mount M1-7, which was removed from an NDE feature adjacent to CVN specimens C1-7A and C1-7B (4% Nital Etchant).

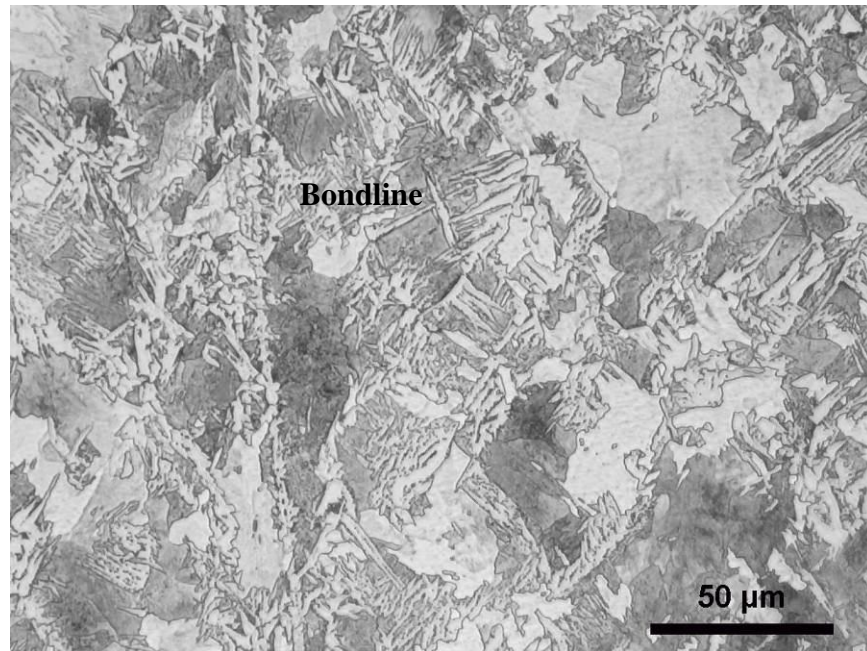


Figure 23. Light photomicrograph showing the microstructure adjacent to the bond line of transverse Mount M4-1 (4% Nital Etchant).

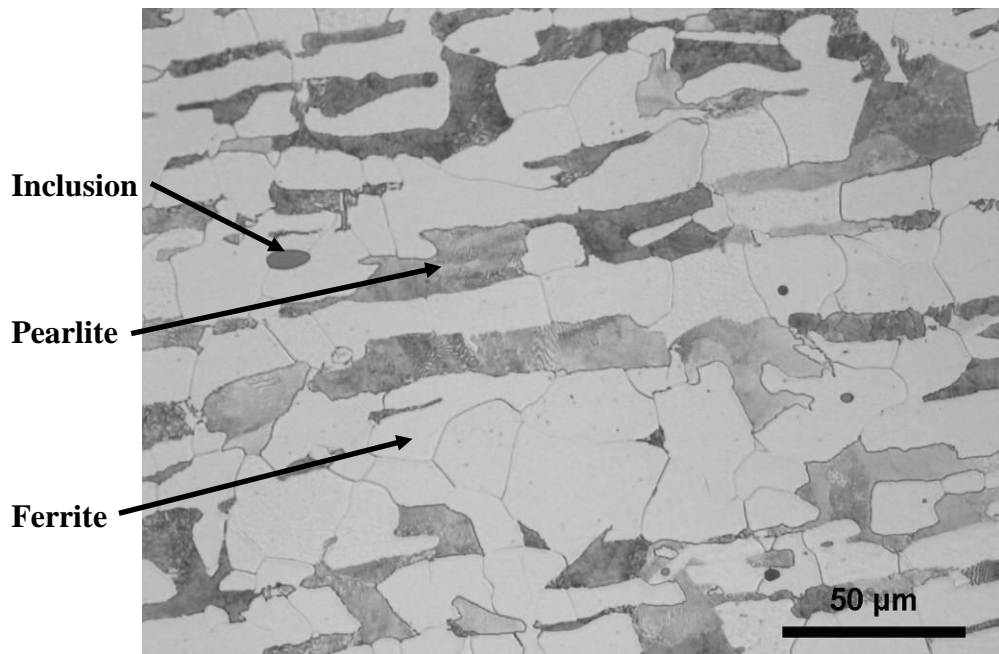


Figure 24. Light photomicrograph showing the typical base metal of transverse Mount M4-1 (4% Nital Etchant).

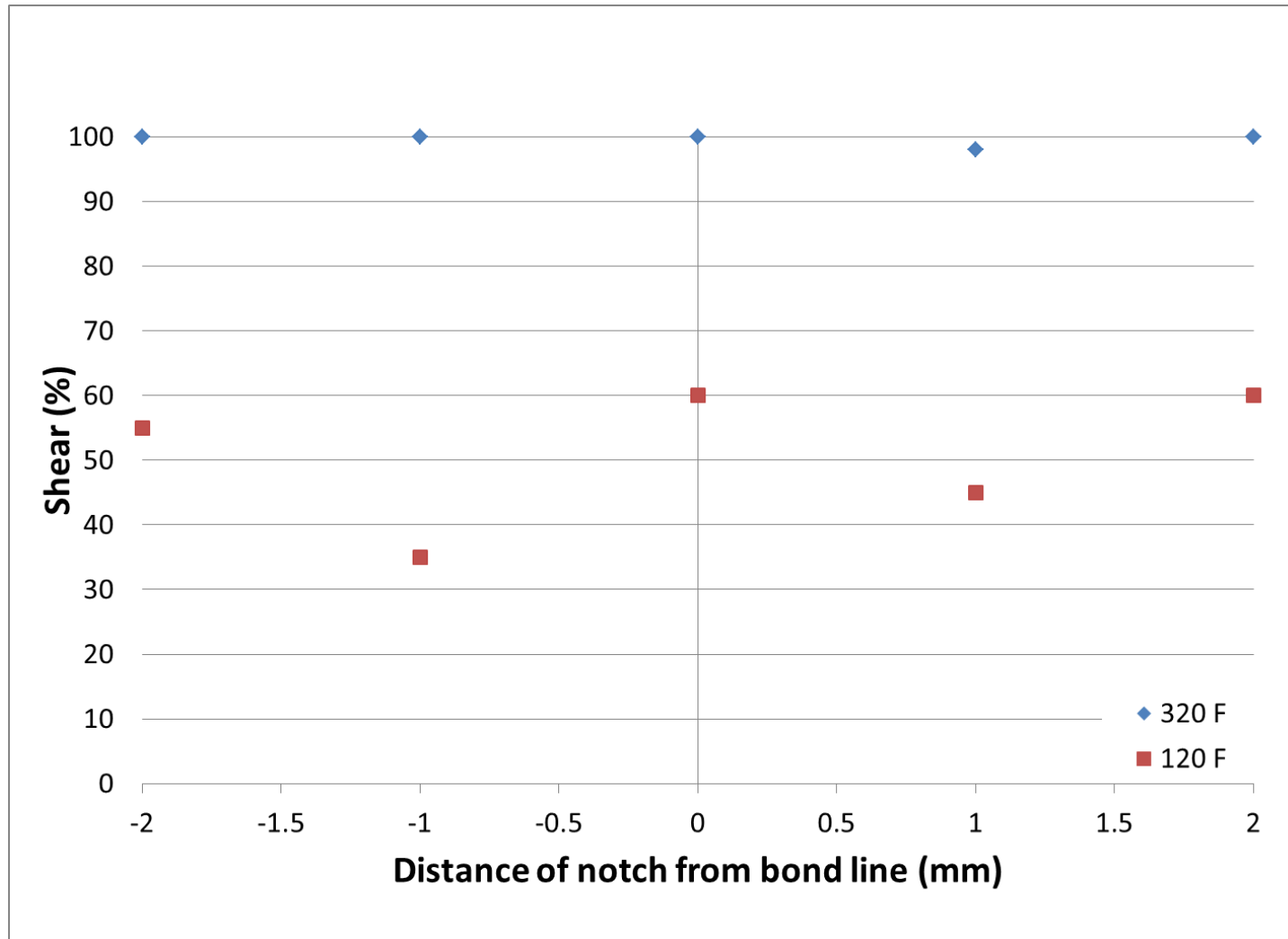


Figure 25. Plot of percent shear vs. distance of the notch from the bond line for Pipe Section 1.

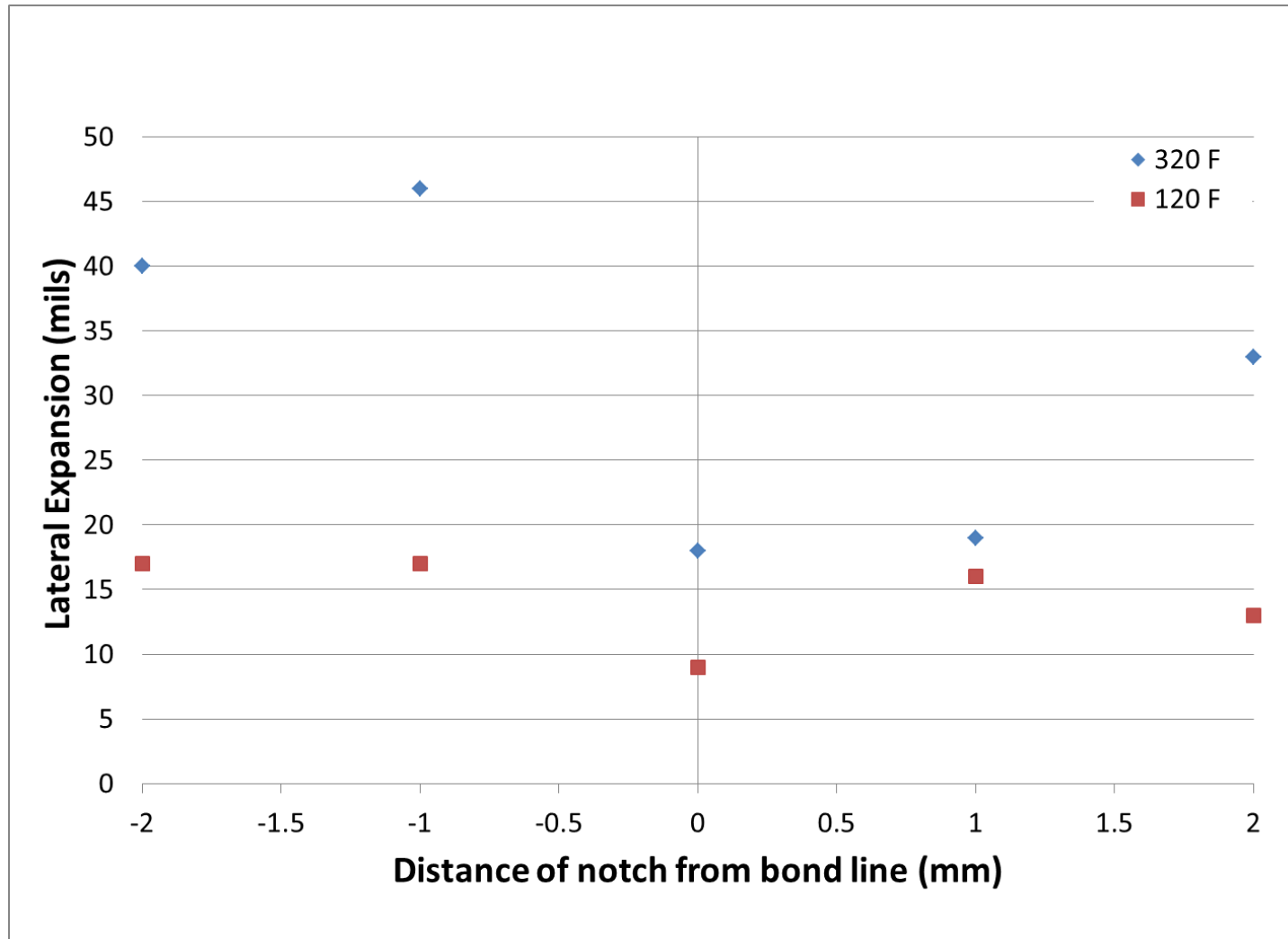


Figure 26. Plot of lateral expansion vs. distance of the notch from the bond line for Pipe Section 1.

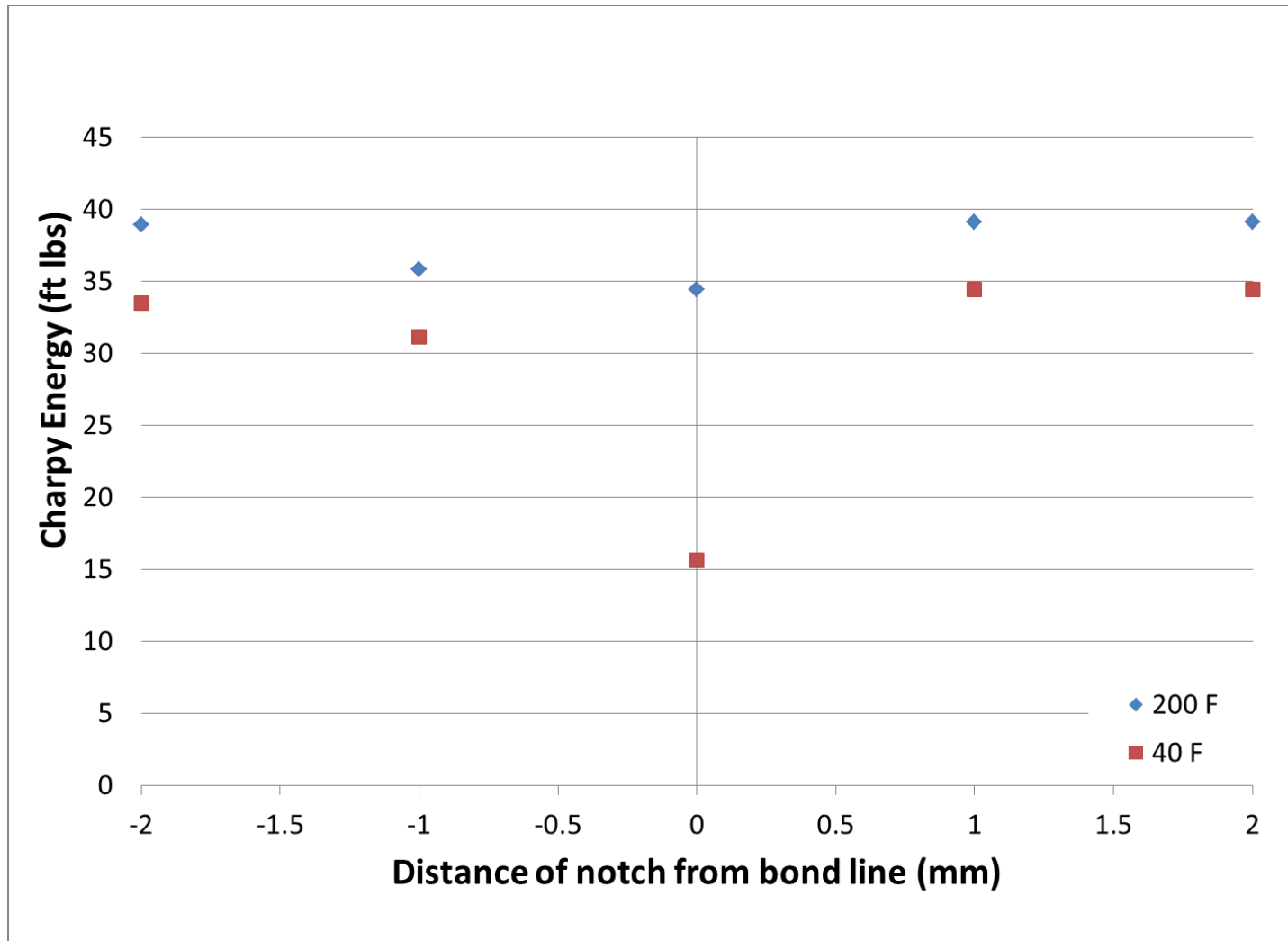


Figure 27. Plot of Charpy energy (full-size-equivalent) vs. distance of the notch from the bond line for Pipe Section 4.

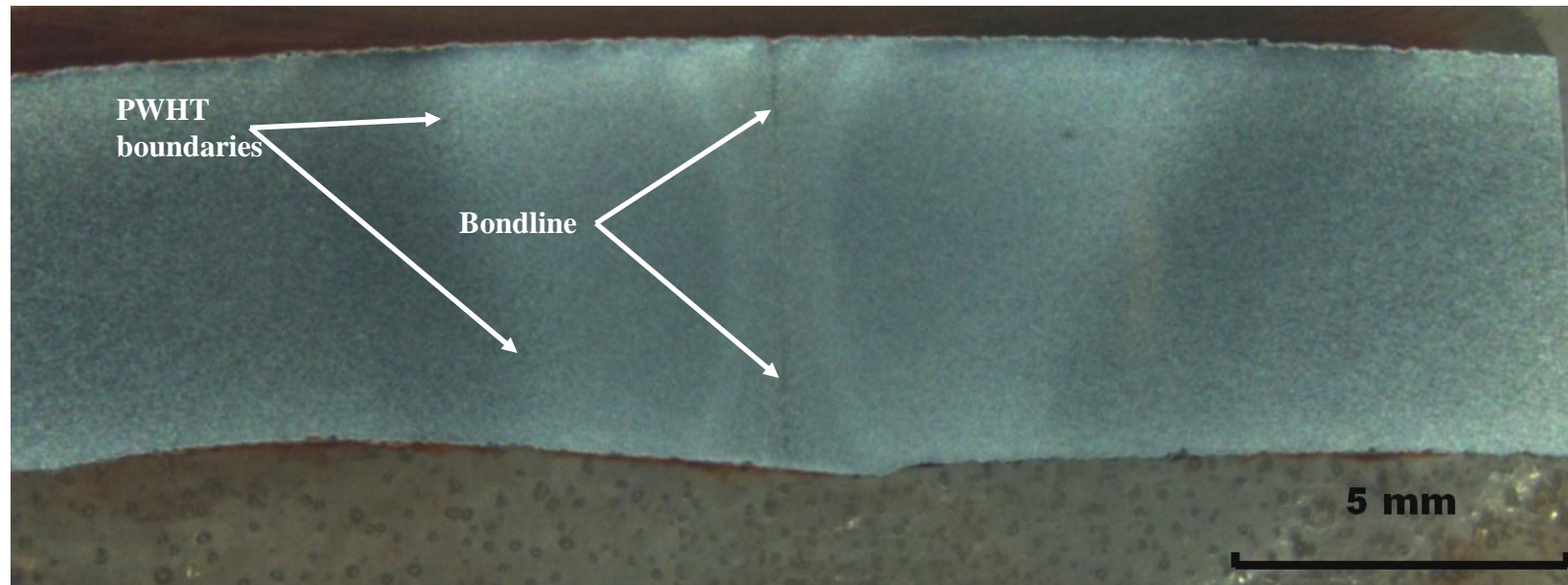


Figure 28. Stereo light photomicrograph of transverse Mount M4-1, which was removed from an NDE feature adjacent to CVN Specimens C4-1A and C4-1B (4% Nital Etchant).

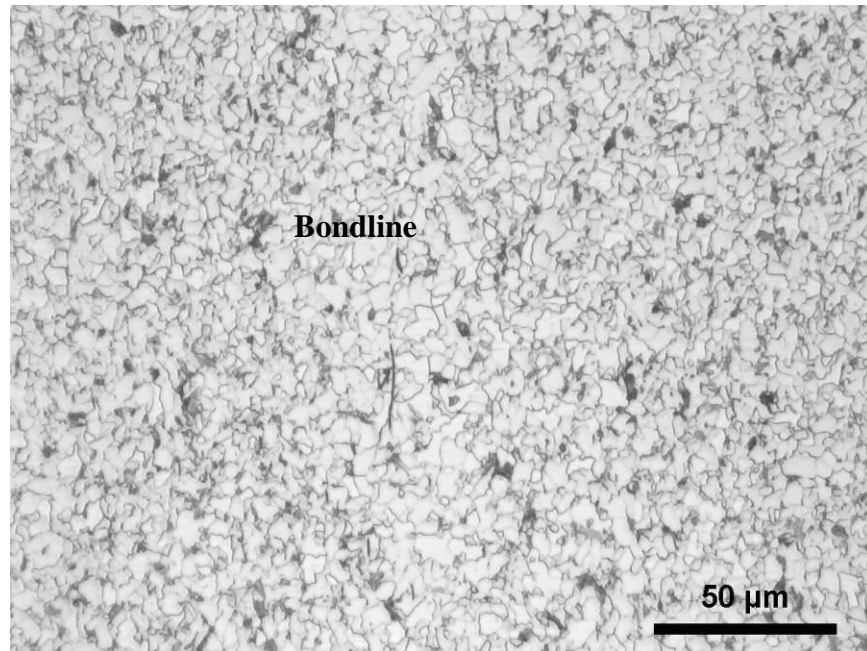


Figure 29. Light photomicrograph showing the microstructure adjacent to the bond line of transverse Mount M4-1 (4% Nital Etchant).

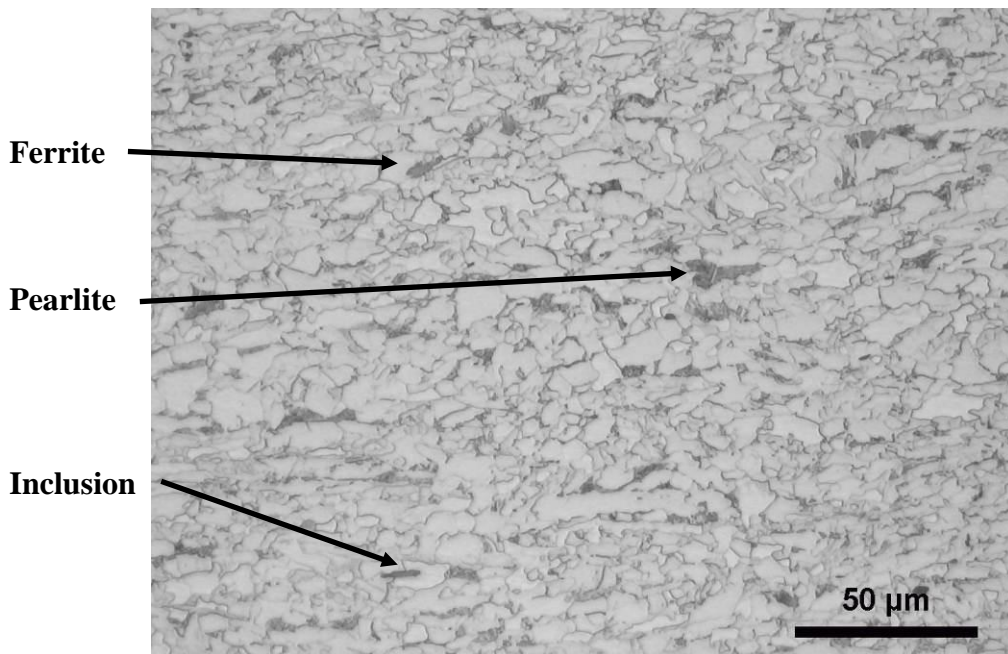


Figure 30. Light photomicrograph showing the typical base metal of transverse Mount M4-1 (4% Nital Etchant).

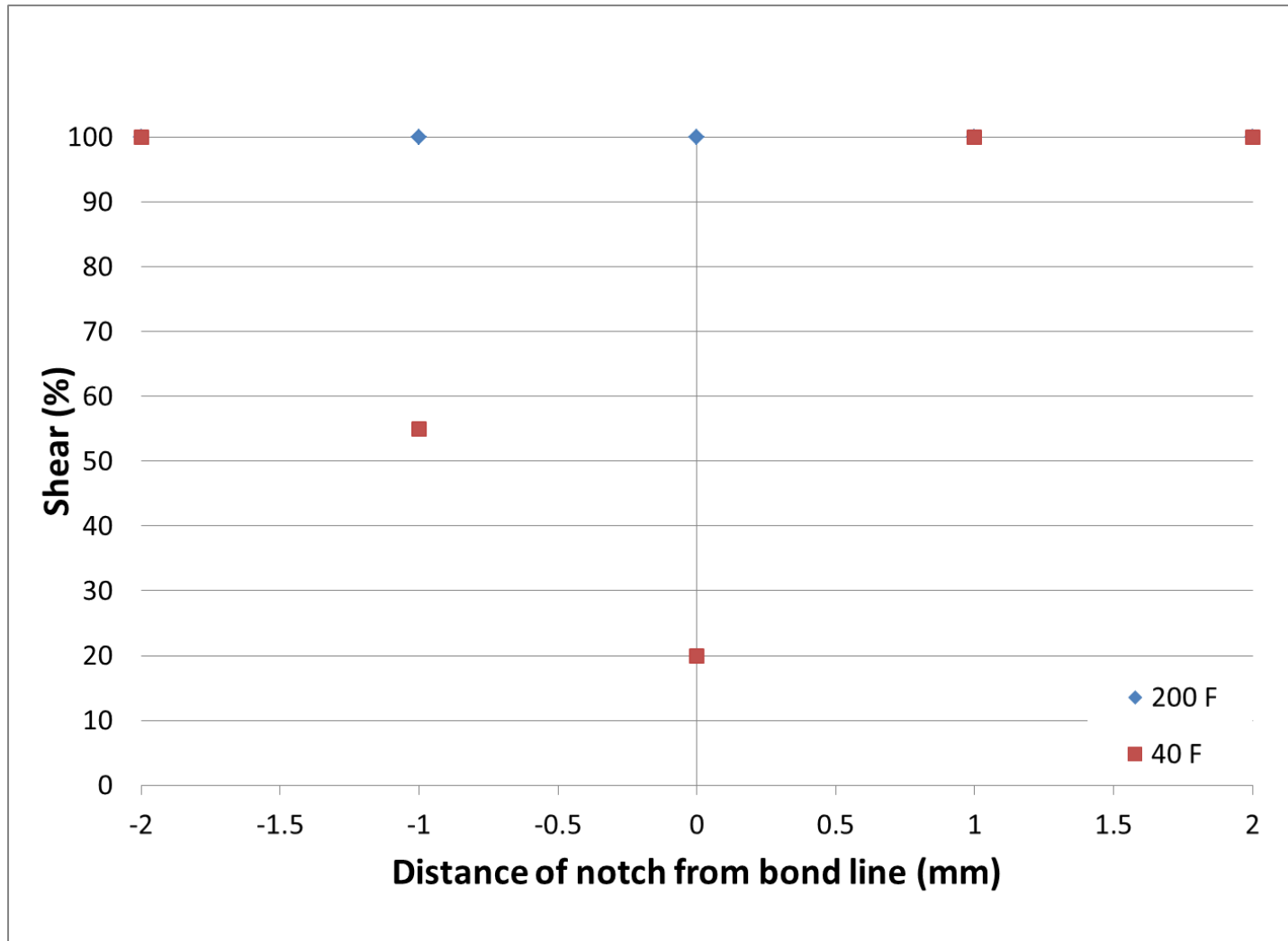


Figure 31. Plot of percent shear vs. distance of the notch from the bond line for Pipe Section 4.

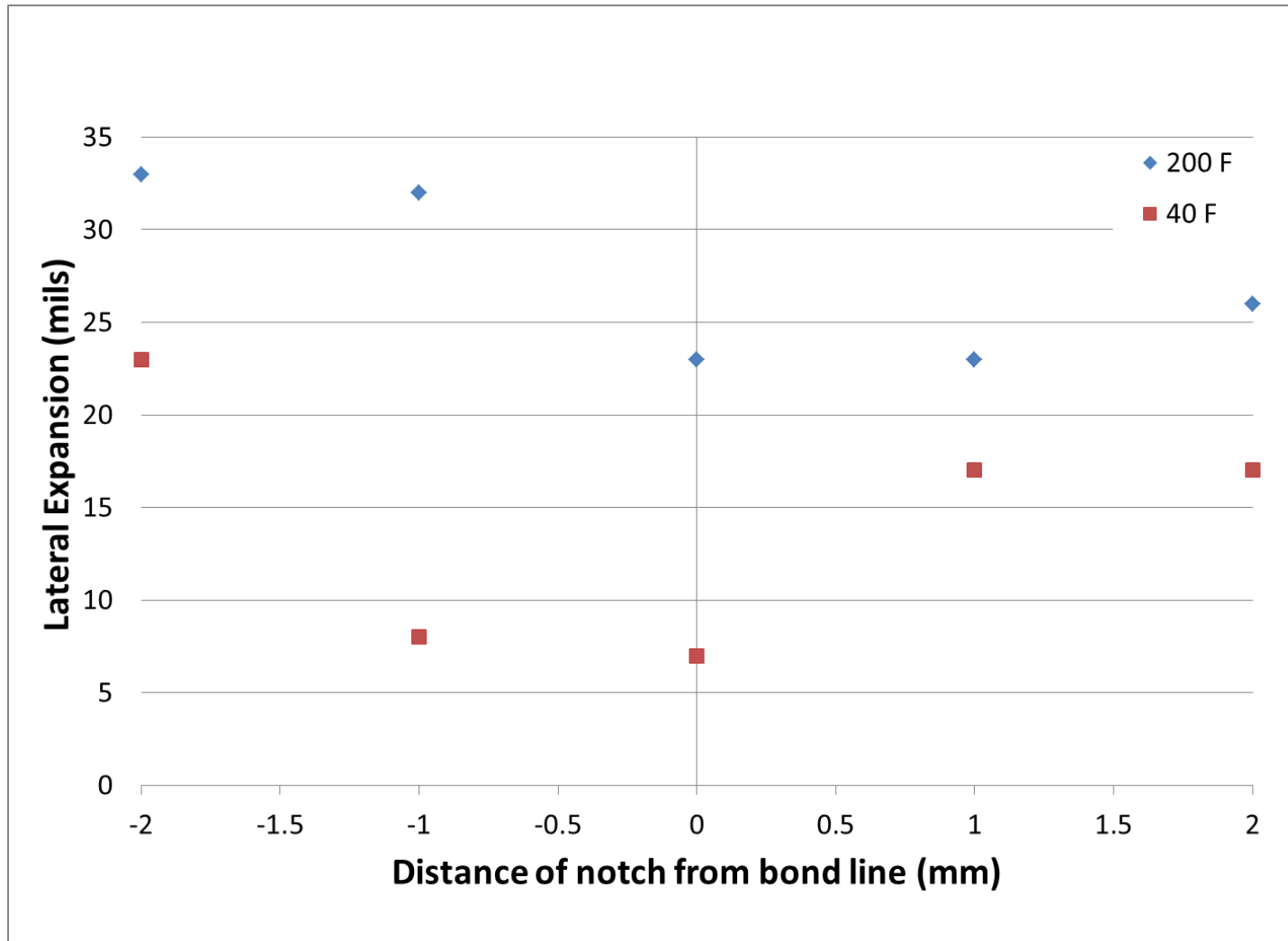


Figure 32. Plot of lateral expansion vs. distance of the notch from the bond line for Pipe Section 4.

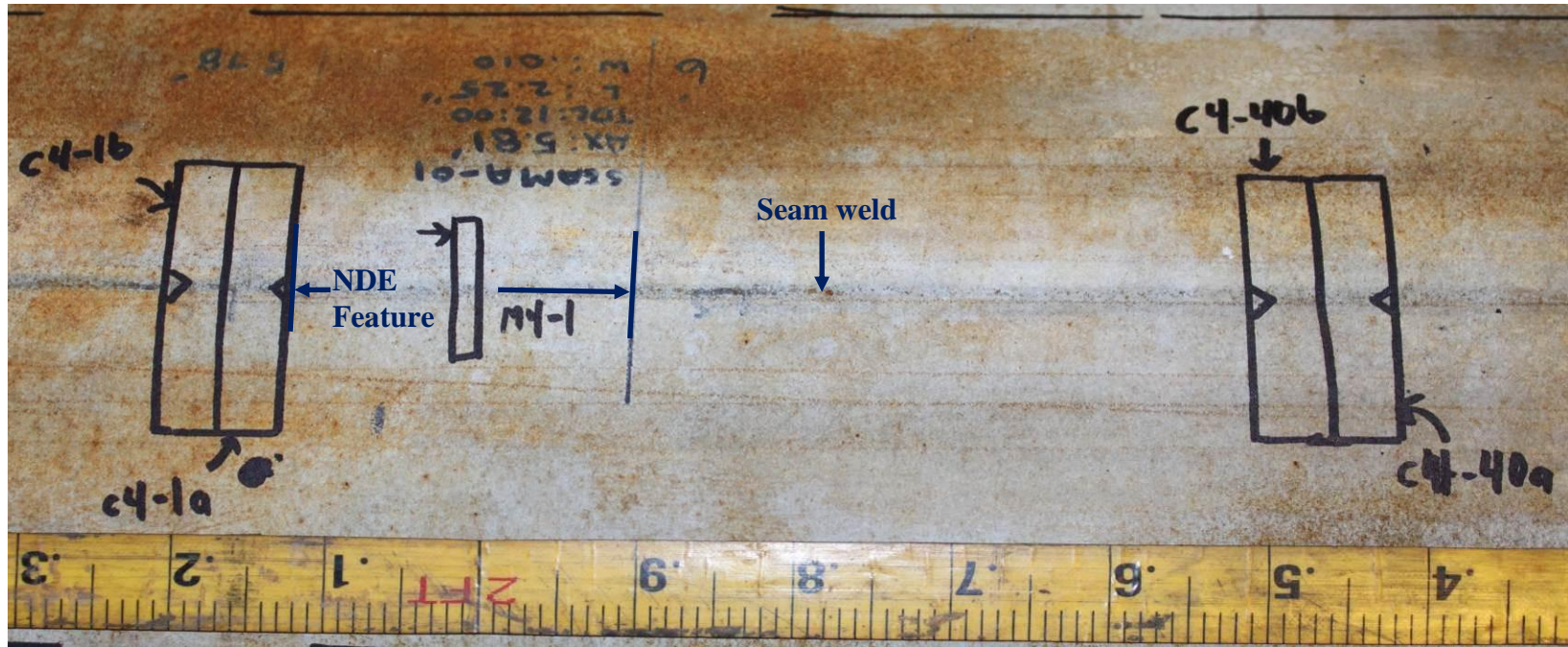


Figure 33. Photograph of a portion of Pipe Section prior to removal of Mount M4-1 and CVN specimens C4-40a/b and C4-1a/b.

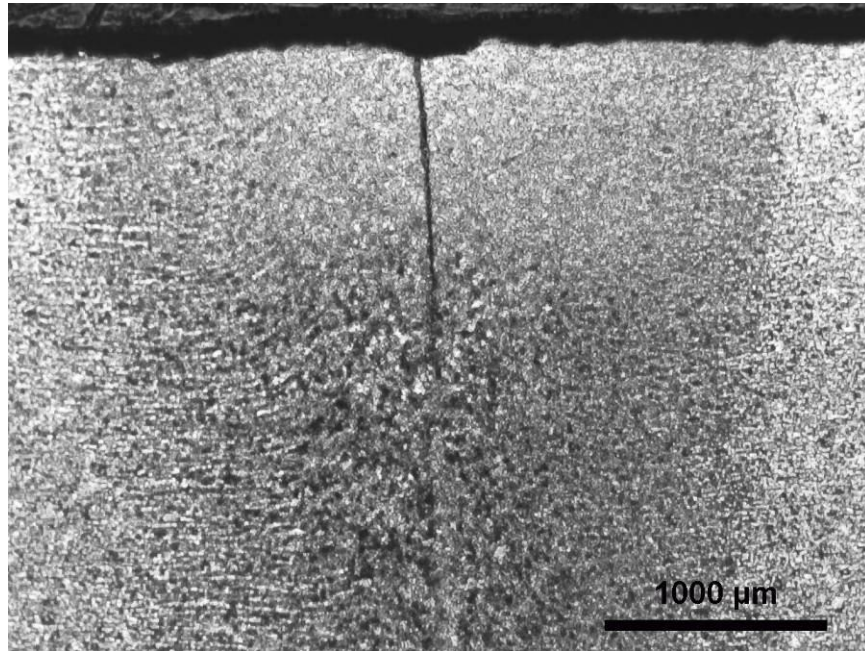


Figure 34. Light photomicrograph of transverse Mount M1-8, which was removed from an NDE feature adjacent to CVN specimens C1-8A and C1-8B (4% Nital Etchant).

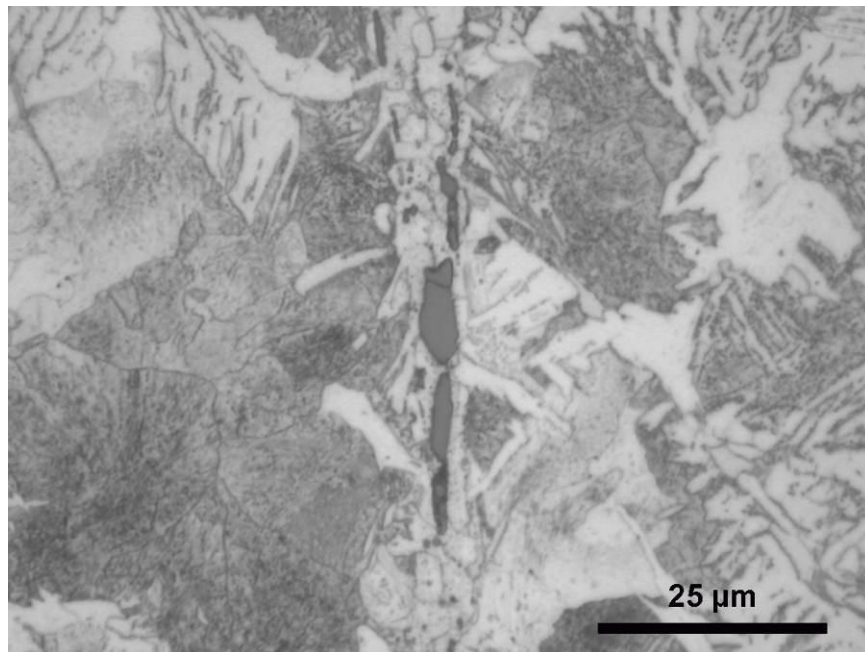


Figure 35. Light photomicrograph of transverse Mount M1-5, which was removed from an NDE feature adjacent to CVN specimens C1-5A and C1-5B (4% Nital Etchant).

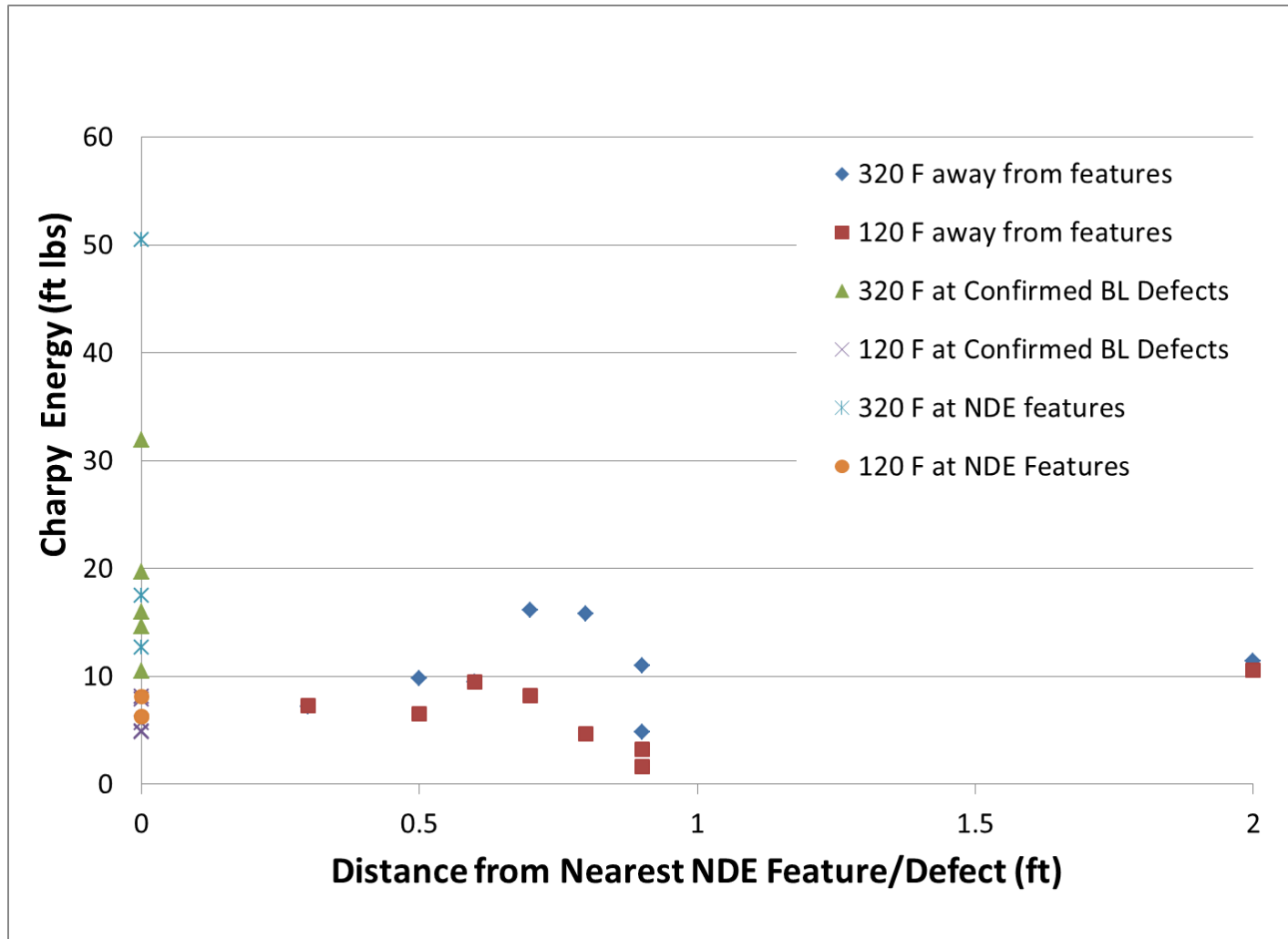


Figure 36. Plot of Charpy energy (full-size-equivalent) vs. distance from NDE features and confirmed bond line defects for Pipe Section 1.

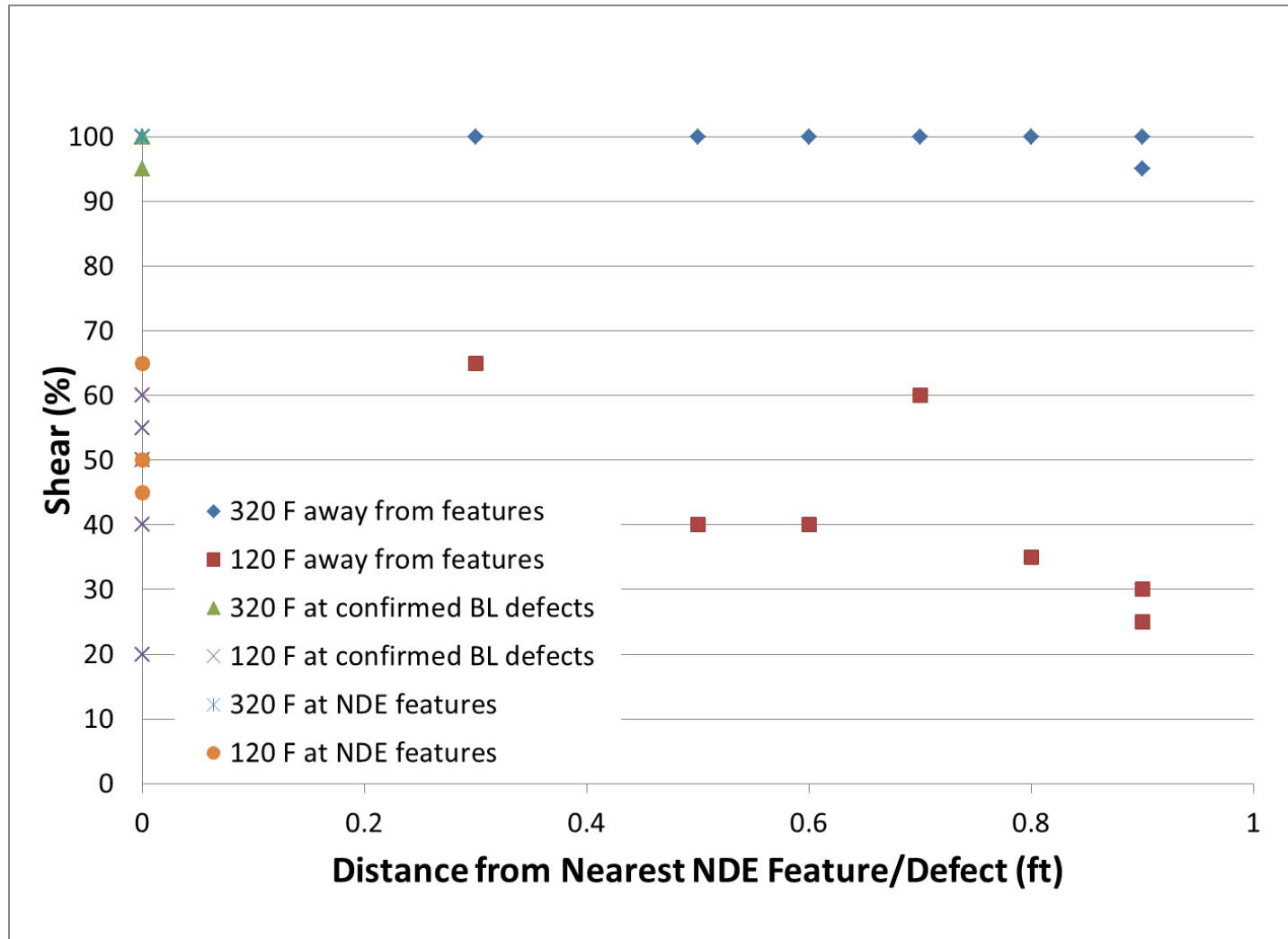


Figure 37. Plot of percent shear vs. distance from NDE features and confirmed bond line defects for Pipe Section 1.

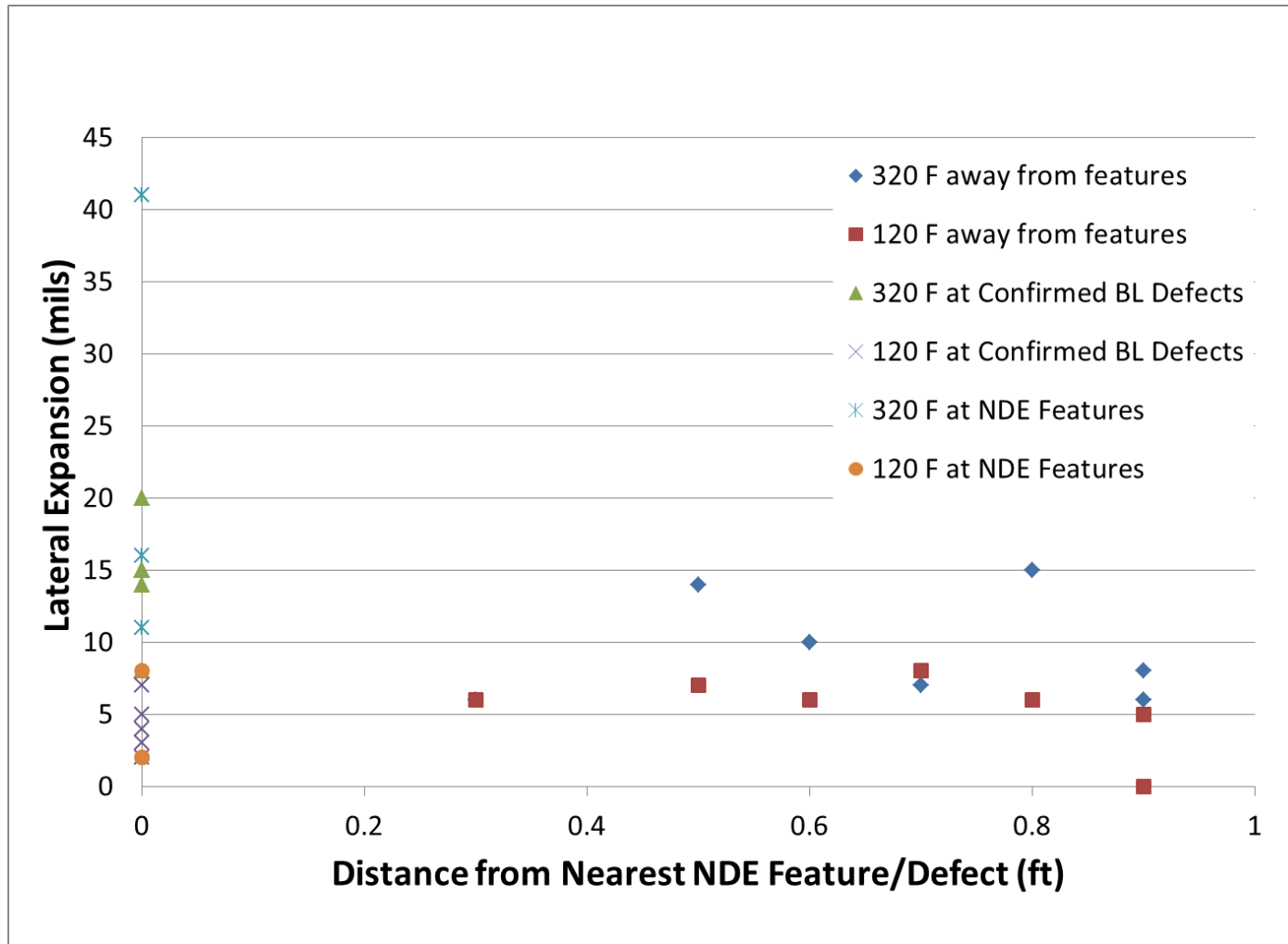


Figure 38. Plot of lateral expansion vs. distance from NDE features and confirmed bond line defects for Pipe Section 1.

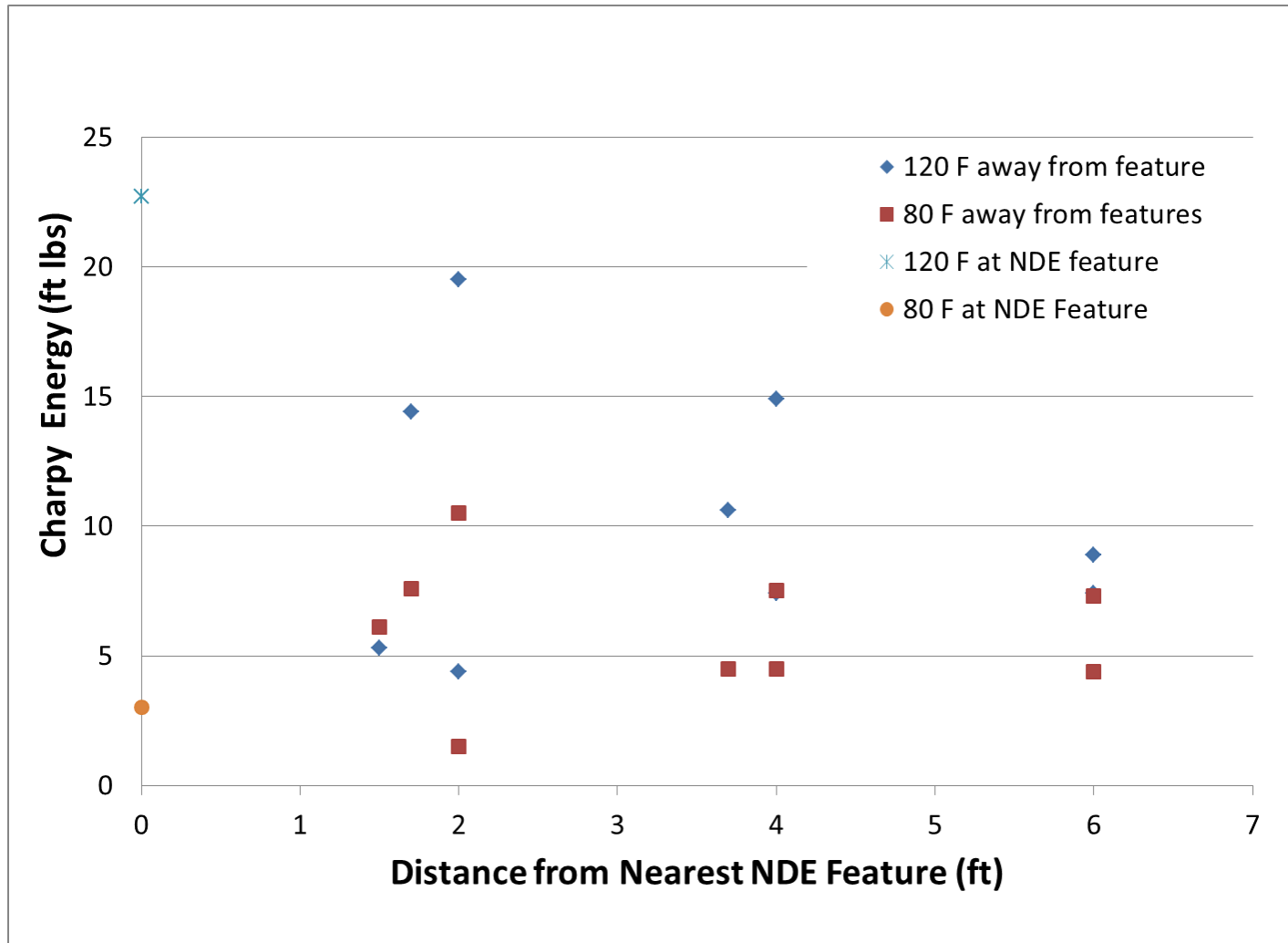


Figure 39. Plot of Charpy energy (full-size-equivalent) vs. distance from an NDE feature for Pipe Section 2.

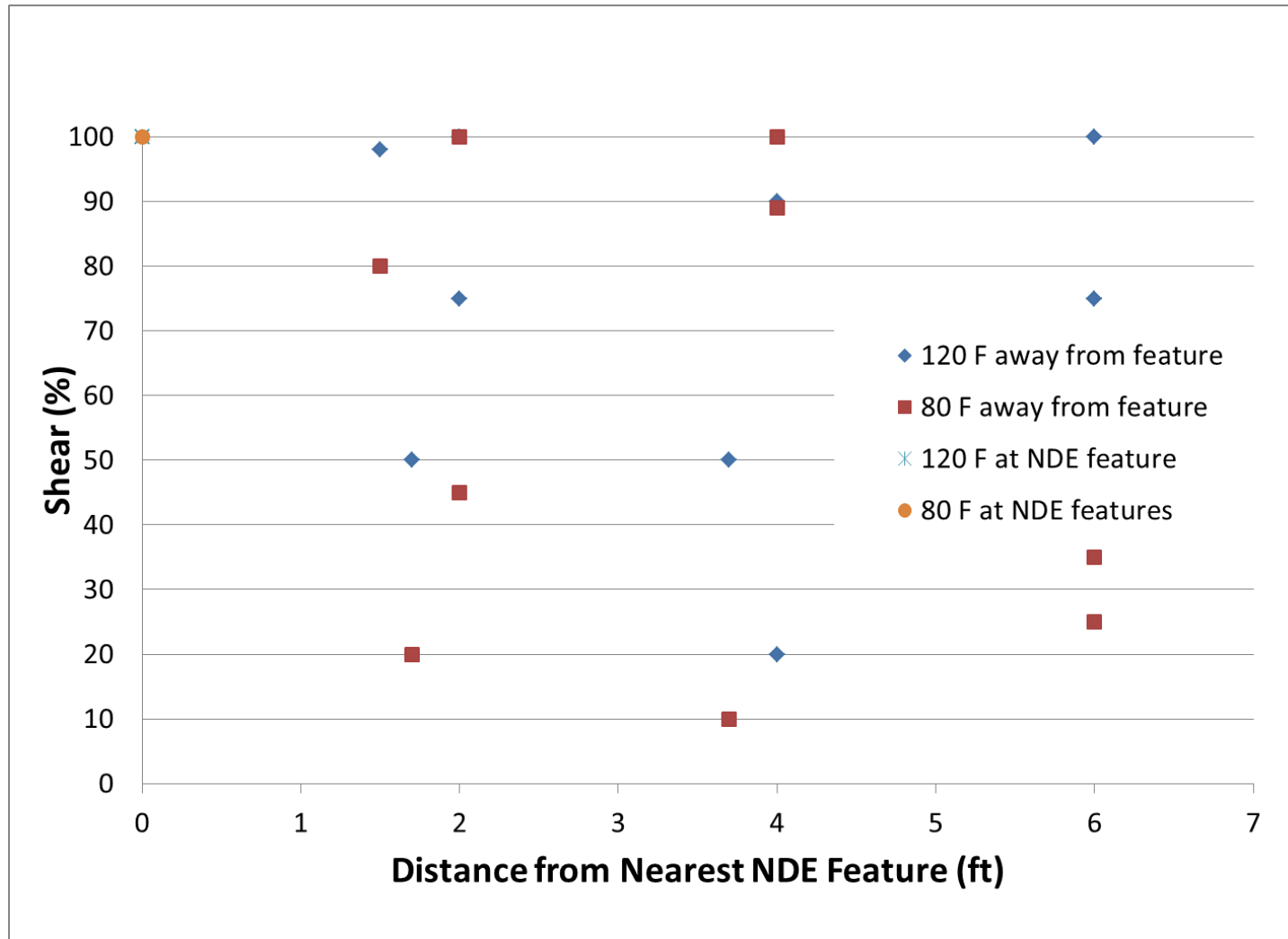


Figure 40. Plot of percent shear vs. distance from an NDE feature for Pipe Section 2.

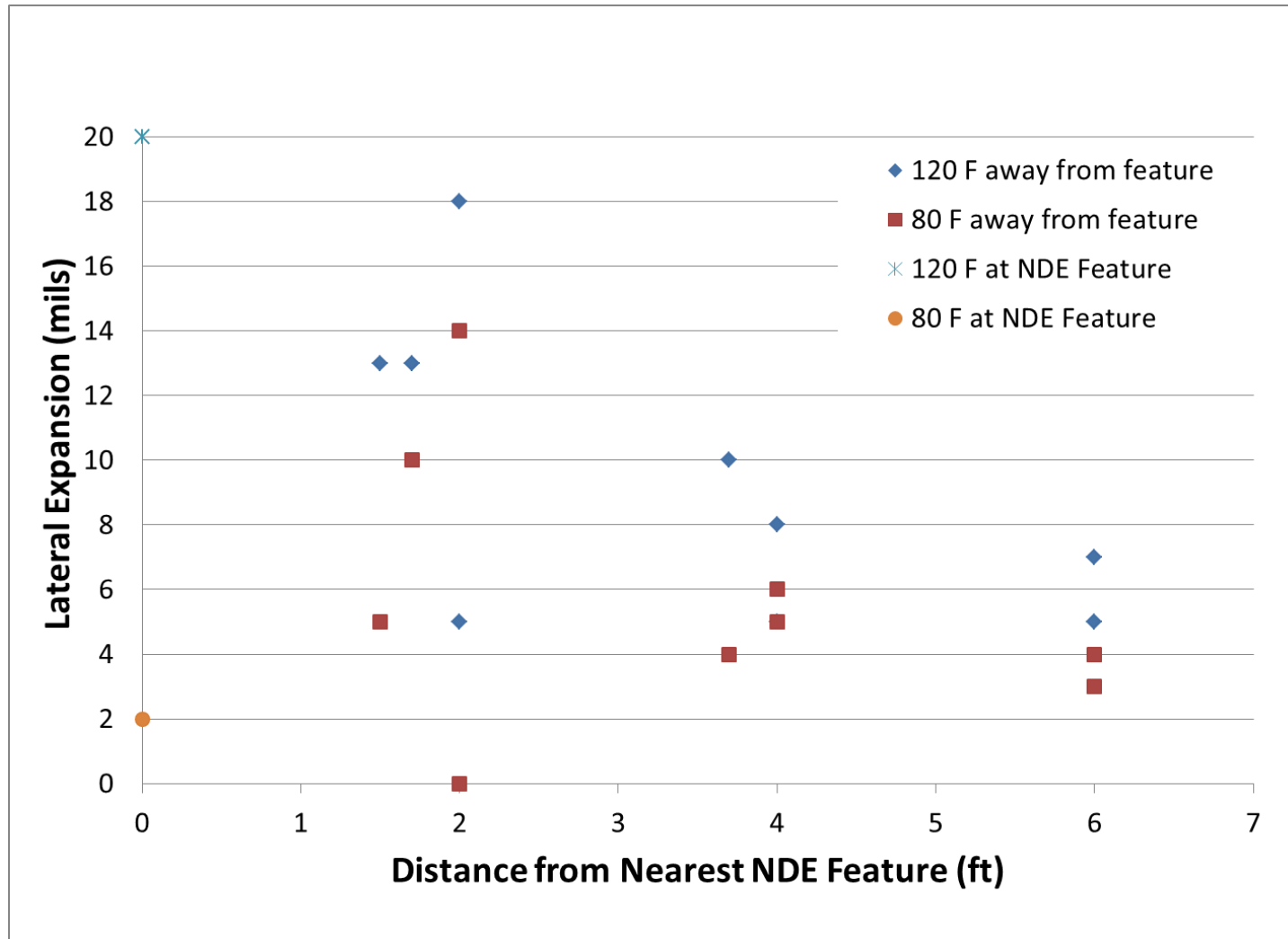


Figure 41. Plot of lateral expansion vs. distance from an NDE feature for Pipe Section 2.

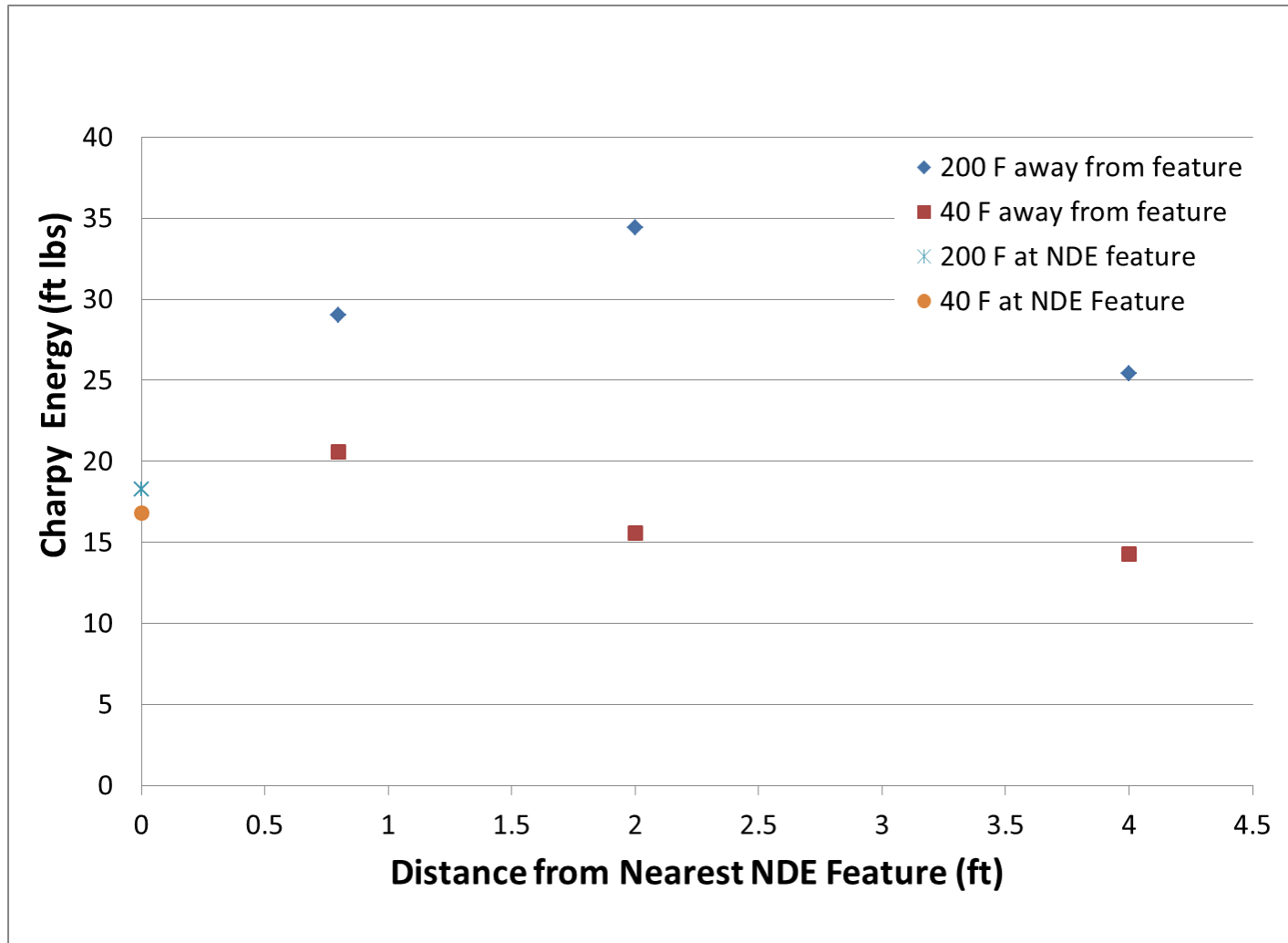


Figure 42. Plot of Charpy energy (full-size-equivalent) vs. distance from an NDE feature for Pipe Section 4.

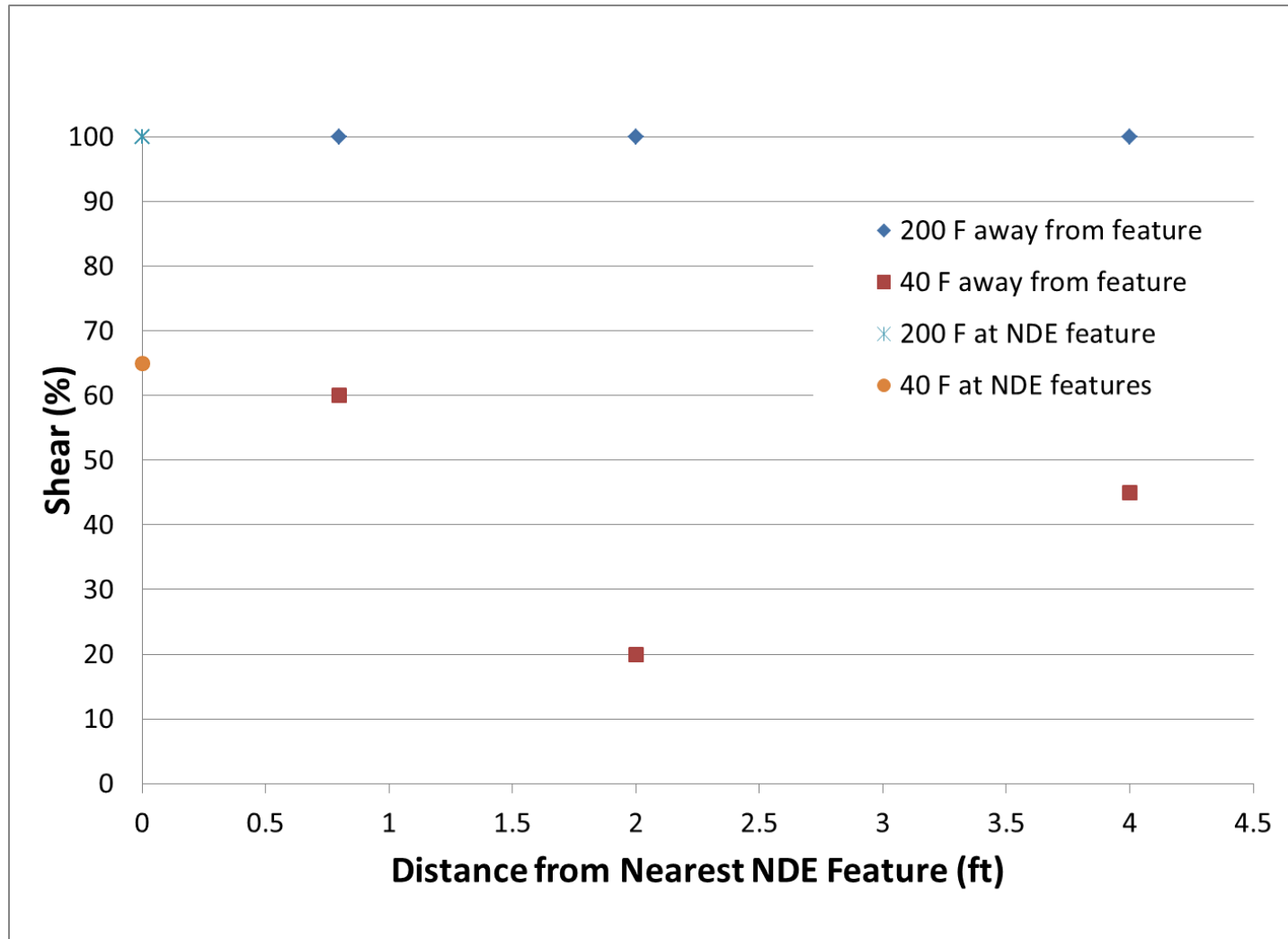


Figure 43. Plot of percent shear vs. distance from an NDE feature Pipe Section 4.

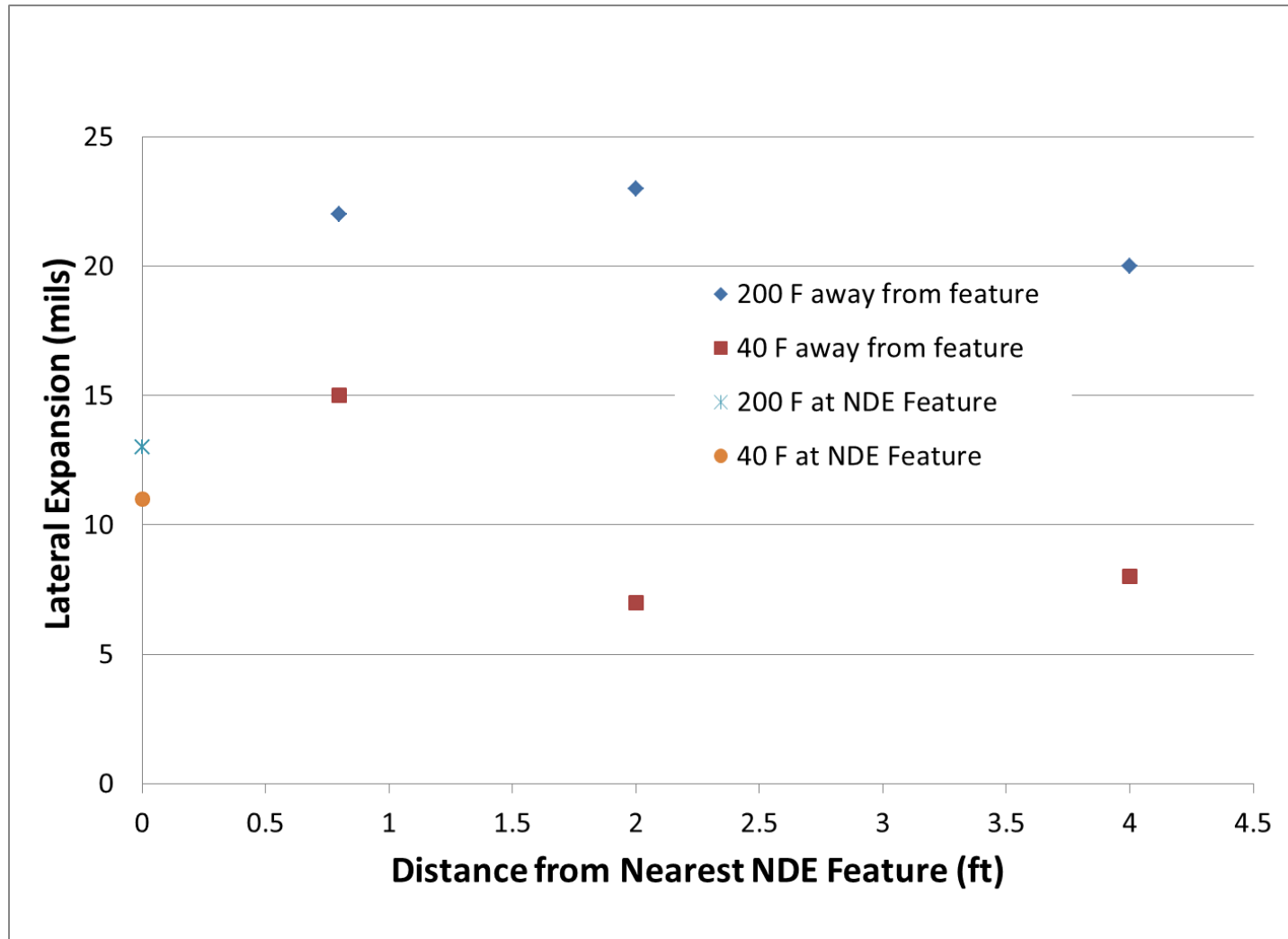


Figure 44. Plot of lateral expansion vs. distance from an NDE feature for Pipe Section 4.

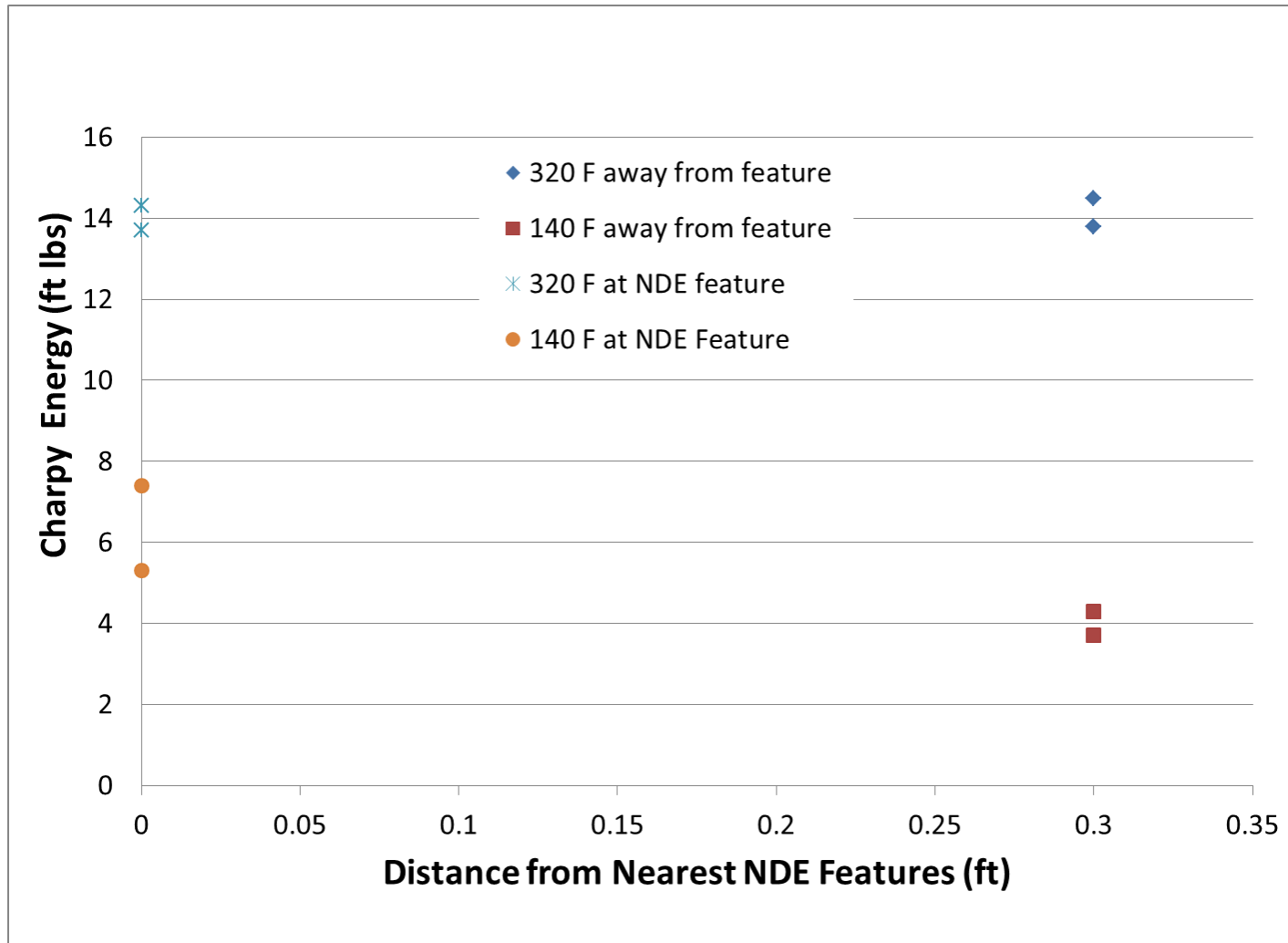


Figure 45. Plot of Charpy energy (full-size-equivalent) vs. distance from NDE features for Pipe Section 5.

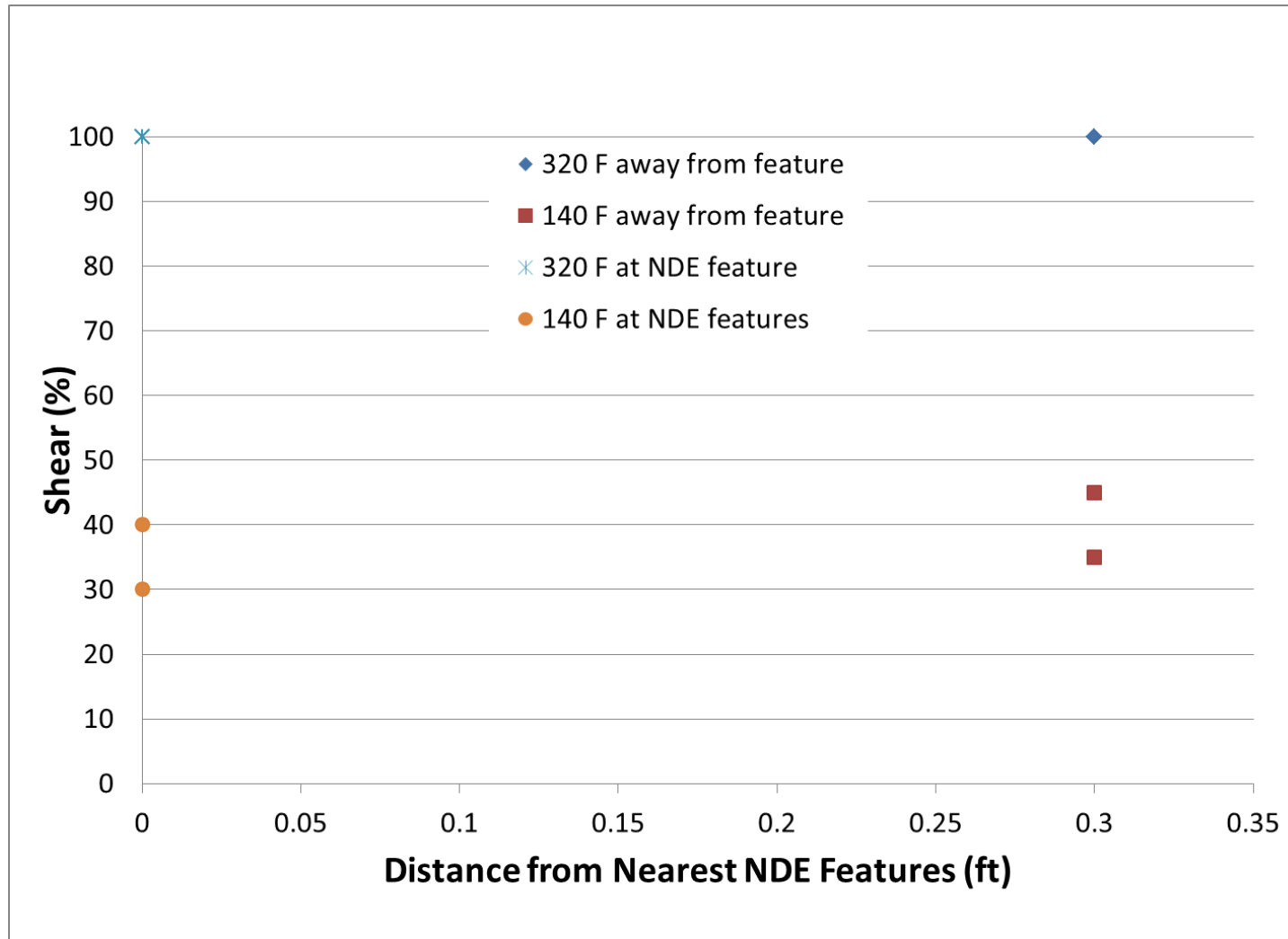


Figure 46. Plot of percent shear vs. distance from NDE features for Pipe Section 5.

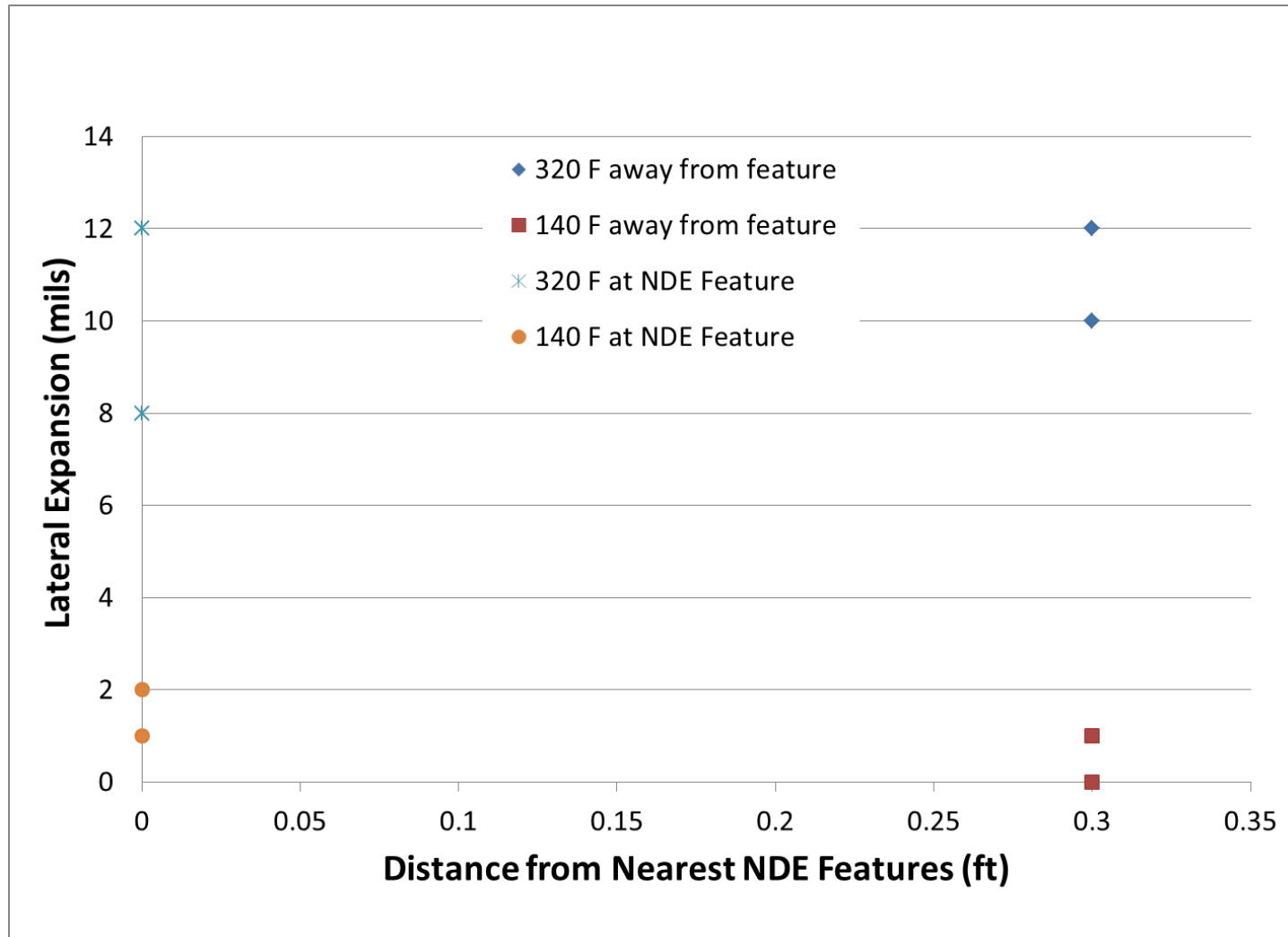


Figure 47. Plot of lateral expansion vs. distance from NDE features for Pipe Section 5.

Det Norske Veritas

DNV is a global provider of knowledge for managing risk. Today, safe and responsible business conduct is both a license to operate and a competitive advantage. Our core competence is to identify, assess, and advise on risk management, and so turn risks into rewards for our customers. From our leading position in certification, classification, verification, and training, we develop and apply standards and best practices. This helps our customers to safely and responsibly improve their business performance.

Our technology expertise, industry knowledge, and risk management approach, has been used to successfully manage numerous high-profile projects around the world.

DNV is an independent organization with dedicated risk professionals in more than 100 countries. Our purpose is to safeguard life, property, and the environment. DNV serves a range of industries, with a special focus on the maritime and energy sectors. Since 1864, DNV has balanced the needs of business and society based on our independence and integrity. Today, we have a global presence with a network of 300 offices in 100 countries, with headquarters in Oslo, Norway.

Global Impact for a Safe and Sustainable Future

Learn more on www.dnv.com